

Giovanni Marin

# Inclined lithography and photoresist optimization for fabrication of 3D mesh structures

School of Electrical Engineering

Master thesis

Espoo 18-11-2014

Supervisor:

Prof. Sami Franssila

Instructor:

Ville Jokinen, PhD



**Aalto University**  
School of Electrical  
Engineering

Author: Giovanni Marin

Title: Inclined lithography and photoresist optimization for fabrication of 3D mesh structures

Date: 18-11-2014

Language: English

Number of pages: 80

Department of Applied Materials Science

Professorship: Microtechnology

Code: MT 301-3

Supervisor: Prof. Sami Franssila

Advisor: PhD Ville Jokinen

The goal of this thesis was to fabricate 3D structures using SU-8 with a novel inclined exposure setup and process. The structures are 3D meshes whose final shape is dependent on both pattern on the photomask and SU-8 layer thickness. 3D structures were successfully fabricated on layers 100, 70 and 50  $\mu\text{m}$  thick. Different patterns were tested to analyse the relations of the sizes and distribution of the holes in the mask with the final structures. SEM imaging confirmed the hypothesis that the shape of the 3D mesh is controlled by the pattern in the mask, the layer thickness and for a certain extent by the exposure dose. During the fabrication defects, caused by the behaviour of the resist during exposure, are observed in the structures. Most of the defects were eliminated or reduced in the optimized samples. The final structures fabricated had apertures in the mesh ranging from as small as 10  $\mu\text{m}$  up to 40  $\mu\text{m}$  and it was demonstrated that they can be fabricated inside microfluidic channels. Improvements to the process and potential applications are presented at the end of the thesis.

Keywords: Microfabrication, Inclined lithography, 3D structures, mesh, photoresist

## Preface

When I graduated from my bachelor degree I had no idea that I would end up doing research in a facility like Micronova at the other side of Europe. I was just sure that I will continue my work as a Scientist not in the country where I lived almost all my life.

The first path for my research carrier appeared when I got an unexpected summer position in Sami Franssila's Microfabrication group. From that moment the direction of my studies became clearer and clearer the more I was working on all the different projects I was part of.

Now that my university studies are finally over I'm quite sure of what my scientific carrier will be and I even found another country that I can call home. And funnily enough many of the applications of my research are in the field of Biology, a study path that I abandoned after high school after choosing to be a Material Scientist.

Of course I could have never get this far without the help and support of many people inside and outside my university life.

I would like to thanks first of all Sami for giving me the opportunity of entering the microfabrication world. During these years it has been the beginning of my scientific carrier and the financial support I needed as well.

All the colleagues in the Microfabrication group that helped me with all the problems and questions I had during my research, in particular Joksa for being the instructor in the thesis and always available for offering the help I needed.

Since Science is fun but still needs some additions during the free time I want also to thanks Mario and Joonas for being friends also outside of the office (and again thanks Mario for all the science help and awesome ideas).

All my friends (and girlfriend) are also included for the thanks because every person helped me at some point of my life and all of that made possible for me to be here now.

Last I want to thanks all my family because they always supported me in every way possible in my decision to move to Finland.

To conclude I want to point out that Science is what is moving the human civilization forward. If people want to find the answer to their question they should put some effort in it and, following the scientific method, do experiments and elaborate conclusions. All of this done with a critical mind set, because not everything in Science is done correctly. Science is done by people and people make mistakes. We need to push forward, remembering the mistakes but trying to avoid them in the future. Every Euro invested in Science is a Euro invested in the future.

## Table of Contents

|   |                  |
|---|------------------|
| <b><i>Preface</i></b> .....   | <b><i>I</i></b>  |
| <b><i>Table of Contents</i></b> .....                                       | <b><i>II</i></b> |
| <b><i>List of Abbreviations</i></b> .....                                   | <b><i>IV</i></b> |
| <b><i>1. Introduction</i></b> .....   | <b><i>1</i></b>  |
| <b><i>2. Microfabrication</i></b> .....                                     | <b><i>3</i></b>  |
| <b><i>2.1 Lithography</i></b> .....   | <b><i>4</i></b>  |
| Positive photoresists .....   | 7                |
| Negative photoresists .....   | 8                |
| SU-8.....   | 8                |
| Lift-off negative resist (ma-N 1400) .....                                  | 10               |
| <b><i>2.2 Metallization</i></b> .....                                       | <b><i>12</i></b> |
| PVD (physical vapour deposition) .....                                      | 13               |
| CVD (chemical vapour deposition).....                                       | 16               |
| ALD (atomic layer deposition).....  | 16               |
| <b><i>2.3 Etching</i></b> .....   | <b><i>16</i></b> |
| <b><i>2.4 Lift-off</i></b> .....  | <b><i>17</i></b> |
| <b><i>2.5 Bonding</i></b> .....   | <b><i>19</i></b> |
| <b><i>3. Inclined lithography</i></b> .....                                 | <b><i>20</i></b> |
| <b><i>3.1 Principle</i></b> .....   | <b><i>20</i></b> |
| <b><i>3.2 Different techniques</i></b> .....                                | <b><i>23</i></b> |
| <b><i>4. Materials and methods</i></b> .....                                | <b><i>31</i></b> |
| <b><i>4.1 Substrate and masks</i></b> .....                                 | <b><i>31</i></b> |
| <b><i>4.2 Photoresists</i></b> .....  | <b><i>31</i></b> |
| SU-8.....   | 31               |
| Lift-off negative resist .....  | 32               |
| <b><i>4.3 Other materials</i></b> .....                                     | <b><i>32</i></b> |
| <b><i>4.4 Lithography and process equipment</i></b> .....                   | <b><i>33</i></b> |
| Negative resist processing optimization .....                               | 33               |
| General process flow for SU-8 processing .....                              | 34               |
| SU-8 with inclined lithography (process flow used in the experiments) ..... | 35               |
| Inclined lithography tools .....  | 37               |
| <b><i>4.5 Characterization equipment</i></b> .....                          | <b><i>40</i></b> |
| SEM SUPRA 40.....   | 40               |
| Contact angle measurement setup .....                                       | 40               |

|   |           |
|---|-----------|
| <b>5. Results and discussion .....</b>                                      | <b>41</b> |
| 5.1 Negative resist optimization (maN-1407) for lift-off applications ..... | 41        |
| 5.2 SU-8 with inclined lithography .....                                    | 44        |
| Fabrication .....   | 44        |
| Bonding .....   | 46        |
| Exposure results .....  | 48        |
| Analysis of the mesh structures .....                                       | 51        |
| Contact angles measurements .....   | 54        |
| Defects and possible improvements .....                                     | 55        |
| Multiple exposure experiments .....   | 57        |
| <b>6. Conclusions and final remarks .....</b>                               | <b>58</b> |
| <b>References .....</b>   | <b>62</b> |
| <b>Table of figures .....</b>   | <b>67</b> |
| <b>APPENDIX A (Inclined exposure additional data and pictures) .....</b>    | <b>70</b> |
| <b>APPENDIX B (Scanning electron microscope) .....</b>                      | <b>73</b> |

## List of Abbreviations

|       |   |
|-------|---|
| IC    | Integrated circuit                        |
| MEMS  | Micro electro mechanical system           |
| SEM   | Scanning electron microscope              |
| PVD   | Physical vapour deposition                |
| CVD   | Chemical vapour deposition                |
| ALD   | Atomic layer deposition                   |
| DRIE  | Deep reactive ion etching                 |
| PEB   | Post exposure bake                        |
| SB    | Soft bake                                 |
| UV    | Ultra violet [light]                      |
| DC    | Direct current                            |
| MFP   | Mean free path                            |
| SVHC  | Substance very high concern               |
| MIF   | Metal ion free                            |
| PR    | Photoresist                               |
| PDMS  | Poly dimethylsiloxane                     |
| PMMA  | Poly methylmethacrylate                   |
| TMAH  | Tetramethylammonium hydroxide             |
| NMP   | N-methylpyrrolidone                       |
| PVA   | Polyvinyl alcohol                         |
| PGMEA | Propylene glycol monomethyl ether acetate |
| DQN   | Diazoquinone – Novolak                    |
| DQ    | Diazoquinone                              |

# 1. Introduction

During the early days of the microelectronics [1] the advancement of the technology started the development of a research field of its own, called microfabrication. The term refers to the science and technology used to fabricate devices with features size in the order of micrometres ( $\mu\text{m}$ ). The early development of the microfabrication technology was dragged forward by the microelectronic, which was developing fast after the invention of the transistors and consequentially the microprocessor [2].

The fast development of microfabrication was led by the semiconductor industry, with its development of new techniques. At the beginning, silicon was the most used substrate material with few exceptions like glass and some polymers. Metals were used for electrical contact, as thin films, while polymers were mostly used as photosensitive materials in the patterning processes. Nowadays, after the introduction of new materials and techniques, silicon is not the only major player anymore. Polymers, such as SU-8 and PDMS, are gaining popularity thank to their lower cost and simplicity of fabrication [3]. New technique like ALD (atomic layer deposition) are pushing the thickness of thin films down to few nm. The same old materials can now be used in different ways and the application possibilities grew to the point where microfabrication is not restricted to the electronics industry alone. A simple google Scholar search will reveal that, in the last year, the number of papers published using 'microelectronics' or 'microfluidic' in the title are roughly the same. This is showing how microfabrication is now used to fabricate devices from the most advanced microprocessors to medical analysis [4] [5] to sensors of every kind [6] [7].

The need for better resolution in the fabrication pushed for the development of polymers. The introduction of novel polymers has been beneficial for the whole field. Ultimately this led to the introduction of polymers that can also be used as structural materials to fabricate devices directly. The silicon and glass are kept only as support materials. These polymers are used extensively in the microfluidic science, where the small dimensions of the device makes possible the use of small amounts of liquids (nano or even picoliters). Medical and biological applications benefitted greatly from this and thanks to the biocompatibility of most of the polymers used. Silicon and glass are still utilized for microfluidics applications [8] [9] but they are starting to get replaced by polymers like PDMS that also presents surface properties that are easily tuneable for a specific application [10].

The work in this thesis is mostly focused on the optimization of photoresist polymers processing and the development of the novel process of inclined lithography. Inclined lithography is an evolution of the traditional lithography technique and it uses the same principles, but with the substrate being inclined by a certain angle during the exposure. This small, but fundamental, difference is opening new possibilities for the fabrication of new and different devices that were not easy, or possible, to fabricate with traditional lithography.

An iconic example of a structure fabricated with inclined lithography can be a 3D mesh structure used as a filter or alternatively as particle splitter [11]. The mesh are fabricated inside a microfluidic channel and the device is made utilizing only SU-8 with glass as support. The advantages of inclined lithography over traditional is resting on the fact

that only vertical cylinders would be obtained with traditional lithography, making the particle splitter structure impossible to fabricate.

Starting from the examples found in the literature [12-16] my work was to develop a new inclined lithography setup and then optimize all the processing for the fabrication of mesh structures in SU-8. The fact that the inclined lithography is not a fully developed techniques makes my work significant in the development of the technology contributing to the widely availability of inclined structures.



## 2. Microfabrication

Microfabrication is the technology used to fabricate devices with features in the micrometre scale and, if the definition is broadened, we can also include nanometre structures (usually fabricated using nanofabrication). Both use the same principles and the only difference is in the final features size and precision requirements. Microfabrication techniques are used to machine bulk material, pattern thin films or to create polymeric structures using moulding techniques. The techniques used in microfabrication are presented in this section starting from the beginning of the processing, with photolithography, and ending with etching and eventually bonding after the metallization [17].

The modern microfabrication is an evolution of the techniques invented in the IC industry [18] when the same processes are adapted to different material other than silicon. Silicon has been used in integrated circuits for its semiconductor properties and the quality of its oxide but silicon is also mechanically strong with good heat conduction [19] and it is used often in many different applications. MEMS (micro electro-mechanical systems) is one of the most widely diffuse field nowadays where silicon is used for fabricating many different structures from cantilevers to mirrors to gears for micro motors and these are just few examples [20]. Sensors make use of different properties of silicon when used for light detection [6] or as a floating mass in a bulk accelerometers [7].

The advancements in the technology have made possible the creation of integrated devices using many different materials together to obtain better devices. These materials are silicon, glass, metals, polymers and, in the recent years, biological material that are added to the bulk silicon to create the integrated devices. The fact that most of the processes and the material are compatible with IC technology, sensors and other devices are often fabricated in the same wafer (and together in the same chip) with the needed electronics component in order to enhance the performances of the final device [21]. A simple example is glass bonded on top of a silicon chip to achieve protection of the sensor from the atmosphere while keeping the optical path open to the sensor [22].

The integration of polymers with silicon or glass, used as bulk or support materials, is often used in microfluidic. Combining the characteristic of all the materials can be beneficial for the final products [23]. The new properties available thanks to physics of fluid in the microscale [24] [25] can now be tackled using the wide range of techniques in microfabrication. However every materials still maintains its own advantages. Beside cost and biocompatibility in some cases, another big advantage of polymers over glass or silicon is that they can be easily bonded together at low temperatures.

Glass still presents many of the same features of polymers and it is still widely used for similar applications [26]. The fragility and the lack of photosensitivity can be big limitations. Added to this is the fact that polymers are fabricated with less expensive tools [27] with good reproducibility it is not a surprise that the use of polymers is steadily increasing in microfabrication.

Polymers are processed either using direct lithography patterning when they are photosensitive (the resist solution contains some photoactive compound while the resin

forming the structures does not react with light) or by moulding using a master (typically made of SU-8 or silicon). An example of moulded polymer is PDMS (poly dimethyl siloxane), an elastomer, that can replicate with good precision even complicated patterns on the mould [28] down to nm sizes [29]. On the contrary photosensitive polymers are patterned directly using UV light and a mask [30]. These polymers are used to the direct fabrication of devices.

## 2.1 Lithography

The fabrication of devices with micro or nanometre sized feature cannot be practically done by directly machining the substrate due to the small dimensions of the features. Few exceptions exists but they are not developed enough to be relevant [31]. Because of this, a way to transfer a pattern from a mask to the substrate is needed.

The pattern is first transferred to a photosensitive polymeric resin that can be patterned shining ultraviolet light through the mask with the pattern on it. The exposed areas in the resist will undergo a chemical change and, after development, only the needed pattern remains on the substrate. The open areas are now leaving access to the substrate so that further processing can be carried out while the areas with resist on top will be protected. Removing (or adding in some cases) selectively material from the substrate is the way to transfer the pattern from the mask onto the substrate (Fig. 1).

To summarize the process:

1. *The pattern is designed with a CAD software and, if needed, transferred on a mask*
2. *The resist is spinned on the substrate*
3. *The pattern is transferred to the photosensitive polymer either using the mask or by direct writing*
4. *The polymer is developed with a specific solution so that only the necessary areas remain on the substrate*
5. *The area that are unprotected by the polymeric resin are open to further processing such as etching of the underlying layer, surface modification or deposition.*

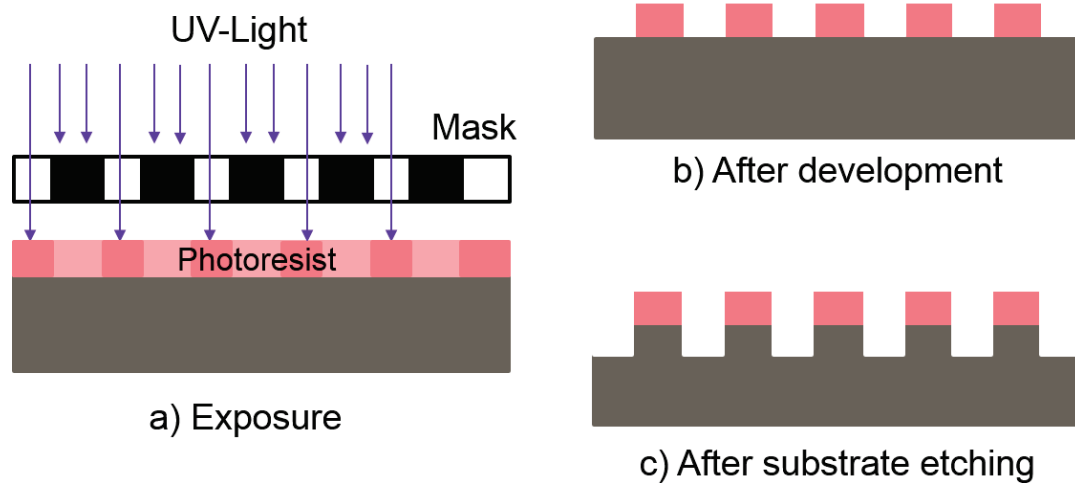


*Fig. 1 Fabrication of a device using a single step lithography and a positive tone photoresist. a) Exposure of the resist through a mask, b) Development of the resist will dissolve away the exposed areas, c) The substrate is etched only in the areas non protected by the resist.*

There are two different ways available for the exposure of the photoresist. The first consist in using a beam (laser, ions or electrons) to write the pattern directly on the photoresist exposing only the needed area. The other rely on a mask, where the pattern is previously drawn, that let the light to get to the photoresist only through the open areas. Each method present both advantages and disadvantages among which speed of processing and resolution of the pattern can be considered the most important.

While direct writing is slow and can expose only one sample the design of the pattern can be varied between samples making this the ideal method for testing different patterns [32]. The resolution of the pattern is fixed by the physical dimensions of the writing beam. Laser writing is limited to some  $\mu\text{m}$  while electron beams can draw feature as small as few nm.

The use of photomask, on the other end, makes the exposure of multiple samples cheaper and substantially faster. The pattern is transferred during one exposure that transfers the whole pattern at once. The mask can then be reused again to expose another sample. The disadvantages of the photomask are the opposite of the ones of the direct writing, masks are usually expensive and the pattern cannot be modified once written on the mask. Masks are generally used for pattern that are tested already and are ready for batch production. Masks are typically made of glass transparent to the UV light. The dark areas on the mask are coated with a Chromium layer that is reflective on one side and non-reflective on the side in contact with the photoresist. The resolution of glass masks is limited by the one of the direct writing technique used to process them.

The exposure of the photopolymer is done using a mask aligner that provides the UV light utilizing a filtered mercury lamp (to eliminate the deep UV part of the spectrum). The equipment is composed by different parts, depending on the complexity of the machine, with the basics being the UV light source, a mask holder and a wafer holder. In this way simple single exposure lithography can be performed (only one pattern can be transferred on the substrate).

When the fabricated devices become more complex the process will need multi-layered structure, each one of them requiring an exposure step. In this case the different patterns need to be aligned to the previous one. The necessary parts are added to the mask aligned so that the wafer can be moved relatively to the mask so that the two patterns are aligned. Aligning the mask to the pattern on the back side of the wafer is also possible.

The photosensitive polymer used to transfer the pattern is called photoresist. Photoresists are divided into two categories, positive tone resists and negative tone resists. The composition of the two kinds of photoresist is different resulting in different behaviour of the resist after exposure. Positive tone resists are insoluble in the developer when unexposed and the light will catalyse reactions that will increase the solubility of the exposed areas by an order of magnitude. When the resist is developed the exposed areas will be removed from the wafer at a much faster rate compared to the unexposed areas. The opposite situation is happening in a negative tone photoresist with the light catalysing the polymerization of the resist so that the exposed areas will be insoluble in the developer and will remain on the wafer after development.

As visible in Fig. 2 the other difference between the resist tones is the sidewall slope. The positive resist will generally result in positive sloped walls with straight walls possible thanks to optimized resist formulations and processing [33]. The walls in a negative resist will commonly have negative sloped walls. The reason of this behaviour is again visualized in the Fig. 2.

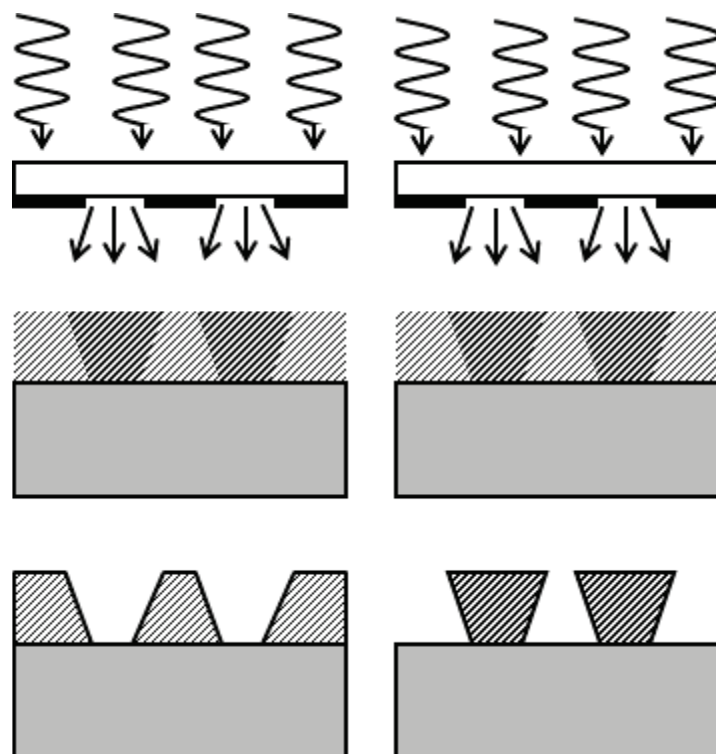


*Fig. 2 Difference between the positive tone resist on the left and the negative resist on the right. After development the exposed areas will be removed in the positive resist resulting in positive sloped walls while in the negative resist the exposed areas remain with negative sloped walls. From [20]*

The top layer of the resist will receive a higher light dose resulting in a V shape in both cases. Then the fact that the developer will remove the exposed resist or not will cause the difference in the walls slope. Every resist has its own optimal exposure dose that will provide the best results. The exposure dose is the measure of the light energy per area reaching the sample ( $\text{mJ}/\text{cm}^2$ ) and it is calculated multiplying the power of the UV lamp (mW) with the exposure time (s).

The general photoresists solutions are composed of a resin (typically Novolak resin), a photo initiator (Diazquinone for positive resists and a photoacid generator for negative ones) and an organic solvent. The resin is the component that forms the structures and it is dissolved in the solvent to keep it liquid during the processing. The optically active compound (photo initiator) is added to provide the light absorption properties to the resin. The processing starts with liquid resist that can be spun on the substrate. After the spinning the solvent is evaporated to obtain the solid resist layer. The thickness of the layer is mainly dependent on two variables: the ratio resin/solvent in the starting solution and the spinning speed. The faster the spinning the thinner the resist layer will be. The resist formulation determine the thickness range that can be achieved with different spin speeds. The time of the spinning is also determining the final thickness but it is not as critical as the speed.

### Positive photoresists

In the positive tone resists the chemical reaction induced by the UV light is weakening the polymer by scission or breakage of the molecular chains. This render the exposed resist more soluble to the developing solution (10 time more soluble when exposed). The dark areas on the mask will transfer on the resist layer.

There are two main class of positive resists, single component PMMA (poly methylmethacrylate) and the two-component DNQ (diazquinone ester DQ and phenolic novolak resin N).

PMMA is the oldest photoresist in use. It is a slow photoresist with a required dose of  $>250\text{mJ}/\text{cm}^2$  and sensitive at low  $\lambda$  (below 240nm). Its light sensitivity can be increased with the addition of a photosensitizer (t-butyl benzoic acid) and the required exposure dose is reduced to  $150\text{mJ}/\text{cm}^2$ . PMMA is, nowadays, used in electron beam, ion beam and x-ray lithography.

DQN based resist are the most widely use positive resist nowadays. They are sensitive to the 365-, 405-, 435nm mercury lines and highly alkali soluble (when exposed) thanks to the photochemical reaction that transform it to a polar product [34]. The main component of the photoresist is the Novolak resin. The Novolak is normally soluble in alkaline solutions but is rendered insoluble by the addition of the DQ (20-50 %wt) that is working as both solubility inhibitor and photoactive compound. When DNQ based resists are exposed to the UV radiation the DQ molecules in it are transformed into carbenes that rearrange into ketones. The ketones react with the water present in the resin becoming indene acid. The solubility inhibition of the DQ is removed and the Novolak resin is again soluble in basic solutions (developer). The indene acid makes the resist hydrophilic and aqueous solution easily wet it. During the reaction  $\text{N}_2$  gas is released making the exposed area foamy so that the developer reaches the bottom of the resist layer easily. In addition the novolak resin is absorbing the light below 300nm

so the long chains are broken during exposure, helping the dissolution of the exposed resist.

### Negative photoresists

In negative tone resists the UV radiation will promote the polymerization of the resist rendering insoluble the exposed areas. The light areas in the mask will be transferred on the resist layer.

Two ways are available to achieve polymer insolubilization. Either the UV light increase the material molecular weight through the formation of longer polymer chains starting from the soluble monomers or, the material is rendered insoluble by photoreactions that form new insoluble products. In the latter case also the hydrophobicity or hydrophilicity can be modified to introduce preferential solubility of unexposed resist.

The polymerization of the resist is the method used in the old type of negative resist and it is still widely used. The polymerization is started during exposure but a post exposure bake is required to promote the complete polymerization of the exposed areas. The light shined on the resist could not be sufficient to expose the layer all the way to the bottom. This is particularly problematic when processing thick resist layers. The photons arriving on the resist layer are absorbed by the top layer first and less photons will reach the bottom of the resist. The time of exposure needs to be increased or, when needed, this behaviour can be used to emphasize the V shaped walls of a negative resist.

### SU-8

SU-8 is a negative tone photoresist mainly used as a structural resist due to its good mechanical and optical characteristics. It is composed of Bisphenol A Novolak epoxy (Fig. 3) dissolved in an organic solvent (gamma butyrolactone GBL or Cyclopentanone depending on the formulation) and up to 10 wt% of mixed Triarylsulfonium/hexafluoroantimonate salt [35]. The amount of solvent determines the viscosity of the

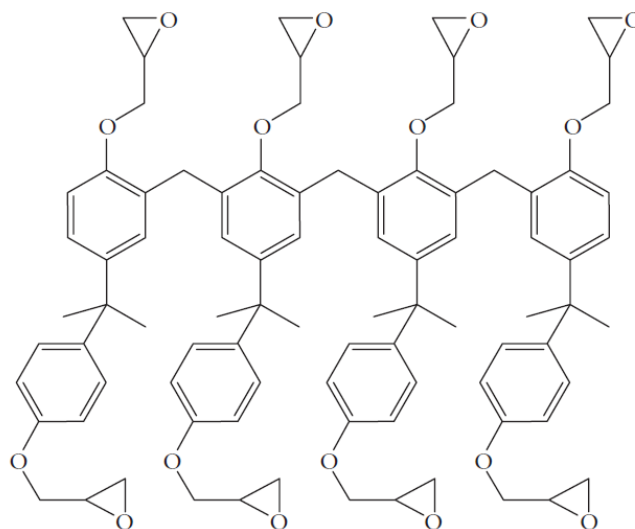


Fig. 3 Chemical formula of the Novolak resin, main component of SU-8.  
From [53]

material (hence the range of available thicknesses) while the salt act as photoacid generator.

SU-8 belongs to the family of chemically amplified resists thanks to the fact that a single photon can generate a cascade of polymerization reactions in the resin [36] [37]. The light irradiation activates the photoacid compound that creates a low concentration of a strong acid (hexafluoroantimonic acid) that protonates the epoxides on the oligomer. The protonated oxonium salts are then reacting with the neutral epoxide sites on other oligomers in a series of cross-linking reactions catalysed by the temperature during the post-exposure bake step. Every oligomer in the resist has eight epoxy sites (from here the name SU-8) so the high crosslinking degree in the exposed areas is possible making the cured resist mechanically strong [38].

Lithography of SU-8 follows the traditional procedures used for most resists with a more control of the baking steps. The spinning is done usually in a cover spinner to maintain the condition as stable as possible during the solvent evaporation. Most of the solvent that remains after the spinner is evaporated during the soft bake. The baking is performed rising the temperature slowly, and through steps, to get to 95°. The time of this step is dependent on the layer thickness. The temperature is then brought back to room temperature with a slow ramp down. This phase is critical because lower temperature or shorter time would leave high solvent content and this will introduce high stresses in the next baking step. A temperature higher than 137°C will initiate thermal crosslinking of the unexposed resist rendering the material useless for lithography [37]. The exposure is performed utilizing a suitable exposure dose for the resist thickness. After exposure the sample has to be baked in order to improve the crosslinking all the way to the bottom of the resist layer. The post exposure bake is a critical step (as the pre bake) since, due to a non-ideal temperature ramping, high stresses are introduced in the material when all the solvent is evaporated [39].

Cured SU-8 has excellent chemical and thermal resistance thanks to the high degree of crosslinking. The glass transition temperature is >200° C while it degrades at temperature around 380°C. The mechanical properties are good too with a Young module of 4-5 GPa [37].

In the market several different SU-8 are available. The company “Microchem” is producing different products with some differences in the chemical composition. Table 2 presents the different chemical composition of the SU-8 available from the company. The number of the resist refers to both the series and the thickness range achievable. The SU-8 50 and SU-8 2050 will have different composition but similar thicknesses at the same spin speeds.

The different additives in the resist are influencing its properties. The additional substances added to the SU-8 3000 are helping with its adhesion to the substrate and with reduced stresses. This is not always critical so if the adhesion is not an issue in the processing the use of the cheaper SU-8 2000 may be beneficial while obtaining similar results.

|                          | Thickness range ( $\mu\text{m}$ ) | Resin   | Solvent                      | Additives   |
|--------------------------|-----------------------------------|---|------------------------------|---|
| <b>SU-8 50</b><br>[35]   | 1-100                             | Epoxy   | Gamma Butyrolactone (22-60%) | Propylene Carbonate (1-5%)  |
| <b>SU-8 100</b><br>[40]  | 80-250                            | Epoxy   | Gamma Butyrolactone (22-60%) | Propylene Carbonate (1-5%)  |
| <b>SU-8 2000</b>         | 1-350                             | Epoxy<br>Formaldehyde polymer (1-30%)<br>Cycloaliphatic epoxy (1-30%) | Cyclopentanone (20-60%)      | Propylene Carbonate   |
| <b>SU-8 3000</b><br>[41] | 1-350                             | Epoxy<br>Formaldehyde polymer (1-30%)<br>Cycloaliphatic epoxy (1-30%) | Cyclopentanone (20-60%)      | Propylene Carbonate<br>Polyglycidyl ether<br>Silane<br>Surfactant |

#### Lift-off negative resist (ma-N 1400)

The ma-N 1400 series photoresist is a high performances negative resist that is optimized for lift-off applications. The resist is design to result in negative sloped walls of the pattern and the lift-off will give good results if the metal layer will not be more than a third of the resist thickness. The negative slope will prevent the metal to deposit on the wall of the resist thus making the removal of the resist possible.

The ma-N 1400 is an aromatic bisazide/novolak resin based resist not chemically amplified (Fig. 4). The reaction mechanism is radically based with one electron starting one chemical reaction. The exposed resist will polymerized upon exposure with the molecular weight also incising slightly.



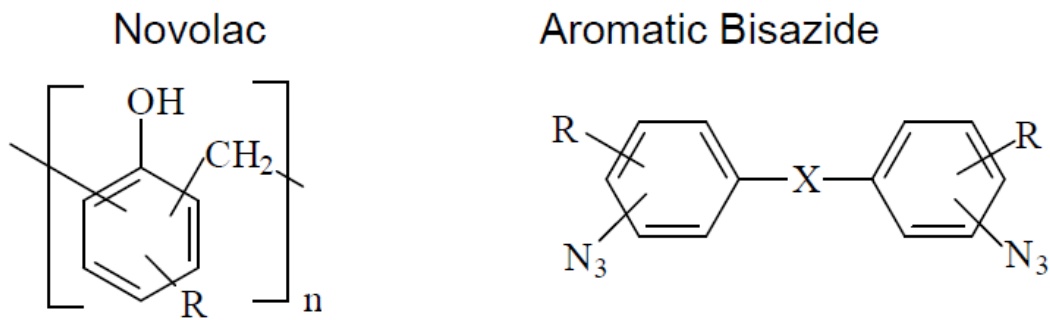


Fig. 4 Components of the ma-N 1400 series resist. The Novolak is the main component of the resist while the Aromatic Bisazide is the optically active one.

The structural properties of the resist such as viscosity, layer formation, temperature stability and etching stability are provided by the Novolak resin that is the principal component of the resist. In order to make the resist UV light sensitive, the photoactive aromatic Bisazide is added. This molecule will determinate the adsorption sensitivity and exposure wavelength of the resist. The solvents added to the Novolak are 2-methoxy-1-methylethyl acetate (PGMA) and Anisole ( $C_7H_8O$ ) and they will contribute to the viscosity and solubility of the resist determining the bake/drying parameters.

The chemical reactions that are initiating the polymerization of the novolak resin are started by the UV exposure of the resist (Fig. 5). This will activate the nitrenes groups in the bisazide (photoactive compound) that will then reacts with the Novolak resin that will start polymerizing forming the products with increased molecular weight (Fig. 6). The areas where the polymerization takes place are then insoluble in the developer giving the ma-N its negative characteristic.

### Generation of nitrenes

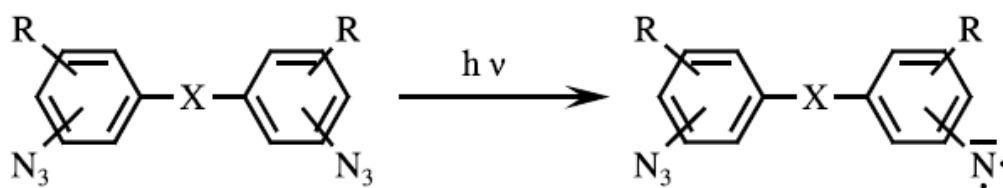


Fig. 5 Generation of nitrenes during the exposure of the resist. This reaction is the starting point of the polymerization of the novolak resin.

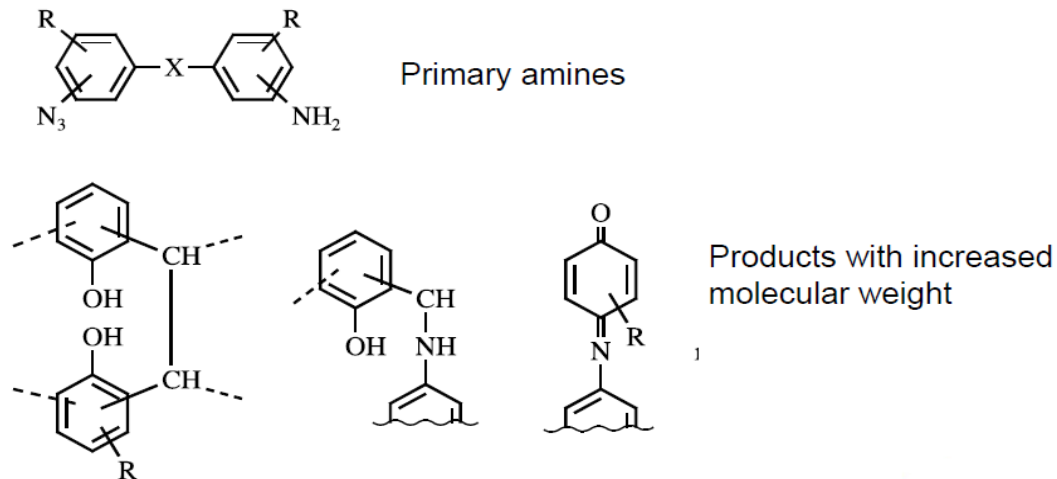


Fig. 6 After the Aromatic Bisazide is activated it will promote the polymerization of the Novolak resin resulting in higher molecular weight compounds.

With this resist, adjusting the time of development, it is possible to control the degree at which the negative slops will results. The resist is polymerized already during exposure and the light is absorbed before in the top layers of the film while less light will reach the bottom layers. The polymerized Novolak resin will also absorb some of the light. This will cause the bottom layers to receive lower dose and thus be less polymerized, compare to the top layer. The unexposed resist is soluble in the solvent while the polymerized is not (or very little). The bottom layer is not completely polymerized (when using an adequate exposure dose) so it will be eroded with a higher rate than the top layer. For these reasons the exposure is still a critical step but the slope of the walls is controlled mostly by the developing time. If the sample is overexposed than the UV light dose will be enough for the polymerization of all the resist thickness and the slope of the walls cannot be controlled tuning the developing time. The soft bake temperature (and time) will also impact the developing rate of the resist with higher temperatures making the resist less soluble in the developer.

The control of the inclination of the resist's walls is possible by the particular behaviour of the resist that differs from the one of traditional negative resists. Usually, in resist such as SU-8 the light starts the polymerization and the subsequent PEB is polymerizing the whole thickness. Underexposure in traditional negative resists will not affect the inclination of the walls.

## 2.2 Metallization

Metals are extensively used in Microfabrication for all kind of applications ranging from electrical contacts to structural functions and masking layers. They are mostly deposited as thin films on top of the substrate or on structures already present on the wafer. When a metal is used as conductor layer its thickness is usually in the range of few hundreds on nanometres while, if used as adhesion layer, the thickness will be much smaller, in the order of few tens on nm. Thicker layers, in the order of micrometres, are also used if the bulk characteristics of the metal are needed (thin films' physical properties differs

from the one of the bulk material and some of these properties are layer thickness dependent e.g. optical properties).

Metals, generally, cannot be directly patterned using lithography for the obvious reasons that they are not photosensitive. A chemical solution or gases in combination with atom bombardment are used to remove the metal from all the exposed areas. These solutions are called etchant and they are specifically design for the etching of a certain metal. Some techniques are available for patterning metal layers directly removing material using a focused laser beam to "draw" the pattern in the layer (e.g. laser ablation [42]).

Many depositions techniques are available and each one of them offer some advantages while carrying some disadvantages. Following is a brief list of the deposition techniques that are more relevant for the work carried out in this thesis. Not all the techniques presented are used only for metals but some of them are mainly used to deposit other layers such as oxides and organic materials used in Microfabrication.

### PVD (physical vapour deposition)

The basic idea of PVD is to physically remove material from a source made of the material that is needed (the target) and transfer it on the substrate where it will form the film. The process can be done using both thermal and kinetic ways to remove material from the target dividing the PVD techniques in two categories: Evaporation and Plasma techniques.

#### Evaporation

This techniques is based on the thermal evaporation of the target material. The evaporated atoms travel from the source to the sample with low kinetic energy deriving only from the thermal energy (the temperature of the deposited layer is basically room temperature) and a good vacuum is needed to avoid collisions during the travel. High vacuum ( $\sim 10^{-7}$  Torr) or ultra-high vacuum ( $< 10^{-10}$  Torr) is used so that the evaporated atoms have a mean free path (MFP) longer than the chamber dimensions (distance target-substrate). The high vacuum ensure also that gases that could contaminate the film are not present (or in negligible amount) inside the chamber. Evaporation is used mostly for metals but also other materials can be deposited by this techniques. Alloys and composite compounds are problematic since high vapour pressure materials evaporate faster than low vapour pressure materials. If an alloy is composed of two elements with very different vapour pressure the resulting deposited film will have a composition that differs a lot from the original alloy composition.

Metals with relatively low melting point can be evaporates simply with direct heating of the crucible. When we have to evaporate refractive materials we need to use an electron beam that is focused on the material and provide enough energy to evaporate the atoms. The electrons can transfer higher energies (high voltage is used to accelerate the electrons, 10-20kV and the electron beam gun is operated at 10-50kW up to 150kW) to the target's atoms and therefore evaporate high melting point materials [43].

The fact that the atoms are thermally evaporated gives them a perpendicular direction when the leave the target. The long MFP allows them to travel in a straight line so that this techniques produces very directional films [44]. The film deposited with an

evaporator are high quality and with low defects. The deposition rate of the evaporation can be quite high but it can also be as low as few Å per second. Thanks to this films of few nm can be deposited with a great thickness control.

### Sputtering

Sputtering is maybe the most used techniques for the deposition of thin films [45]. A wide range of materials can be deposited by sputtering among which metals, alloys and oxides are the most common. Sputtering is based on a simple principle: a plasma discharge is created in the chamber when a voltage difference is applied between the target and the substrate. The positively charged atoms present in the plasma are accelerated towards the target by the potential difference and hit the target material with a certain kinetic energy that depends on the voltage applied and the pressure in the chamber. The impact of the ions generates sputtered atoms from the target that fly (with a certain angle) toward the substrate where they deposit on the surface creating the film. The energy of this atoms influence the properties of the deposited film for example when the pressure is low in the chamber the sputtered atoms have higher MFP therefore higher speed so the resulting film is denser than one deposited at higher deposition pressure.

The pre deposition vacuum is also very important in particular when a reactive gas is used during the deposition to deposit oxides or nitrides since unwanted gases present in the chamber will contaminate the deposited film. For this reason sputtering machines work at high vacuum and ultra-high vacuum usually achieved with the combination of a mechanical pump, to reach the rough vacuum, and then a turbo pump that brings the vacuum to values  $<10^{-5}$  Torr. The atoms have a MFP shorter than the chamber dimensions. This is due to the fact that the pressure during the process is relatively high (around  $10^{-3}$  Torr) and the atoms have enough kinetic energy to arrive on the substrate even after several collision. Notice that this makes the sputtering a non-line-of-sight technique.

One of the most significative differences between sputtering and evaporation is that evaporated film are very directional with almost no cover of vertical walls while with sputtering that is almost impossible to achieve. On the other hand sputtering is a more performing technique when it comes to deposition speed and simplicity of the process without forgetting the reactive deposition possibility. Sputtering machines can also be completely automatized, something that is not possible with other techniques such as evaporation.

There are three main sputtering techniques: Diode sputtering, magnetron sputtering and rf-sputtering (radio frequency) [45].

The basic idea is to have two conductive plates in a vacuum chamber connected to a power supply. In one of the two we have the target (composed of the material we want to deposit) and in the other one we have the substrate and they are cathode (-) and anode (+) respectively. An inert gas (usually Argon) is introduced in the chamber after the high vacuum is reached. When a voltage is applied between the two plates and its intensity is greater than the threshold breakdown voltage a plasma discharge is formed and charged atoms from the gas are driven to towards the cathode. The impact of the atoms on the target material will sputter it in the direction of the substrate where it will

form the desired film. The electron in the plasma are ionizing the gas atoms but after that they are attracted by the anode or the grounded walls and they are lost. Because of this the ionization rate of DC diode sputtering is not very good. More complicated but for that more efficient system are normally used.

In order to improve the plasma density in the DC generated plasma the electrons needs to be confined in the vicinity of the target. To achieve this, in the 1970s, the magnetron source was developed. It uses a magnetic field to trap the electron in the vicinity of the magnetron where the target is located [45]. In this way we have the plasma concentrated on the surface of the target and the electron are not lost so the plasma is self-sustained. The operation pressure of magnetron sputtering systems is usually between 1 mTorr and 10 mTorr. The magnetic field produced by the magnetron is engineered so that the field lines will be parallel to the substrate surface so that the drift force  $\mathbf{E} \times \mathbf{B}$  (the  $\mathbf{E}$  is perpendicular to the surface as in the normal DC diode sputtering) will confined the electron in cycloidal orbits parallel to the surface maximising the ionising collision with the plasma's gases.

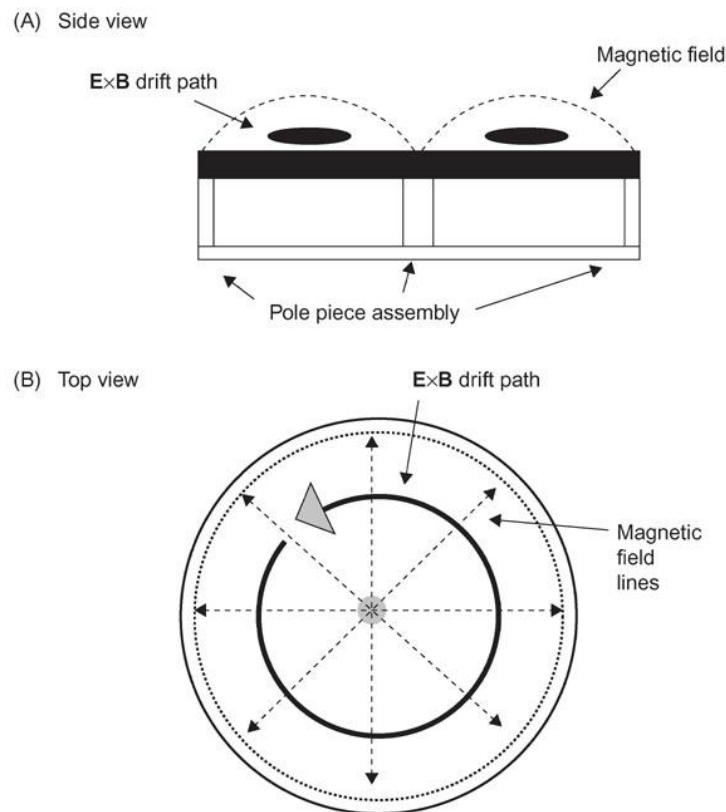


*Fig. 7 Magnetic and electric fields in a magnetron. a) The magnetic field is going from one magnet to the other and it is perpendicular to the electric field at half of the magnets distance creating the  $\mathbf{E} \times \mathbf{B}$  drift path where the electrons are confined. In b) the drift path can be notice in its spiral motion over the target.*

As shown in Fig. 7 the magnetic field has the nodes in fixed positions and the maximum plasma concentration is thus also fixed. In this configuration the sputtering impacts will happen in a fixed region of the target, where the fields are stronger, eroding it non-

uniformly. To optimize the erosion the magnet of the magnetron can be rotated during the process so that the area of high density will be spread across the surface of the target. One of the big plus of the magnetron source is that the magnet configuration can be adapted to the substrate we need to coat [46].

Sputtering systems can also be used in reactive mode where some reactive gas are introduced during the deposition making possible to deposit compounds films like metal nitrides or oxides [47]. To obtain some specific plasma confinement or to bring the plasma to the sample (cleaning of the surface during deposition) the configuration of the magnetic field is changed so that some of the electrons will not be confined in the vicinity of the target. All this different configurations makes sputtering a vital technology in the field of Microfabrication since it can deposit almost all the needed thin films.

#### CVD (chemical vapour deposition)

Chemical vapour deposition is a technique that uses chemical reaction at the surface of the sample to deposit a certain material. The reaction is happening in gas phase and the material that we want to deposit is present in the precursor molecules. These molecules are inserted in the chamber and the hot temperature (300°C usually) is decomposing it on the sample's surface. The film material is then chemically attached to the surface and the film grows.

#### ALD (atomic layer deposition)

Atomic layer deposition is a technique that is similar to CVD but has the advantage of depositing one atomic layer at the time. The deposition is pulsed meaning that the precursor is flowed into the chamber and it reacts with the surface of the sample until the layer is formed. At this point no more reaction will happen and the chamber is flushed with inert gas. The cycle is then repeated to deposit the next layer. The conformity of the deposition is excellent and the extremely good control of the layer thickness are the big advantages of this deposition technique. Multilayers of different materials are simple to deposit also with ALD.

## 2.3 Etching

The word etching refers to the group of techniques used to remove a specific material from the substrate. If used after a lithography step, etching, can transfer a pattern any layer on the substrate as long as a suitable etchant exists (see Fig. 1). Etching solutions (liquid or gas) are mostly material specific and they etch selectively the material or a group of material. When the sample is placed in the etchant solution (or in the etching machine if the etchant are in gas form) the areas exposed to the etchant will be removed. The areas protected by the photoresist layer will remain unaffected.

The etching techniques are divided into two big categories: wet and dry etching. As the name suggest the wet etching makes use of liquids solution as etchants while dry etching is using either gasses or kinetic forces (accelerated ions hitting the target and sputtering the material away) or a combination of the two.

Wet etching is generally characterized by being isotropic meaning that the etching will proceed at the same speed in the vertical and in the lateral dimension. The result is the undercut of the etched layer under the masking layer. There are example of anisotropic

wet etching done on metals for example but this is not a common technique [48]. Metals are usually etched using wet etching techniques due to the fact that those are, most of the time, the easiest and cheapest. If very small features, in the order of the thickness of the layer, are to be produced the anisotropy of wet etching may cause problems. When a layer with a thickness of 100 nm is wet etched the same amount of material will be removed from the vertical and lateral dimensions. The under etch under the masking layer (lateral dimension) will be 200 nm (100 nm from each side) when the vertical etching will go through the whole 100 nm layer. This phenomena is a limit to the minimum feature size achievable with wet etching.

Silicon wet etching is a particular case due to the monocrystalline form in which the silicon is used. Using the difference in etching rate between the different crystal planes, particular shapes are obtained. Anisotropic etching can be performed using liquid etchant such as KOH and TMAH (Tetramethylammonium hydroxide) [20]. When a silicon wafer with orientation [100] is etched with KOH the [111] plane has a lower etching rate (0,004:1) compared the [110] plane. The etching will proceed in the [110] direction faster than in the [111] while, at the bottom of the etched area, the [100] direction is etched at a rate roughly half of the [110]'s. The angle between the bottom and the walls will always be  $54,7^\circ$  due to this situation. Orienting the pattern different angles with respect to the wafer flat (representing a specific crystallography direction of the monocrystal) many different structures can be fabricated. Since the walls will never be straight using wet etching of silicon the only way to obtain vertical walls is to use dry etching methods.

Dry etching is used mostly for anisotropic etching in order to get straight walls in the structure [49] using DRIE (deep reactive ion etching) [50] or other techniques like Bosch process [51]. When using  $\text{XeF}_2$  vapour to etch silicon [52] the walls of the structure will result similar to the one from wet etching. Not all the dry etching techniques are anisotropic. Most of the material will need its specific etchant that will etch the material isotropically or anisotropically.

## 2.4 Lift-off

Lift-off is a techniques that uses the resist as a sacrificial layer to pattern a layer (usually metallic). The idea is to spin and then pattern a photoresist layer before the deposition of the layer. After the deposition on top of the patterned photoresist the layer will cover both the resist and, in the open regions, the substrate. When the resist is dissolved away, using acetone or a proper resist removal solution, the material on top of it is also removed. The final result of Lift-off is the same as the etching since, in both cases, only the necessary areas of the layer will remain on the substrate with the way this result is achieved being somehow opposite. The metal layer is patterned with no etching necessary (Fig. 8).

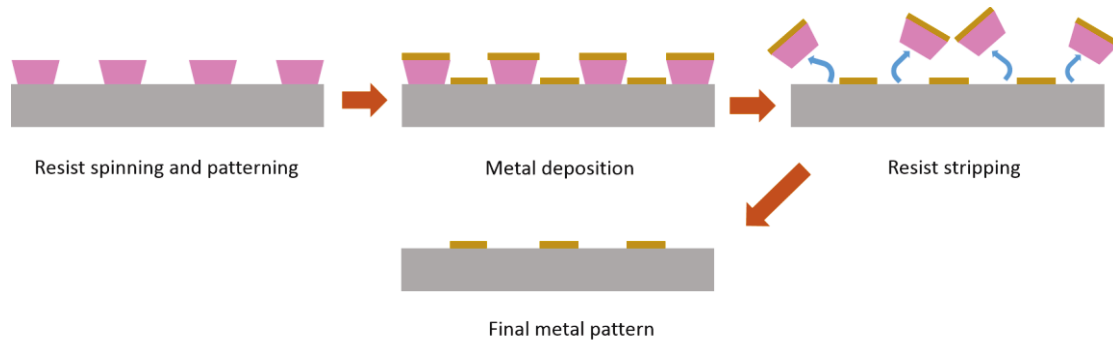


Fig. 8 Lift-off processing work flow. The resist used is negative tone to obtain the V shaped walls that will help the stripping of the resist using acetone or a proper resist stripping solution.

The use of lift-off makes possible to pattern metals or other materials that would otherwise be really hard to etch. Sometimes the etching step would result in non-optimal definition of the pattern or in limited resolution. On top of that the etching time needs to be timed right in order to avoid over etching of the layer. The timing is not always precise enough when the fabrication requires small structured to be patterned. The elimination of the etching step gives to the lift-off techniques high importance in many application (mostly in the research applications).

In order to achieve good results the resist layer must be at least 4-5 times than the metal thickness (lift-off is mostly used for metal patterning) to avoid the metal deposition on the vertical walls. Thicker resist layers are less sensitive to non-directional deposition but, on the other hand, a thinner layer is beneficial for the precision of the patterning. If the side walls of the resist are coated, the remover will have difficulties to penetrate everywhere making the dissolution of the resist impossible or not complete.

In order to avoid the side walls coating, while still maintaining a good precision in the patterning, we need to make use of a characteristic of the negative tone resists. The tendency of negative resist is to have negative shaped walls (V-shape) with resists like the ma-N 1400 optimized for enhancing this behaviour. These resists works so that the dark erosion of the resist is dependent on the exposure dose. Dark erosion refers to the rate at which the exposed resist is developed away compared to the un-exposed one. All positive resists exhibit dark erosion while, usually, negative ones are immune to it due to the high degree of polymerization of the cured resin.

Lift-off resists are negative resist with a certain dark erosion rate that depends on the soft bake temperature together with the exposure dose. The higher the temperature the lower the dark erosion with the same behaviour at high exposure doses. The final goal of the lift-off resist is to obtain V-shaped walls and for that the resist's top layer will need to receive a higher dose than the deep layer. The exposure needs to be optimized so that the bottom layer will receive enough dose and the optimization is anyway done in conjunction with the developing time.



## 2.5 Bonding

With bonding is intended the process used to bond together two or more layers. They can be made of the same or different material. Bonding is used to fabricate a more complex, multi-layered devices or to encapsulate parts of them. There are three main bonding techniques: Anodic, Fusion and adhesive bonding.

The first method uses relatively low heat (between 180 and 500°C) and voltage (200 to 1000V) to bond sodium rich glass and silicon together. The real bonding mechanism is not yet fully understood but the best explanation suggest that the migration of sodium from the glass towards the cathode (the silicon layer) leaves negatively charged empty spaces in the glass. Since a voltage is applied, the two layers are pulled together by the electric field and the high temperatures. The result is the formation of strong and durable covalent bonds at the interface between silicon and glass [53].

When two silicon surfaces needs to be bonded together the fusion bonding techniques comes into play. It is based on the chemical reaction between the OH groups that are found in the native or the grown oxide layer over the silicon surface. The bonding is actually happening between two oxide layers, not directly between the silicon. The two wafers are brought into intimate contact using pressure and the temperature is raised up to 800°C. The bond is completed in some tens of minutes. The requirement for a good fusion bond are strict, the surface roughness must be in the order of few nanometres compared to micrometres in anodic bonding. Furthermore the high temperature is also preventing the use of this techniques if delicate IC component are present in the wafer. Again, the working principle of the process is not fully understood but the polymerization of the silanol bonds on the oxide surfaces seems to be the best explanation [53].

The third bonding technique is based on the use of polymers as bonding layer and it can also be used to bond different polymeric layers together. The polymers are typically UV sensitive and they can be patterned by lithography before the bonding. Channels can be fabricated and then a polymeric capping layer can be bond on top of them to close them. The advantage of using polymers as bonding material can be seen when using both traditional materials like glass, silicon or metals and when bonding all polymeric structures. Polymers can be used to bond almost any material to another and the surface roughness requirement is very relaxed since the polymer will adapt to the irregularities. Bonding is also the way to go when a full polymeric chips is fabricated. More information about all these techniques are found in [53] [20]

## 3. Inclined lithography

### 3.1 Principle

The basic principles of inclined lithography are the same as the traditional lithography with the main difference being the fact that the sample is tilted in respect of the light source (Fig. 9). The light is coming straight from the top (the light source is not tilted) but it will expose the resist on the substrate with an angle. This arrangement makes possible the exposure of 3D structures with inclined walls so geometric shapes such as pyramids or cones are directly fabricated with a single exposure [13].

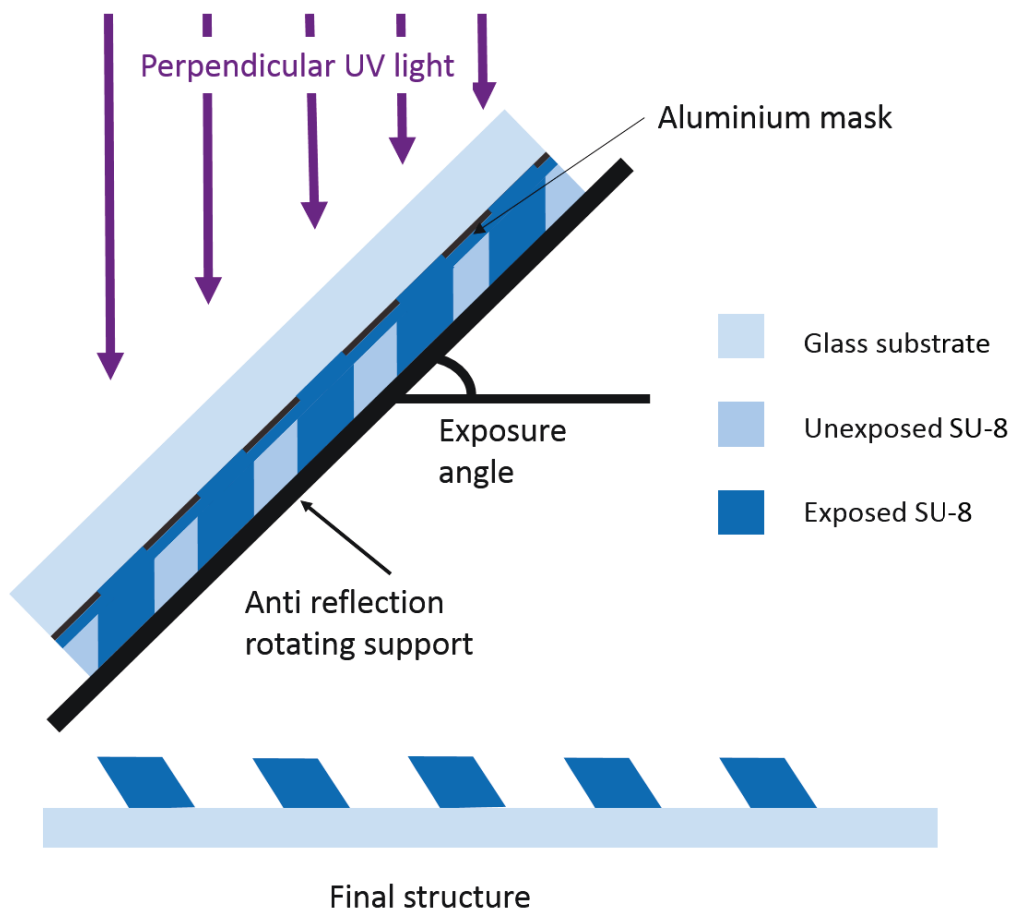


Fig. 9 Schematic of the inclined lithography and the final structure resulting from it..

The inclined exposure can be performed exposing from both sides of the wafer. If top side lithography is performed the mask needs to be on top of the photoresist layer while when back side exposure is performed the mask has to be placed on the back side of the sample. In this case, between the resist and the mask there is one additional layer, the substrate. This gap created by the substrate (that needs to be transparent) is affecting the precision of the lithography. The light has to travel to various layers with different refractive indexes. The refractions of the incident light needs to be eliminated as much as possible to obtain good results.

The optimal way to perform back side lithography is placing the mask between the substrate and the resist so that the gap is eliminated with the resist being in intimate contact with the mask. The refraction at the surface air substrate will not affect the exposure of the pattern that happens at the interface substrate-SU-8. The mask will be directly patterned on top of the substrate and, if the resist is not released from the substrate, it will be used only once, being trapped between substrate and resist. The most efficient way to utilize backside lithography is to release the PR layer after the fabrication and reuse the substrate with the mask. Even if the mask will be used only once the better precision in the fabrication is worth the trouble of getting another mask on the new substrate.

The Fig. 10 is presenting visually the difference between the exposure from the front and from the back. The PR is positive tone but the same idea applies to the negative tone resists.

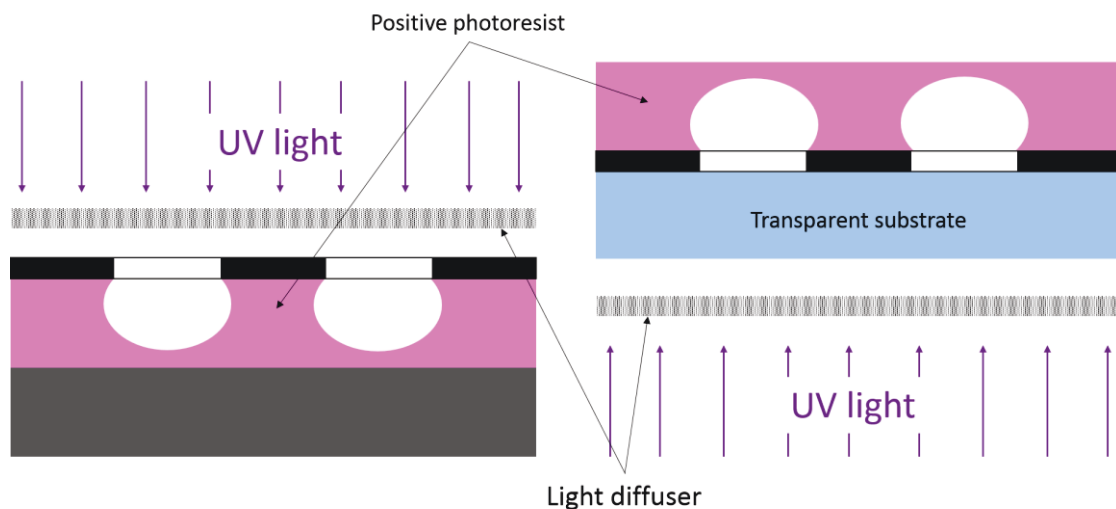


Fig. 10 Differences of the front side lithography on the left and the back side lithography on the right. On both picture the resist is positive tone and it is easy to visualize the exposed areas that are removed. When the exposure is performed from the bottom the base of the structures will be attached to the substrate. The opposite situation will happen with front side lithography. The diffuser in the picture is inspired by [66]

The setup required for the backside exposure is simpler since only a tilting support for the sample is needed. If the mask is not embedded in the sample, the setup would have to provide a support also for the mask adding complexity to the system.

Inclined exposure can be also performed while the sample is rotating. Cones are the first and easier shape that the rotation of the sample will provide. When exposing cones in the resist the difference between front and back side exposure will emerge quite strongly. The tip of the cone will be touching the substrate when exposing from the back while the opposite situation (base of the cone touching the substrate) will result when exposing from the top side. Example of the fabrication of cones, together with other structures, can be found in [13].

The exposing angle in the lithography is an important parameter together with the exposure dose since it directly affect the inclination of the walls in the structure. The refraction of the light is playing here a big role since the mask is placed after the transparent substrate (in the back side exposure) and the light will travel through that

before reaching the mask and then the sample. The refracting index of air and glass (usual material used as substrate) is different and the incoming light direction will be changed first, when going from air to glass, and again when going from the glass to photoresist. The angle of the exposed substrate will thus always be lower than the exposing angle. The relation between the exposure angle and the resulting angle in the structures when using glass and SU-8 can be found in [54]. The Fig. 11 is showing the relations between the incident angle of the UV light to the glass substrate with the final angle of the structures in the SU-8.

Snell's law will give the relations between the refractive indexes and the angles:

$$n_1 \sin \theta_1 = n_2 \sin \theta_2 = n_{31} \sin \theta_3$$

Where the  $n_1, n_2, n_3$  are the refractive indexes, as in the Fig. 11, of air, glass and SU-8 respectively and  $\theta_1, \theta_2, \theta_3$  the incident angles of the light on air, glass and SU-8 respectively.

The refracted angle in SU-8 can be obtained knowing refractive index of air and SU-8 and the incident angle of the light  $\theta_1$  using the formula:

$$\theta_3 = \sin^{-1} \left( \frac{n_1}{n_3} \sin \theta_1 \right)$$

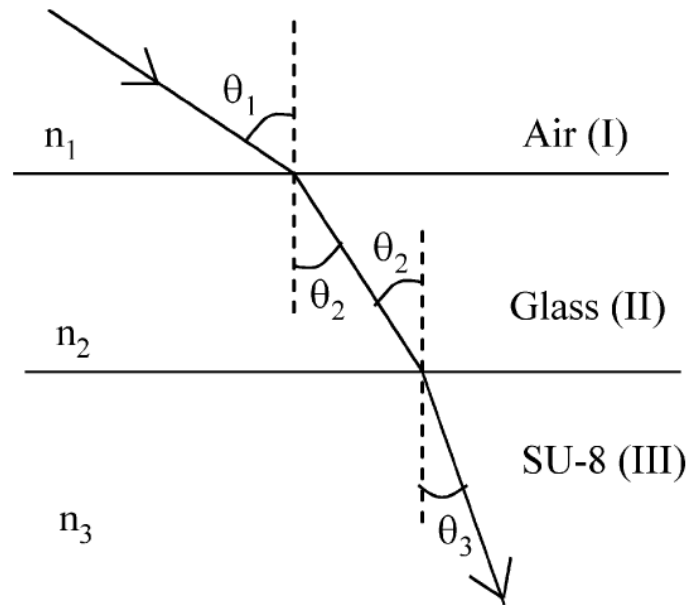


Fig. 11 Relations between the incidence angles of the UV light when refracted travelling through different materials (air to glass and finally to SU-8). From [56]

The refractive index of non crosslinked SU-8 during exposure at 365 nm before PEB is 1.67 [40]. From this data we can construct a graph (Fig. 12) showing the theoretical refracted angle of the exposed structures in relation to the exposing angle.

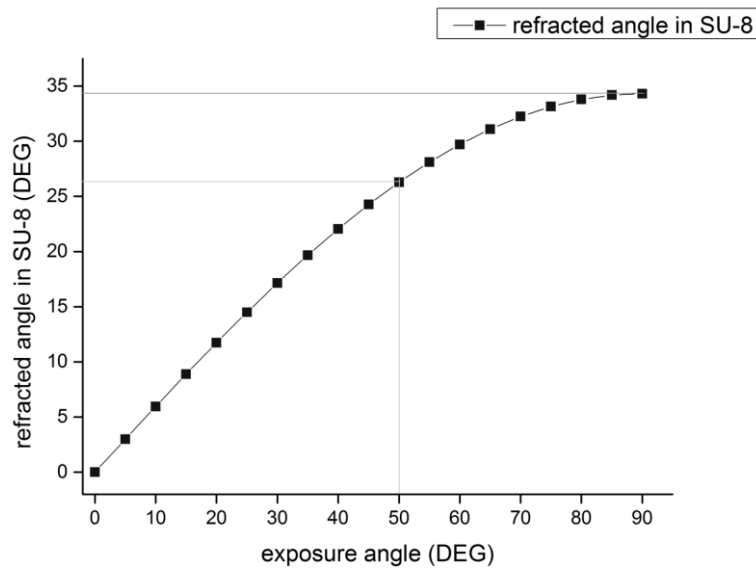


Fig. 12 Relation between exposure angle and refracted angle in the SU-8. The angle in the SU-8 is always smaller than the exposure angle and it is limited to values below 35°.

From the graph we can notice two main facts. The refracted angles in the SU-8 (the angles of the final structures) are, as expected, always smaller than the exposure angles. The other interesting fact is the limit of refracted angle that cannot be higher than 35° even when the exposure angle raised. The difference in diffraction index is creating a limiting angle for the structure's walls. The highest possible inclination for the structures is limited and some adjustments to the refractive indexes has to be made to overcome the limitation. The background material can be changed to match the glass's refracting index better than air. Using deionized water would make higher angles of exposure possible ( $n_{\text{water}} = 1,33$  vs  $n_{\text{air}} = 1$ ).

### 3.2 Different techniques

Inclined lithography is a relatively new techniques and the literature on the topic is still not so vast. The fact that the technique is in its infancy means that there is huge room for improvements. In addition the science is still focusing on the fabrication of the inclined structures more than their use. The applications of the technology are still limited because a reliable and developed technique is needed before switching to the fabrication of real devices. Today research is aimed towards the investigation of the different ways the inclined lithography can be used. Examples of inclined structures fabricated to be used in devices can be found in [55], [15]. Examples of inclined structures used as an intermediate step to fabricate different structural materials in combination with various coatings are presented in [12].

Starting from the more traditional setups using inclinable supports and a fixed UV light source we will then move to the more original setups and some applications for the

structures fabricated. This collection of different setups is showing how the technique is not at all standardized.

The first setup [13] uses a tilting stage (and then a rotating stage in conjunction to it) to expose the resist from the top using a mask on top of it (Fig. 14). In most of the literature the inclined lithography is used with negative tone resists so that the exposed structure would remain on the wafer. In this way is easy to fabricate beams and similar structures.

The structure that can be fabricated exposing the resist from the top side are obviously inverted compared to the one done using backside exposure (Fig. 13). The point where the light enters the resist is on top of the structure and the structures have the base on the substrate's surface. In the case of rotating inclined lithography this will result in cones with the base on the substrate and the vertex on the surface of the resist.

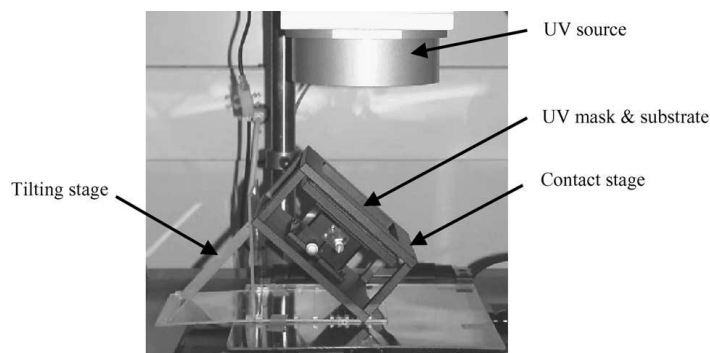


Fig. 14 Inclined lithography setup used in [13]. The setup is using just a UV light source and a tilting stage to hold the sample with a rotating motor integrated in it.

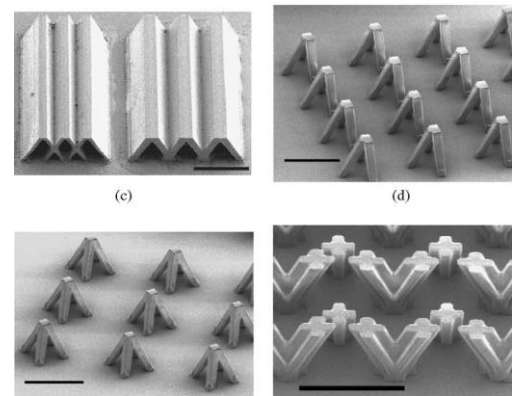


Fig. 13 Structures fabricated with inclined lithography from the top side and bottom side on the bottom right. From [13]

One feature/problem of the topside exposure is the fact that the light coming from the top will be reflected on the substrate surface (silicon polished surface is a good reflecting surface) if no specific coating is applied. In the article the authors use this feature to fabricate V shaped structures using only one exposure. One beam will be formed directly by the incident light while the other will form due to reflection of the light on the substrate's surface (Fig. 15).

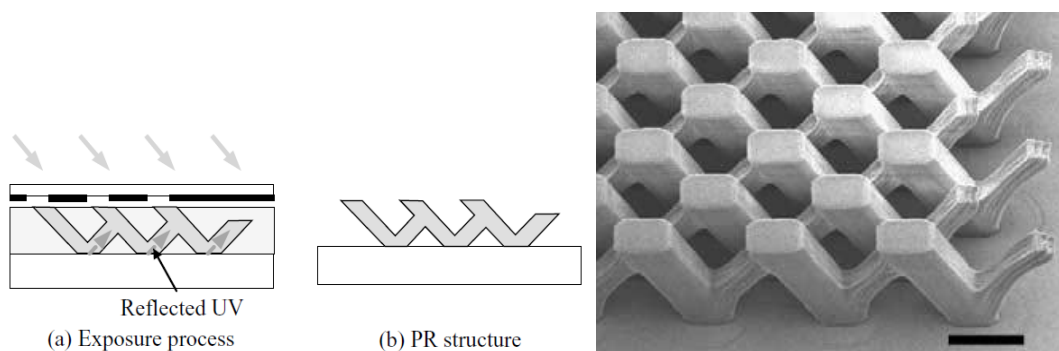


Fig. 15 Schematic of the topside reflection inclined lithography and the resulting structures on the right. From [13].

Another example of a work that is focusing only on the fabrication point of view is found in [56]. The authors are focusing on both traditional perpendicular lithography from the back side and inclined lithography from the front side. Only the part about inclined lithography is considered here bringing another example of front side exposure. The schematics of the exposure and the setup used are presented in the Fig. 16.

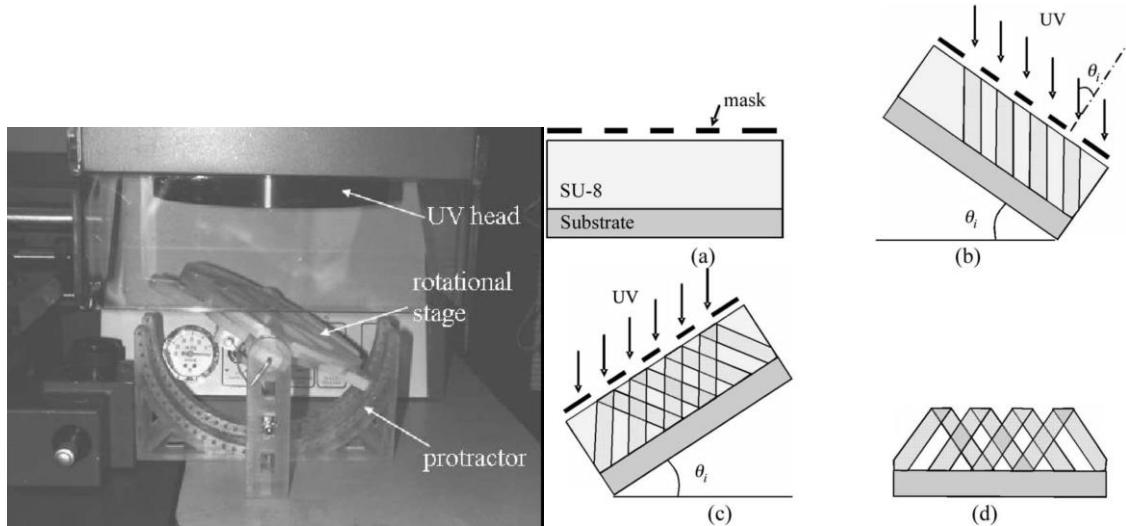


Fig. 16 On the left the setup used for the inclined exposure and on the right the process flow followed by the authors. (a) The mask is placed on the topside of the resist layer, (b) First exposure at a certain inclination angle, (c) second exposure at the same angle and finally the final structure in (d). From [56]

The structures fabricated in this work are similar to the one in my work with the difference of being exposed from the top side. The authors claim that the use of front side exposure is beneficial because the mesh structure and the microfluidics channels shown in Fig. 18 are fabricated with the same exposure step. Using backside exposure the same situation is achievable with one lithography step. The advantage is that, with the addition of another lithography step, the channel are fabricated with vertical walls and only the needed structures are fabricated inclined.

The application mentioned for the structures shown in Fig. 17 is to work as a filter in a microfluidic channel, the same idea that can be found in other works such as [11] or the work in this thesis.

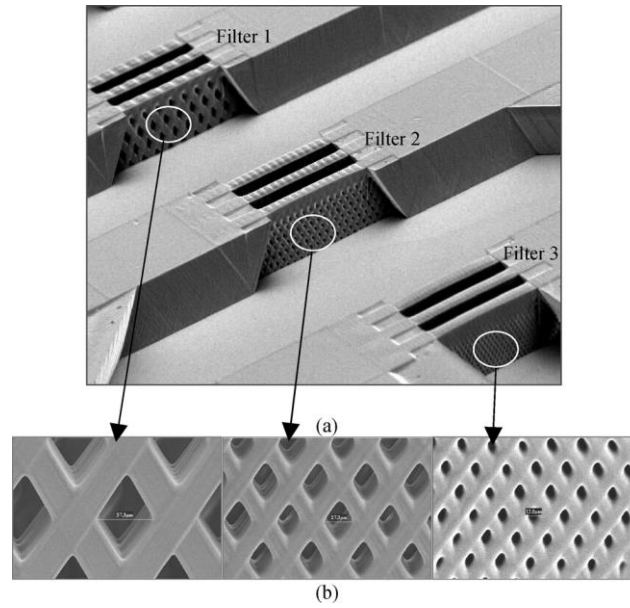


Fig. 18 Example of a filter for microfluidics made out of a mesh structure fabricated with frontside inclined exposure. From [56]

The article that has been important as guideline for the starting ideas of this work is the one from Sato et al. [11]. The authors are using backside inclined lithography to fabricate mesh structures used as a filter inside a microfluidic channel.

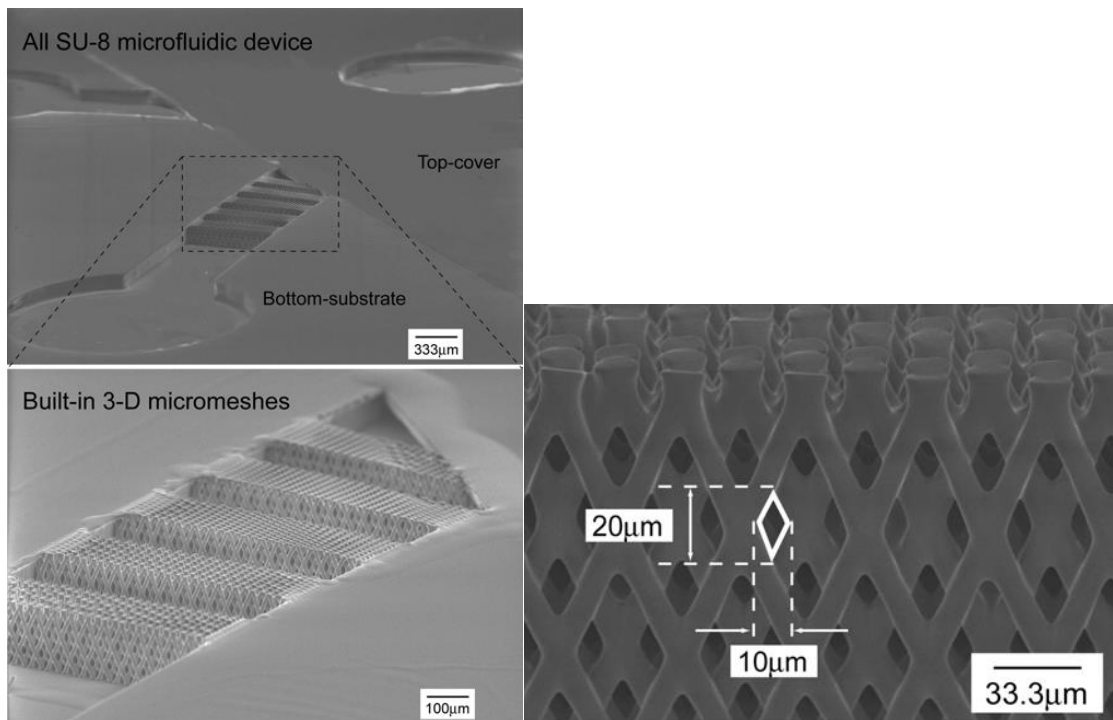


Fig. 17 On the left side the microfluidic channel with the mesh structures inside of it and on the right the zoomed image of the mesh structure where we can appreciate the dimensions. From [11]



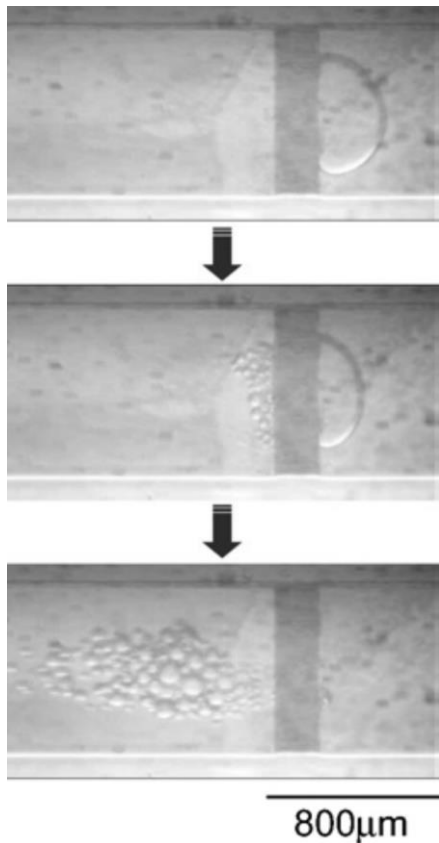


Fig. 20 The mesh structure "filter" in action while breaking a big droplet into smaller ones inside a microfluidic channel. From [11]

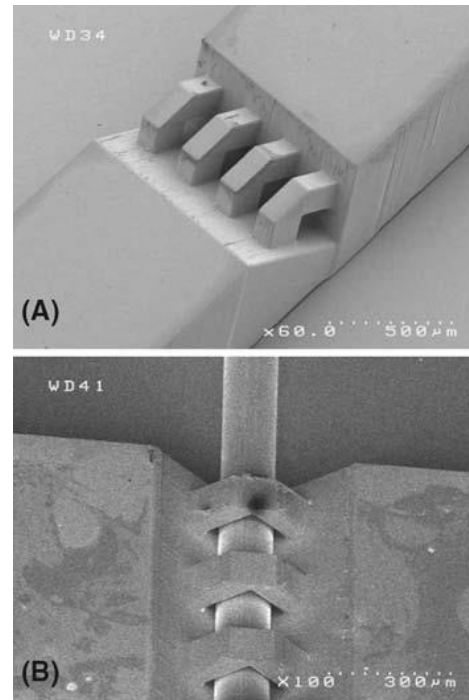


Fig. 19 Holder for optical fibres fabricated with inclined lithography of SU-8. a) the structure and b) with the fibre in place. From [15].

The fact that they are using backside exposure makes possible the exposure of another pattern from the frontside to define the microfluidic channels and other necessary structures before the inclined lithography. The goal of this study is to create an all SU-8 microfluidic device with the inclined meshes used to break apart big droplet to smaller droplet whose size is dependent on the size of the holes in the mesh. The visual explanation on the Fig. 20 The mesh structure "filter" in action while breaking a big droplet into smaller ones inside a microfluidic channel. From is the best way to understand how this works in practice.

To fabricate the device only with SU-8 the authors use a support glass wafer with the mask patterned directly on it. The capping layer is already patterned when it is bonded on top of the unexposed SU-8 on the device. Then a normal perpendicular lithography from the top side is used to expose and define all the microfluidic channels and then the mesh structure is exposed from the backside. At this point the device is released from the glass support dissolving the resist layer that was spun between the mask on the glass and the SU-8 layers. The resulting device is made of only SU-8. This example is the nearest to the work I have done in this thesis.

In a different example the authors needed a support for optical fibre that was in the  $\mu\text{m}$  scale [15]. The structure needed to hold the fibre in place (Fig. 19) and that could not have been done using traditional lithography. The requirement was that the structure would have walls inclined at  $45^\circ$  so normal inclined lithography in air was not possible

due to the limit angle of  $35^\circ$ . The exposure was then done immersing the sample in water making possible the fabrication of structures with  $45^\circ$  inclined walls.

Fig. 19 is showing the fabricated structure and then the optical fibre in place. The fabrication of this structure needs two different exposure, the first to define the supports and the second to define the beams that are actually holding the fibre.

In some cases the inclined lithography structures are used as an intermediate step to obtain a different structure with a different material. In [12] the authors use the mesh structure made out of a photosensitive thiol-ene polymers and coat them with metal (Fig. 21).

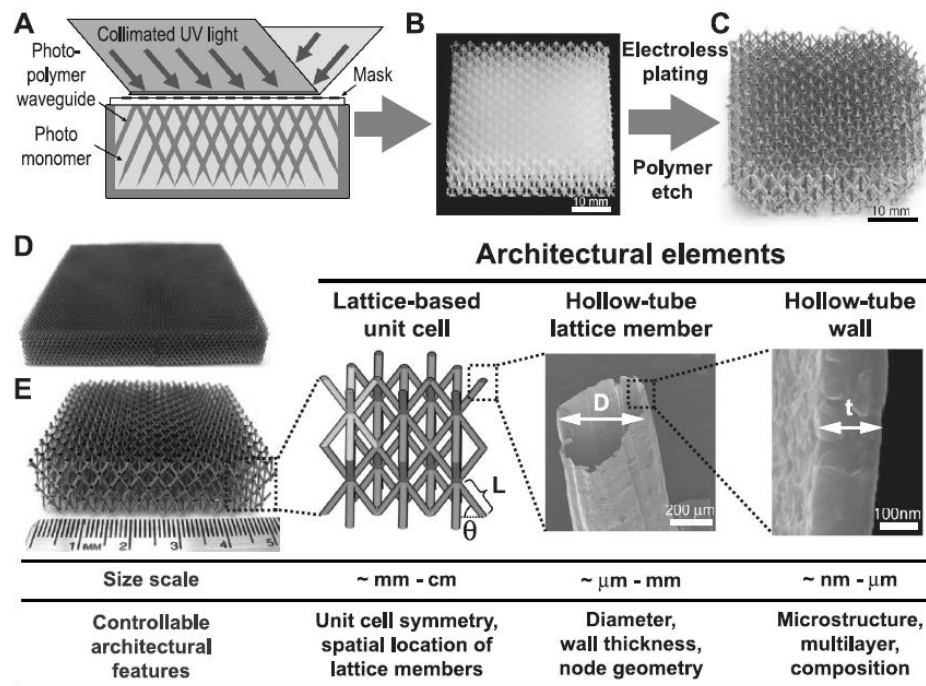


Fig. 21 Inclined lithography of thiol-ene monomers to obtain the final metal hollow metal mesh. a) the schematic of the exposure, b) exposed polymer and c) the polymer structure coated with the Nickel. The details of the structure are also illustrated. From [12]

The resist is then removed from inside the metal coat leaving a hollow metal mesh structure. This structure is made using Nickel and it is considered to be a metamaterial since it possesses some characteristics that are not available to a traditional structure made of the same metal. Basically the hollow structure is having a very small volume of metal to the total volume and the weight of the sample is very low. The sample has also the ability to support quite high compression since the structure is acting like a spring going back to the original form with minor damages. The compression can be repeated several times without causing any more damages on the structure.

The last example of the use of inclined lithography is coming from the work of Jiang G. et al. [54] where the authors are using prisms to improve the inclined lithography or to make a valid alternative to it (Fig. 22). Since the inclined lithography done in air is limited in the structures angle to values below  $35^\circ$  different methods are used to overcome this, immersing the sample in water or in this case using a prism. The light travelling into the prism will change direction according to the angle of the prism's face so that the incident angle at the SU-8 surface can be made higher than the  $35^\circ$  limit in fact the angle can be raised up to  $60^\circ$ . Also in this case the SU-8 layer is exposed from the bottom as shown in the schematics.

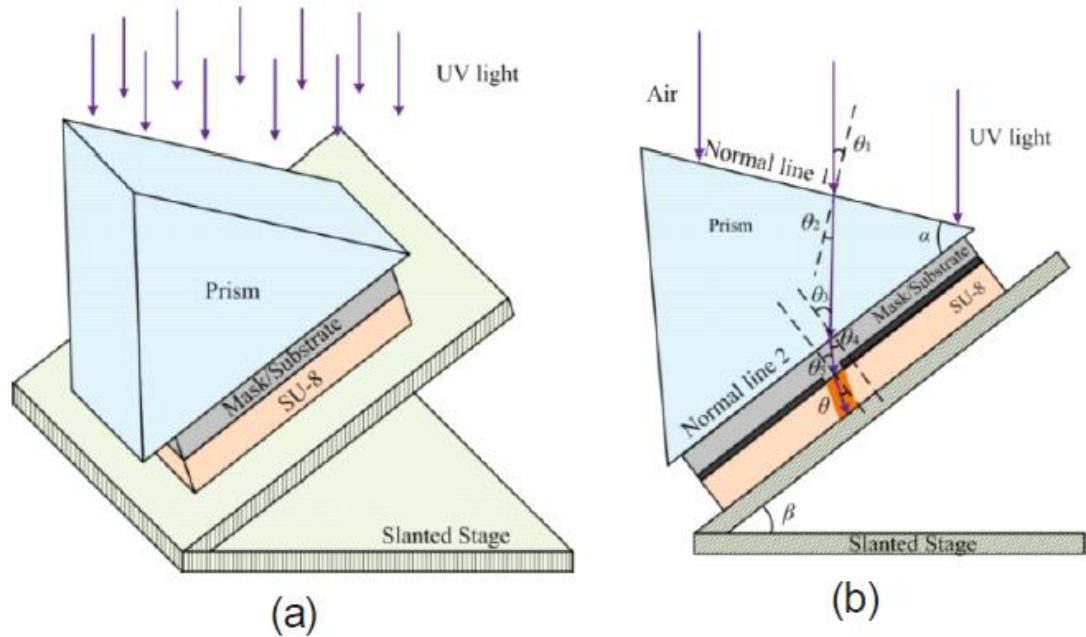


Fig. 22 Schematic of the inclined lithography assisted by the prism. The maxim exposure angle can be raised from  $35^\circ$  to  $60^\circ$  thanks to the reflections inside the prism. From [54]

The idea behind the setup is relatively simple and it is using the changes in the light direction inside the prism to obtain a higher angle at the interface between the mask/substrate and the SU-8. Since the refractive index ratio at that interface cannot be changed in any way the only way to achieve higher exposure angles is to have a higher angle when the light arrives to that surface. The exposures are done with the slanted stage inclined at  $0^\circ$ ,  $27^\circ$ ,  $54^\circ$  and  $85^\circ$  with a  $45^\circ$  prism on top of the substrate to obtain structures in the SU-8 inclined at  $15^\circ$ ,  $30^\circ$ ,  $45^\circ$  and  $60^\circ$  respectively. The SEM images of the structures are presented in Fig. 23.

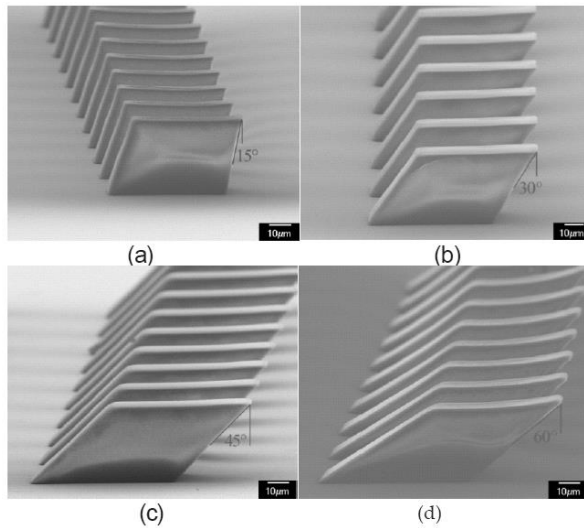


Fig. 23 Inclined structures fabricated using a combination of a slanted stage at different inclinations and a 45° prism. From [54]

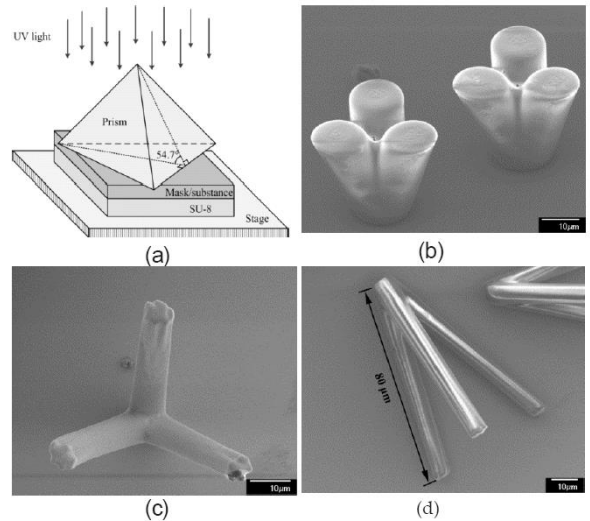


Fig. 24 Structure fabricated in SU-8 using a pyramid prism and traditional lithography. The inclination of prism's walls is refracting the light that creates the inclined structures when exposing the SU-8. From [14]

The application of the prism to traditional lithography opens up some new possibilities since (as shown in Fig. 24) with no changes in the traditional setup and with the addition of a prism we can now expose different shapes and with only one exposure. The prisms can be different in order to fabricate more structures and they are used in combination with a properly design mask.

The use of the prism makes things easier when compared to exposure in a water medium since it can simply done in air.

## 4. Materials and methods

### 4.1 Substrate and masks

All the samples prepared in the work are made using glass microscope slides as substrate. The dimensions of the slide is 7,6 by 5,1 cm (3" by 2") The substrate was chosen for both cost (extremely cheap) and practicality reasons (support and transparency). The small slides are, furthermore, more practical during the fabrication compared to the glass wafers since the rectangular shape helps for the rough alignment during the inclined exposure.

The masks used in the lithography of the aluminium layer and SU-8 were designed on the shape and dimensions of the substrate. The masks were made using 100 mm (4") glass blanks coated with non-reflective chromium. To pattern the mask normal lithography is used. A positive resist is spun on top of the chromium and then exposed using a laser writer. In this way the pattern created with a computer software (CleWin) can be directly transferred on the mask. The photoresist was then developed and the chromium etched away from the exposed areas. These masks were then used for the patterning of the Al mask layer deposited on the glass substrate and for the first of the two exposure of the SU-8 layer.

For dispensing the SU-8 on the substrate a BLE spinner was used together with a programmable Eurotherm HP-220 hotplate for the controlled softbake of the spun resist. The hotplate is connected to a computer where we can load custom programs on the proprietary software deciding the temperatures and the ramping during the baking of the sample.

For the processing of the glass substrate and the Al mask on it a MRC sputter was used to deposit the Aluminium thin film that is then etch, after lithography, using standard wet etching solution. The sputter system is capable of depositing on a very large area and around 20 microscope slides fitted in one run. This was beneficial during the deposition since it saved a huge amount of time and the advantage on the sample is that the uniformity of the film thickness across the different chips is the same. This will then bring further advantages on the subsequent steps since the process is very reliable.

### 4.2 Photoresists

#### SU-8

Different SU-8 compositions were used in these experiments. The viscosity determines the thickness of the layer in relation to the spin speed. The baking times are dependent on the layer thickness. SU-8 is mostly sensitive to the i-line at 365 nm.

SU-8 50 (Microchem – Newton, MA – [www.microchem.com](http://www.microchem.com)) is made for thicknesses from 100  $\mu\text{m}$  to 20  $\mu\text{m}$  when spun at 1000 rpm or 9000 rpm respectively. This composition has a viscosity of 12250 cSt.

SU-8 100 (Microchem – Newton, MA – [www.microchem.com](http://www.microchem.com)) is made for thicknesses from 350  $\mu\text{m}$  to 70  $\mu\text{m}$  when spun at 1000 rpm or 9000 rpm respectively. This composition has a viscosity of 51500 cSt.

SU-8 3050 (Microchem – Newton, MA – [www.microchem.com](http://www.microchem.com)) is made for thicknesses from 100  $\mu\text{m}$  to 30  $\mu\text{m}$  when spun at 1000 rpm or 9000 rpm respectively. This composition has a viscosity of 12000 cSt. This composition is very similar to the SU-8 50 with the addition of some additives that improve the adhesion to the substrate and reduce the stresses after the baking.

### Lift-off negative resist

Ma-N 1407 negative resist (Micro resist technology GmbH – Berlin, Germany – [www.microresist.com](http://www.microresist.com)). The 1407 has to composition tuned to obtain a layer of 0,7  $\mu\text{m}$  when spun at the standard spinning speed of 3000 rpm for 30 s. The spectral sensitivity of the resist is around the i-line (365 nm) in a range from 300 to 410 nm. Recommended exposure dose for the used thickness was  $\sim 250 \text{ mJ/cm}^2$ . The resist is thermally stable up to 160°C when softbaked.

### 4.3 Other materials

#### AZ 826 MIF

MIF developer are TMAH (TetraMethylAmmoniumHydroxide) based. The AZ 826 MIF developer that is 2,38% of TMAH in water with added surfactants to homogenous and fast wetting of the substrate. The surfactants are also removing resist residues formed during development helping with the developing speed but causing a higher dark erosion of the resist.

#### Remover rm-400

The remover rm-400 (NMP free remover) is used in this work for lift-off. The resist is produced by microresists GmbH and it is designed to remove effectively all the novolak based resists [57].

#### Polyvinyl alcohol (PVA)

Polyvinyl alcohol is a colourless, water-soluble polymer resin that is mainly used in treating textiles and paper and in the production of many different organic compounds. PVA is growing in popularity in the microfabrication field [58], [59], [60]. PVA is used in this work as release layer thanks to its water solubility property. The PVA is obtained from Sigma Aldrich in solid form and then dissolved in hot water. The time needed for the dissolution depends on the amount of PVA in the solution. The solution should be heated up to 70°C to speed the dissolution. The PVA solution can be prepared at different w/w% content of PVA in water and this will affect the characteristic of the spun PVA layer. The PVA solution utilized in this work was prepared at 2% and the dissolution took approximately 30 minutes. The PVA layer is cured (to make it solid) at 50°C for 1 hour. For the release of the PVA layer it has to be immerse in water at 70°C for 1-2 hours depending on the layer thickness.

Aqua regia

Etching mixture of nitric and chloric acid (ratio 1:3) used for metals such as Gold and Platinum.

## 4.4 Lithography and process equipment

### Negative resist processing optimization

The optimization of the processing for a new resist is performed following the subsequent steps. The process flow is then adapted for the specific application of the resist.

1. *Starting from the data provided by the manufacturer [61] the basic processing parameters are fixed. The spin speed is fixed at 3000 rpm for 30 s to obtain the 0,7  $\mu\text{m}$  thick layer. The softbake temperature will affect the dark erosion of the resist and is thus fixed at 110°C to avoid too many variables during the optimization.*
2. *The exposure range is chosen based on the required dose and the power of the UV light source.*
3. *The developing time range is chosen with visual inspection of the first exposed sample in order to know the approximate time necessary to develop the pattern. After that, the time needs to be optimized to obtain the needed V-shaped walls.*
4. *The best combination of exposure and developing time is found after some iteration. The lift-off can then be tested with the metal deposition.*
5. *When the lift-off works as well as needed the final device can be fabricated and the process flow is ready. Further optimization will probably enhance the quality of the pattern.*

### General process flow for SU-8 processing

SU-8 is processed as a normal negative resist with particular attention in the baking steps. The thickness of the layer. The thickness of the resist, up to hundreds of micrometres, affects the baking time and the amount of stress present in the final layer. Thicker layers are more prone to high stresses that need to be reduced with a controlled bake.

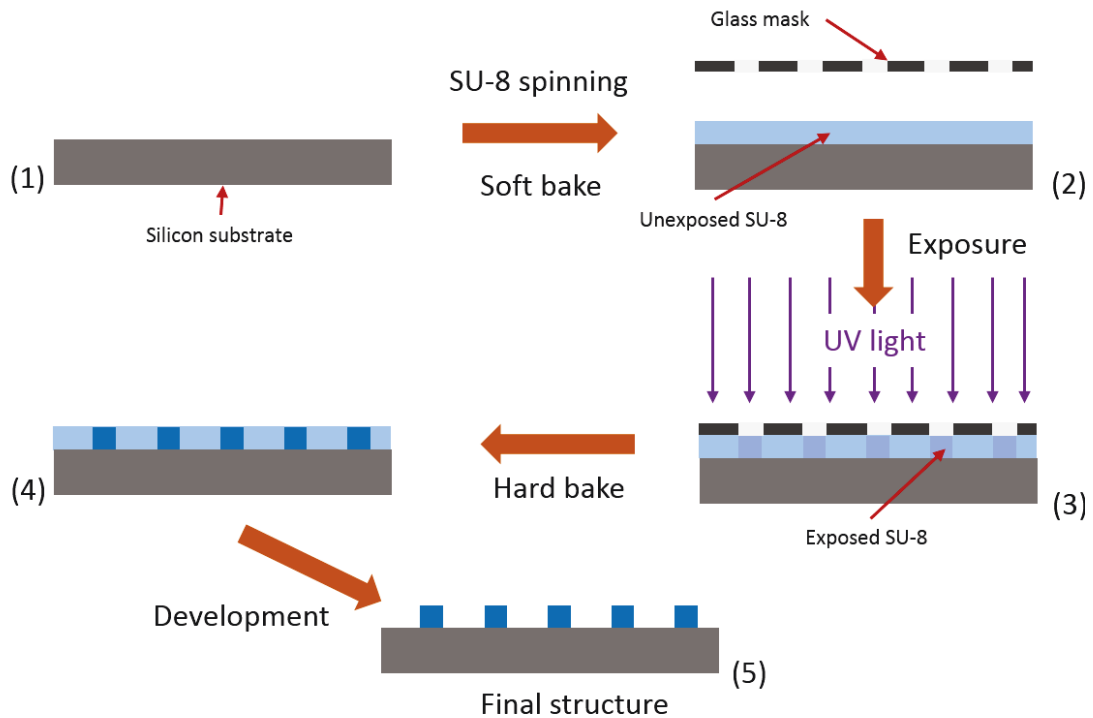


Fig. 25 Process flow for generic back side exposure of SU-8 using a mask directly on the wafer. Information about the steps are found in the text.

Starting from the beginning (the schematic process flow is presented in Fig. 25) the SU-8 is spun on the substrate and, if spun on silicon, does not require adhesion promoters. When the substrate material is different (Aluminium for example) the adhesion is not good and an adhesion promotion steps like oxygen plasma treatment is necessary (step 1).

The spinning speed is decided according to the thickness of the layer, higher spinning speed will result in thinner layers. The range of thicknesses achievable is set by the resist composition with more viscous solution resulting in thicker layers.

The spinned SU-8 is then baked on a hot plate at 65°C and then at 95°C for a certain time depending on the layer thickness to remove most of the solvent. All the baking is done on a programmable hot plate with a ramping in the temperature to avoid stress inside the drying film that will cause cracking and adhesion loss (step 2)

The exposure time is chosen according to the power of the UV lamp used and the thickness of the layer so that the resist will get the required exposure dose. During exposure a mask with the desired pattern is placed between the light and the SU-8 layer and the only the areas exposed to the light will start to polymerize (step 3)



The complete polymerization is achieved in the subsequent baking step (post exposure baking) where the temperature (95°C with the usual ramping) will catalyse the polymerization reaction to completely cure the exposed areas (step 4)

At this point the cured SU-8 can be developed using 1-methoxy-2-propyl acetate or PGMEA (propylene glycol monomethyl ether acetate). The exposed areas will be completely insoluble in the developer so when processing SU-8 overdeveloping is not an issue (step 5)

### SU-8 with inclined lithography (process flow used in the experiments)

The process flow actually used for the inclined lithography differs in some steps from the traditional processing. Exposure is done from the backside through a mask on the glass support. These small differences have quite a big impact on the final structures. The process flow is here reported with the parameters used for the fabrication of the 3D structures in a 50 µm thick layer:

1. **Aluminium mask:** *sputtering using MRC sputter and patterning using AZ 5214E (spinning at 4000 rpm for 30 s, softbake at 95°C for 1 min, Exposure 3.5 s in the mask aligner, develop 45 s and hardbake at 120°C for 1 min. Etching of the Aluminium layer using standard Al etching solution at 50°C for 30 s.*
2. **Thin layer of SU-8 50 (10 µm):** *spinning at 9000rpm for 45 s, Softbake 3 min at 65°C and 5 min 95°C, Flood exposure: 5 s and hardbake 4 min at 95°C.*
3. **Thick layer of SU-8 50 (50 µm layer):** *Spinning at 3000 rpm 30 s, softbake 5 min 65°C and 15 min 95°C.*
4. **First exposure and alignment:** *First exposure in MA-6 mask aligner for 18 s with the mask aligned to the pattern in the metal mask on the sample.*
5. **Inclined exposure:** *Inclined exposure from the back side, two times 3 s with inclination  $\pm 50^\circ$ .*
6. **Hardbake and development:** *hardbake for 15 min at 95°C with a long development (> 1 hour). Washing with isopropanol to remove the residues of developer from the structures.*
7. **Bonding:** *PVA solution at 2% w/w in water is spinned over a plastic transparency. Spin speed 500 rpm for 30 s. Curing of the PVA layer at 50°C for 1 h. Spinning of a 10 µm thick SU-8 layer on top of the PVA and then softbake. The SU-8 layers are brought in contact while on a hot plate at 63°C and bonded manually applying pressure from the top.*
8. **Hardbake and release:** *hardbake of the bonded sample at 95°C for 15 min after flood exposure for 5 s. Release in hot water to dissolve the PVA layer overnight (1-2 hours are sufficient). If the sample needs to be detached from the supporting glass then the aluminium layer needs to be etched.*

The processing of the inclined structures is shown in Fig. 26 below.

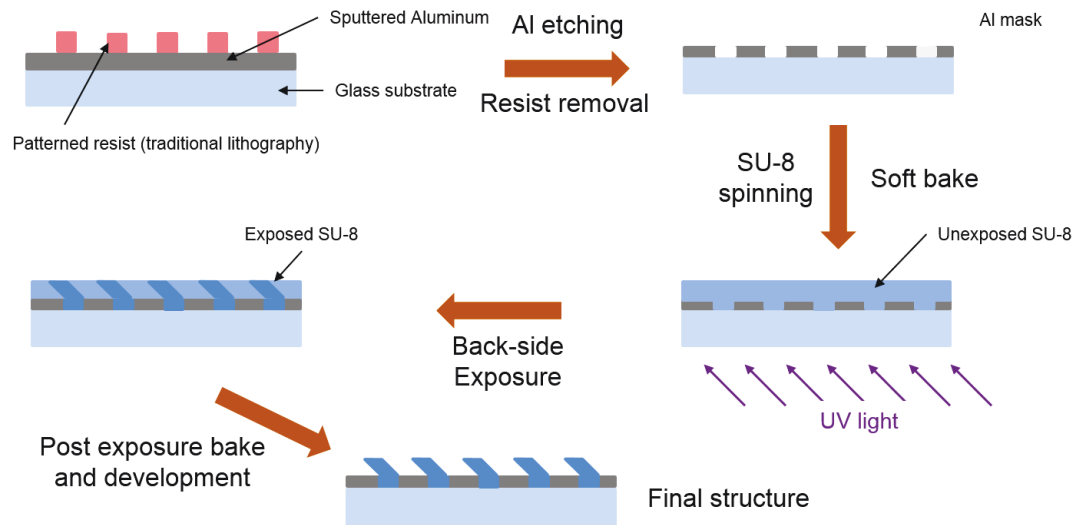


Fig. 26 Process flow for the fabrication of inclined exposure structures.

If SEM images are needed, the sample needs to be coated with a thin layer of metal. Without the metal layer the imaging will be hard and low quality due to the charge accumulation on the insulating SU-8 layer. In this case the sample were coated with approximately 10 nm of gold.

To coat the structures a Bal-Tec SCD 050 diode gold sputter was used. The deposition parameters are not really important but they are reported here for completion. Sputtering base pressure:  $10^{-2}$  mTorr, Sputtering pressure:  $3 \cdot 10^{-1}$  mTorr, Voltage: 40 mV, Time: 60 s.

### Inclined lithography tools

The inclined exposure setup used in this work was designed specifically to meet the needs of the experiments. It was built by Ville Liimatainen from the automation department, Aalto University. Since the inclined lithography is still a new technique the equipment is not available as commercial product and it has to be custom build (Fig. 27).

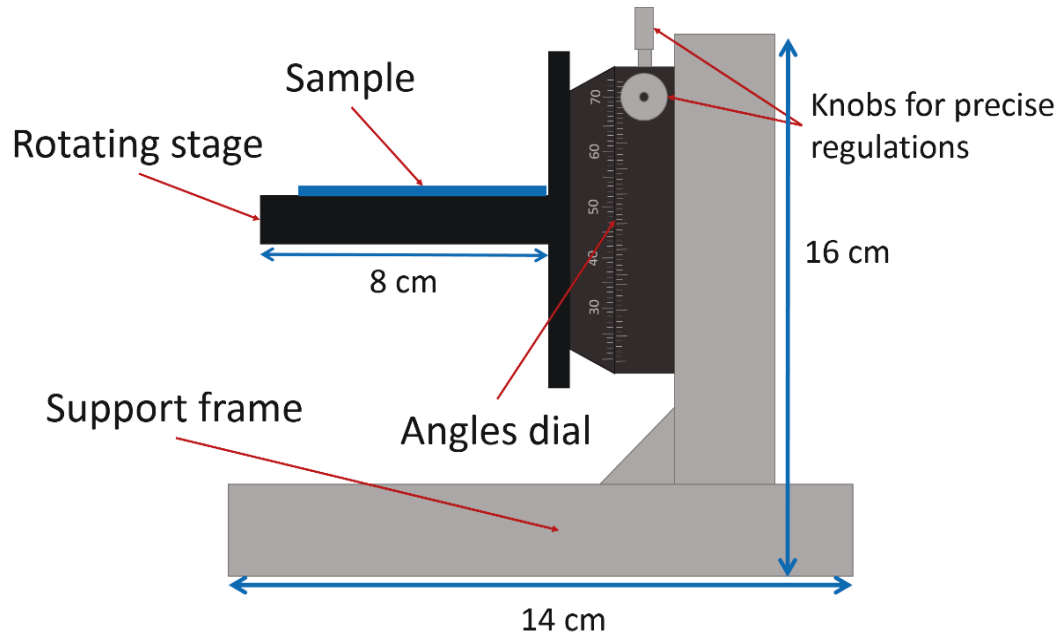
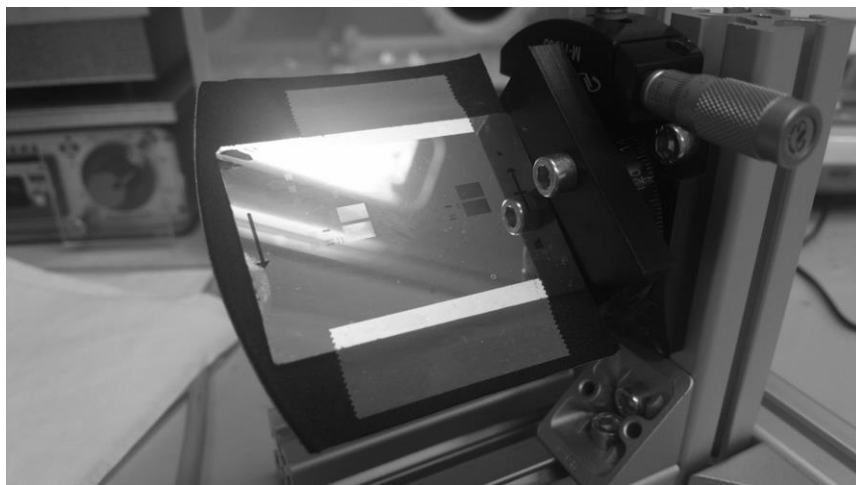


Fig. 27 Schematic of the inclining stage. The support frame is 16 cm high and around 14 cm long. The rotating stage's dimensions are 8 by 5 cm.

The idea behind the setup is to keep it simple while being able to fit substrates as big as a 100 mm silicon wafer (even 150 mm with few modifications). It consists of a simple metal support where a horizontal stage is mounted on a rotating stage (model M-RS65 manufactured by Newport, US). The stage is manually rotated for rough adjustments of the angle and then the chosen position can be fixed with the screw on the top. The bigger screw on the side is used to then make the fine adjustment but that is not needed for this kind of application. On the rotating part of the stage the angles are written (from 0 to 360°) with an increment of 10 degree. The angle can be set with good precision (11 arcsec according to the manufacturer), enough for lithography purposes. This equipment can be used with all the UV setups big enough to fit it (dimensions at least 20x20x20 cm). Just some alignment is needed between the lamp and the equipment to keep the illumination constant between different experiments.

The setup is shown in the Fig. 28 below with a close up of the rotating stage.



*Fig. 28 Sample on the inclined lithography setup before exposure. The sample is attached simply with tape and this is not creating any problems since the SU-8 layer is touching the stage and the tape is attached to the glass support.*

The top side of the SU-8 layer is touching the stage the reflected light will expose the uppermost layer making the structures unusable due to undesired polymerization. This problem is solved using a layer of non-reflective material in contact with the sample. Different materials were evaluated from other resists on glass to layers of antireflective oxides (ZnO for example) but they were all more complicated solution than the one used in the experiments.

The first experiments were performed using a glass piece with a resist layer on one side. The resist would absorb some of the light preventing the reflection. Further experiments were done with an improved the setup, the back of a normal mouse pad was used between the stage and the sample (Fig. 29). The dark and extremely rough surface of the mouse pad's back was perfect to almost eliminate the reflection while at the same time being the easiest and by far cheapest solution. The stage where the sample is attached is made to fit the microscope slides used in this work but it could be simply replaced with some bigger one if different substrate would be used.

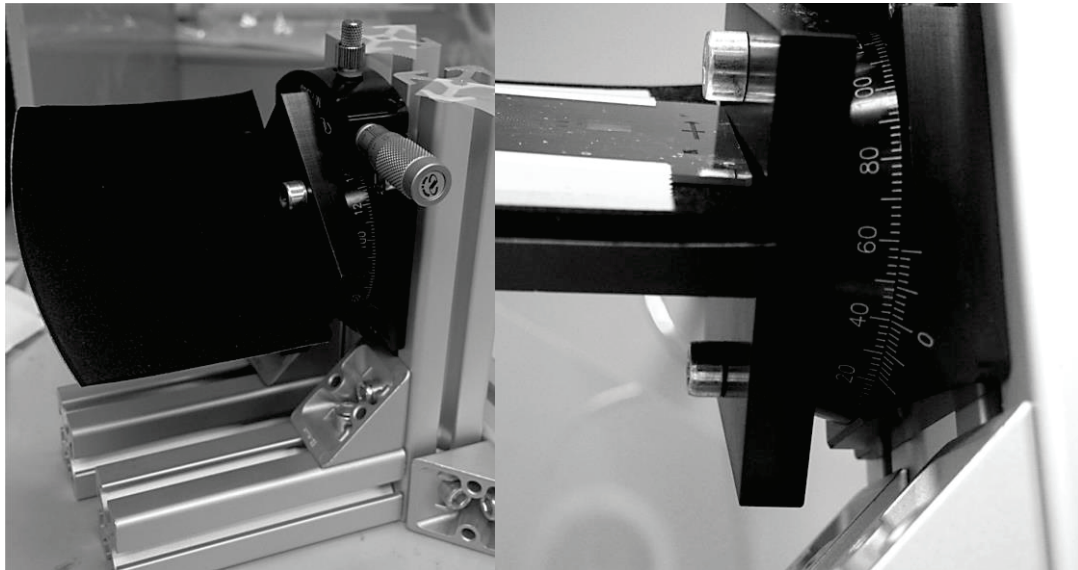


*Fig. 29 Pictures of the inclined lithography equipment showing the supporting frame and the rotating stage with the antireflection material attached. On the right a close up on the angles scale on the rotating stage.*

The sample is attached to the rotating stage after the non-reflective layer is in place, attached with double sided tape. The sample is placed with the SU-8 layer touching the stage so that the mask is in between the resist and the UV lamp. To keep the sample in place some scotch tape is used and that is not giving any problems because the tape is attached to the back side of the sample. The tape needs to be placed so that it is not covering the pattern. At this point the stage can be rotated to the needed angle manually and then fixed in place with the screw on the top of the device. The setup is aligned with the UV source.

The SU-8 was exposed with a Süß MA-6 mask aligner ( $\sim 20 \text{ mW/cm}^2$ ) in the cleanroom of Micronova for the areas that didn't need to be inclined. Using this machine the mask on the substrate was exposed. The alignment of the glass mask with the mask in the sample was also performed with the mask aligner. The light from the Hg source is filtered eliminating the wavelengths below 300 nm.

A DYMAX ECE 2000 Modular flood UV light source ( $100 \text{ mW/cm}^2$ ) was used for the inclined lithography step (Fig. 30). The UV system operates with an unfiltered Hg lamp so all the lines present in the Mercury spectrum are present in the exposing light.



*Fig. 30 DYMAX ECE 2000 setup as used in the experiments. From the manufacturer website.*

## 4.5 Characterization equipment

### SEM SUPRA 40

The scanning electron microscope SUPRA 40 is manufactured by ZEISS (Oberkochen, Germany) and it is a multipurpose high resolution SEM used in Micronova for both imaging and focused ion beam lithography.

The machine is equipped with a 5-axis motorized eucentric stage that allow the hassle free observation with the stage tilted. The whole stage is tilted and not only the sample (as it was in the older SUPRA 35 machine) so that when moving in the x-y plane there is no danger of hitting the column.

### Contact angle measurement setup

The setup used is the model Theta produced by Biolin Scientific (Espoo, Finland).

## 5. Results and discussion

### 5.1 Negative resist optimization (maN-1407) for lift-off applications

The project started from the need of interdigitated electrodes made out of Platinum with lines as narrow as 1  $\mu\text{m}$  with spacing of the same dimension. The device would be then used as a sensor so the good reproduction of the pattern was necessary.

The fabrication of the device was first tested using etching of Platinum with aqua regia. The results was not good due to the small dimensions of the pattern. Aqua regia is a strong etchant and the control of the time is not easy. Small features are challenging and, on top of that, every failed attempt makes the platinum layer unusable. The focus was then shifted to lift-off and for that a new resist (ma-N 1407 lift-off resist) processing needed to be optimized [62].

According to the power of the UV source and the recommended exposure dose, the resulting exposure time is calculated to be around 12 seconds. The exposure dose needed to fabricate the V-shaped structures is lower since less light is needed. The range of exposure times that was tested was kept between 4 and 12 seconds. The first sample was exposed with 6 and 9 seconds and developed until the pattern was visible in the wafer. The approximate developing time in AZ 862 developer was found to be between 4 and 5 minutes.

Now another wafer is exposed with four different times (4 – 6 – 8 – 12 seconds) and developed for the time necessary to develop all the 4 different areas. SEM was then used to observe the results and decide the best exposure time to use forward.

The best results were obtained with 8 s exposure where all the line dimensions from 1  $\mu\text{m}$  to 20  $\mu\text{m}$  were fabricated with enough quality. The developing time is obtained exposing the whole wafer for 8 s (exposure dose 160mJ/cm<sup>2</sup> ) and then try different times for the developing. The range was between 3 and 6 minutes with the best result obtained at 4 min 30 s. The difference in the walls slopes for different developing time is demonstrated with the SEM picture in Fig. 31.

Working with photoresist is always matter of adjusting the exposure and the development times around the optimal values. Usually the exposure time is the parameter that is fixed first and the fine corrections to the processing are done with the developing step. Development time is in the order of minutes and, compared to seconds in the exposure, small variations are not critically affecting the final results.

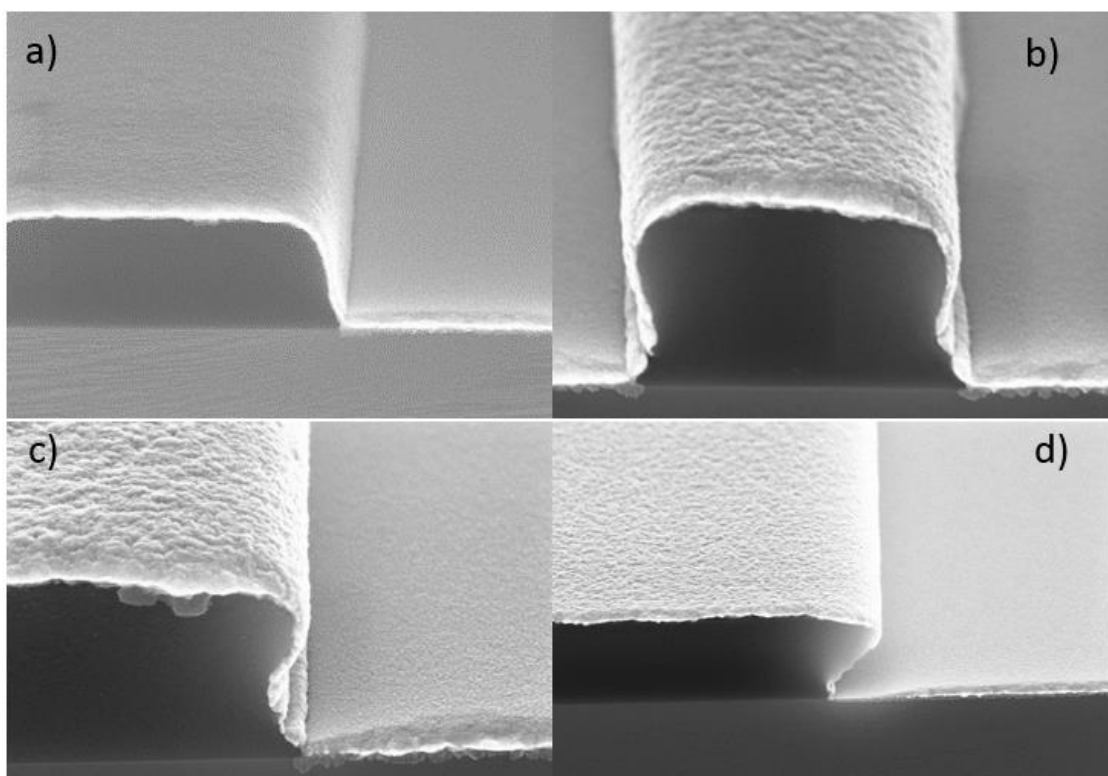


*Fig. 31 Pictures showing the difference in walls slope when the developing time is longer at the same exposure dose. On the picture a) the developing time is 3:30 minutes and in d) 5 minutes. B) and c) are in between with 4 and 4:30 minutes respectively.*

After the optimization of the resist processing, the metallization is tested using Copper instead of Platinum. If the process will work with the Cu (that is substantially cheaper than Pt) than similar parameters will apply to the Pt. The optimization is therefore cheaper and only the final device will use the needed Platinum.

The Copper was first sputtered but the results were not good since the metal was deposited also on the walls of the resist even though they had negative inclination. The metallization method was changed to evaporation. This technique will guarantee the perpendicular direction of the metal atoms coming from the target so that the walls of the resist will not be coated.

The results with the evaporator were excellent and the resulting lines were well patterned on the metal down to the 2  $\mu\text{m}$ . With some more optimization of the whole process also the 1  $\mu\text{m}$  lines could be successfully patterned but keeping in consideration that at that line width the resolution limit of the resist is approaching.



We can see in Fig. 32 how the evaporation works with the 2  $\mu\text{m}$  lines.

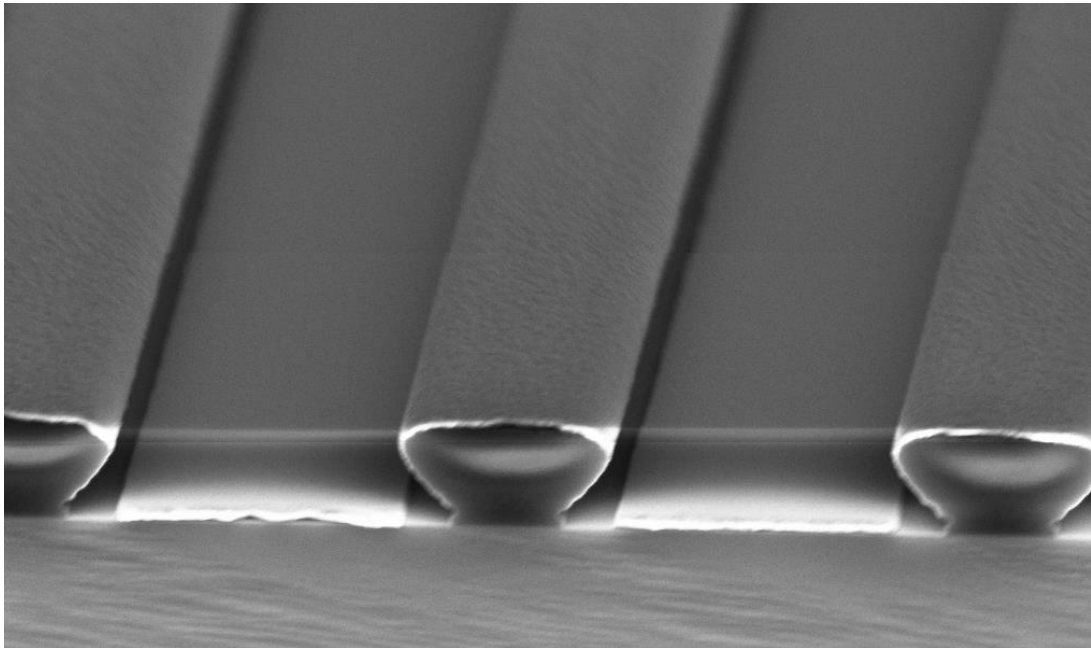


Fig. 32 V-shaped resist's 2  $\mu\text{m}$  lines and an evaporated metal layer that is deposited only in the areas not covered by the resist.

The V shape of the resist is preventing the metal to deposit on the walls and the metal lines are right of the width demonstrating the superiority of the evaporation coating in this specific fabrication process.

With the metallization optimized the lift-off using the resist remover rm-Rem 400 is working perfectly without the need of any ultrasounds. The lift-off can be speed up if the resist is heated to 70°C. The dissolution of the resist on the more difficult areas can be helped using a pipette to spray some remover over them. The use of ultrasounds was tested but it was causing adhesion problems on the thinner metal lines.

Optimized process flow:

1. Wafer priming in HMDS
2. Spinning ma-N 1407 resist at 3000 rpm for 30s
3. Softbake 110°C for 1 min
4. Exposure 8 s at 20 mW/cm<sup>2</sup> (exposure dose 160mJ/cm<sup>2</sup>)
5. Developing time in AZ 826 MIF 4 minutes 30 seconds
6. Metal evaporation 50-150 nm
7. Lift-off in resist remover rm-Rem 400 with the help of a pipette if necessary

|           | Spinning         | Softbake       | Exposure | Development |
|-----------|------------------|----------------|----------|-------------|
| ma-N-1407 | 3000 rpm<br>30 s | 110°C<br>1 min | 8 s      | 4:30 min    |

Table 1 Optimized parameters for the processing of V-shaped walls in ma-N 1407

## 5.2 SU-8 with inclined lithography

### Fabrication

During the work different samples were prepared and some parameters were changed (exposure time mainly together with the layer thickness) after every iteration in order to obtain a better structure every time. The mask was also changed, three times, to test better pattern designs. In Table 2 the list of the optimized fabrication parameters for the tested thicknesses are reported. The list of all the samples fabricated during the optimization is found in APPENDIX A.

| Thickness  | Spinning         | Softbake                   | 1 <sup>st</sup> exposure | 2 <sup>nd</sup> exposure | Post exposure bake |
|--|------------------|----------------------------|--------------------------|--------------------------|--------------------|
| <b>10 <math>\mu\text{m}</math><br/>SU-8 50</b>   | 9000 rpm,<br>45s | 3 min 65°C<br>5 min 95°C   | 10 s flood<br>exposure   | NA                       | 4 min 95°C         |
| <b>50 <math>\mu\text{m}</math><br/>SU-8 50</b>   | 3000 rpm,<br>30s | 5 min 65°C<br>15 min 95°C  | 18 s in mask<br>aligner  | 2 x 3 s                  | 15 min 95°C        |
| <b>70 <math>\mu\text{m}</math><br/>SU-8 50</b>   | 1500 rpm,<br>30s | 10 min 65°C<br>25 min 95°C | 20 s in mask<br>aligner  | 2 x 4 s                  | 25 min 95°C        |
| <b>100 <math>\mu\text{m}</math><br/>SU-8 100</b> | 3000 rpm,<br>30s | 10 min 65°C<br>35 min 95°C | 25 s in mask<br>aligner  | 2 x 6 s                  | 35 min 95°C        |

*Table 2 Optimized process parameters for the different SU-8 thicknesses utilized in the work.*

The processing of the SU-8 will start after the Al mask is patterned on the glass slide (the procedure followed is the standard one for metal patterning, ref Fig.26). At this point if the thick SU-8 layer is spun it will be in direct contact with the glass and Al layers. The structures that will be fabricated on the SU-8 will not be strongly attached to the substrate and they will detach easily. The solution is to spin a thin SU-8 layer that will cover the whole substrate having a good adhesion with it. The structures fabricated are now fabricated on the SU-8 layer eliminating the adhesion problems. The thin SU-8 layer will act as a support for the structures connecting them all together. The thin layer is cured before the thick SU-8 layer is spinned by simply flood exposure

The thick SU-8 layer is spun and softbaked having a good adhesion to the bottom SU-8 and it is ready for the exposure steps (Fig. 33).

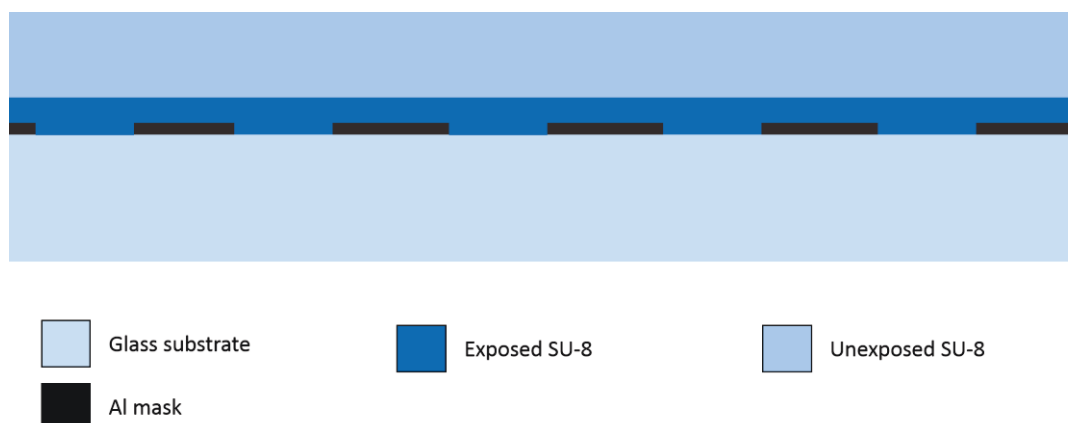


Fig. 33 Schematic showing the sample ready after the multilayer SU-8 is spun. The thickness of the exposed bottom layer is around  $10\text{ }\mu\text{m}$  (and it could be also smaller) while the top unexposed layer thickness varies between samples from  $50$  to  $100\text{ }\mu\text{m}$ .

The lithography of the sample is divided in two steps. The first is a traditional lithography through an external glass mask to pattern all the channels and other microfluidic structures. The second step is the inclined exposure for the 3D structures. A schematic of the two exposures is presented in Fig. 34 below.

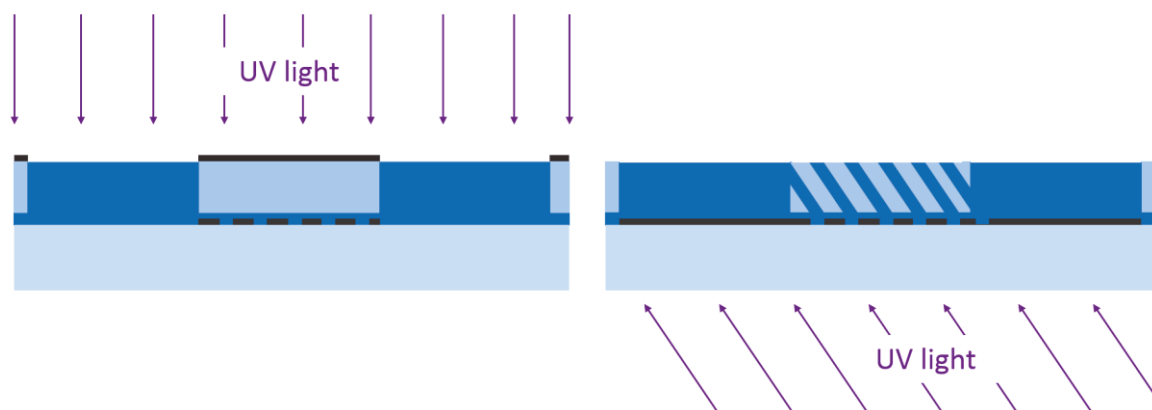


Fig. 34 On the left the schematic of the first lithography to pattern the channels. On the right the second lithography (inclined) is performed to pattern the 3D structures inside the channel.

This first exposure is done aligning the glass mask to the alignment marks present on the Al mask on the substrate. In this way the structures exposed with the traditional lithography will have straight walls and the subsequent exposure will create the 3D meshes aligned to them. The exposure time of the microfluidic channels is certainly not critical thanks to the dimensions ( $50$ - $200\text{ }\mu\text{m}$ ) of these structures.

After the first exposure is done the sample does not go to the post exposure bake step and the second exposure is done immediately. This is the inclined exposure step, performed in the DYMAX UV system utilizing the tilting support to set the angle of exposure to  $50$  degree. The angle that was used for all the sample to keep the processing comparable between the different thicknesses. During this exposure the mask in the sample is aligned already to the microfluidic structures. At this stage the exposure time

needs to be perfectly optimized to obtain good results. An optimal exposure dose is critical in the whole layer thickness.

Every sample was exposed two times, one for each inclination ( $+50^\circ$  and  $-50^\circ$ ) for the same time. The use of the same exposure time for both angles may not be the most optimal procedures since, as it is observed in Fig. 40, the two beams look exposed differently. This may be caused by the fact that the light in the second exposure travels also through the already exposed SU-8. The exposed SU-8 will not absorb as much light as the unexposed SU-8 making possible for the light to get further deep in the layer.

Then the SU-8 is cured as last step of the lithography to complete the polymerization of the areas exposed in both the traditional and inclined lithography steps. When the SU-8 is fully cured it can be develop for a time long enough so that all the unexposed areas are developed away (Fig. 35). The developing time is not fixed since the SU-8 can be left in the developer for long times (overnight) with no issues. There is an optimal time for the development but these structures are much more complicated than structures with vertical walls so the long developing time is chosen to ensure the complete removal of the unwanted resist from inside the structures.



*Fig. 35 The inclined SU-8 structure after development while still on top of the carrier glass wafer.*

The use of two masks (one on the glass slide and an external glass mask) is a great example of the possibility of fabricating the mesh structures in direct conjunction with an existing microfluidic design integrating all the exposures necessary into one multiple exposure of the SU-8 layer. Example of this can also be found in the literature where a full SU-8 microfluidic device is fabricated with mesh structure integrated in the channels and used as a filter [11]. The two masks need to be aligned but the integration of the meshes to the bigger microfluidic structures makes the alignment a non-critical step. The dimensions are big enough to give a wide margin of error (up to few micrometres) to work with. The mesh structures are exposed after the channel so the eventual misalignment will be exposing only exposing areas of the resist that are already exposed.

## Bonding

The device as it is after the fabrication cannot be directly used for microfluidic applications and the top of it must be capped to close the channels. The capping is done bonding a layer of SU-8 to the top of the device. This step is very simple conceptually but in real fabrication can be quite tricky since my structure are not presenting a large surface area on the top, a requirement to make a good bond.

Different bonding techniques have been tested with different results finally founding one that works the best. The first try was done using the method described in [63]. A SU-8 thin layer ( $10\text{ }\mu\text{m}$ ) is spinned on a transparency (3M laminating film) attached to a

glass slide for support. The transparency is cleaned with acetone to remove the adhesive coating on it. After spinning the transparency with the SU-8 is placed on a hotplate to softbake the SU-8. At this point the SU-8 is solid but still not cured and it can be bonded to the SU-8 structures using a temperature higher the glass transition temperature of uncured SU-8 (55°C). The substrate with the structured layer is put on a hotplate at 63°C and then the SU-8 on the transparency is bonded using pressure. At this point the bonded SU-8 layer needs to be cure exposing it with UV light (flood exposure for 5s) and then post exposure baked. The two layer should now be bonded but in the case of my structure that was not happening and the bonded SU-8 was detaching from the structure in some areas remaining attached to the transparency. This is due to the fact that the structures were not presenting the necessary bonding are so the bond of the capping SU-8 was stronger on the transparency side.

Then another method was tried using a release layer between the transparent support and the bonding SU-8 layer. The first trial was done using AZ 5214 E resist as release layer. Then the 10  $\mu\text{m}$  SU-8 layer is spun on the resist (ref. to Table 2) and then baked. The release was tested immersing the slide in acetone to remove the AZ resist. The released worked but it was possible to see traces of the positive resist on the SU-8 layer contaminating the layer. The AZ resist contamination is present only on the outside of the SU-8 capping so the device is not directly affected by it.

The next try was based on the poor adhesion that SU-8 would have when spun on top of a PDMS layer and that would make the release easier. The spinning was good (again same parameters) but the soft baking of the SU-8 cannot be performed without destroying the layer. The adhesion between the two is simply not good enough to keep the SU-8 together during the evaporation of the solvent.

In last method tried PVA (poly vinyl alcohol) is used as release layer (Fig. 36). The PVA can be spun between the support and the SU-8 layer that is bonded with the inclined structures. The PVA can be then dissolve in water after the bonding detaching the support from the bonded SU-8.

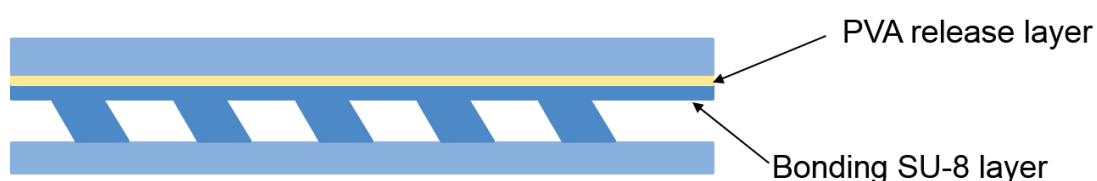


*Fig. 36 Schematic of the bonding method using the PVA as release layer between the capping SU-8 and the carrier transparency.*

A solution of PVA 2% w/w was prepared dissolving solid PVA into water and mixed. The PVA was then spun on a glass slide and then thermally cured. The SU-8 is then spun on top of the PVA layer and baked (for the parameters refer to materials and methods). The sample is then bonded to the structures using the same method previously described again using pressure. The bonded sample is then immerse in hot water overnight and the PVA is dissolved releasing the bonded SU-8 layer. The release time may vary due to the fact that the PVA layer is in between the two SU-8 layers. The water will need some time to infiltrate between the layers to dissolve the PVA. SU-8 is

unaffected by water so the release overnight will just guarantee the complete dissolution of the PVA layer even if the time is longer than the 1-2 hours that are needed.

The release using PVA was successful and the top SU-8 layer was bonded capping the structures as shown in Fig. 37. The sample is still attached to the glass wafer at this point.



Fig. 37 Finished device with the capping layer bonded on top of it. Still the glass carrier is present.

|     | <i>Solution</i> | <i>Spinning</i> | <i>Curing</i>  | <i>Dissolution time</i> |
|-----|-----------------|-----------------|----------------|-------------------------|
| PVA | 2% w/w          | 500 rpm for 30s | 1 hour at 50°C | > 1 Hour at 70°C        |

Table 3 PVA processing parameters for the successful bond.

If the sample needs to be released from the glass support there are some alternatives. The easiest is to simply etch away the Al layer so that the SU-8 structure will be released. This was done leaving the sample in the hot water long enough that the Al layer would have been etched enough for the release. In this way the mask is lost so a release layer between mask and SU-8 would make the release possible preserving the integrity of the mask. The final result was similar to the simplified image in Fig. 38.



Fig. 38 Final all SU-8 device. The inclined structures are enclosed by the bottom layer and the capping bonded layer. At this point all the microfluidic channel are sealed and the device is ready to use.

## Exposure results

The characterization of the fabricated structures is done mainly using a scanning electron microscope to visually inspect the quality of fabricated structures. The stage of the SEM was tilted at 50° to better observe the structures. Observing from the top will reveal information only about how the structures are organized in the space and if defects are present between the different lines (Fig. 52). Many structures are fabricated as if they were used in a microfluidic device so inside of a channel. Some other structures are separated from each other to better understand how single structures are fabricated.

One of the best example of the fabricated 3D mesh structures is reported in Fig. 39. The mesh is fabricated inside of a channel and the quality and apertures dimensions are comparable to the one fabricated in [11]. These structures present only small defects

since the dimensions of the pattern in the mask ( $10\ \mu\text{m}$  holes) match the thickness of the SU-8 layer.

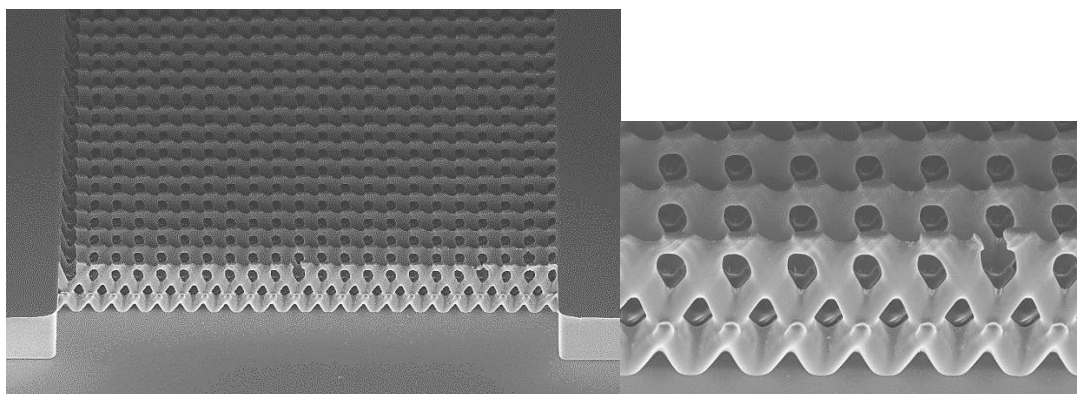


*Fig. 39 The mesh structure inside a microfluidic channel fabricated using  $10\ \mu\text{m}$  holes in the mask,  $50^\circ$  exposure orientation and a  $100\ \mu\text{m}$  thick SU-8 layer. On the right the zoomed detail of the structure.*

The pattern is composed of circles  $10\ \mu\text{m}$  in diameter with a spacing of  $30\ \mu\text{m}$  between each other while the SU-8 layer thickness is  $100\ \mu\text{m}$ . The holes are big enough to let through light necessary to expose the layer all the way to the top (the top layer in Fig. 39 is actually the bottom layer when exposing). There are many points where the beams created from the two different exposures are meeting and the space left unexposed is developed away creating the openings in the structures. In this case the small holes in the mask in combination with a thick resist layer forms two apertures in the mesh. Using bigger holes will result in one or no openings due to the beams not intersecting each other enough. In the table 3 below the different combinations are quickly presented.

|                  | Dimension of the holes in the mask                                     |  |
|------------------|--|--|
|                  | Small  | Big  |
| Thin SU-8 layer  | Few openings, low dose required and low defects formation (thin beams) | No openings, low dose required and no defect formation                   |
| Thick SU-8 layer | Many openings, high dose required and probable defect formation        | Few openings, normal dose requires, low defects formation. (Thick beams) |

*Table 4 How the mesh structure will result from different combinations of pattern dimensions and SU-8 thicknesses. The dose refers to the exposure dose needed to expose the whole pattern.*

The size of the holes in the mask needs to be optimized for the SU-8 layer thickness. Then both of the parameters have to be chosen considering with needed look of the final structures. Differently from the optimized parameters for the structures in Fig. 39 when the choice is done wrong the result will be the useless structure in Fig. 40. In this case the dose of UV light was not sufficient for the exposure of the whole layer.

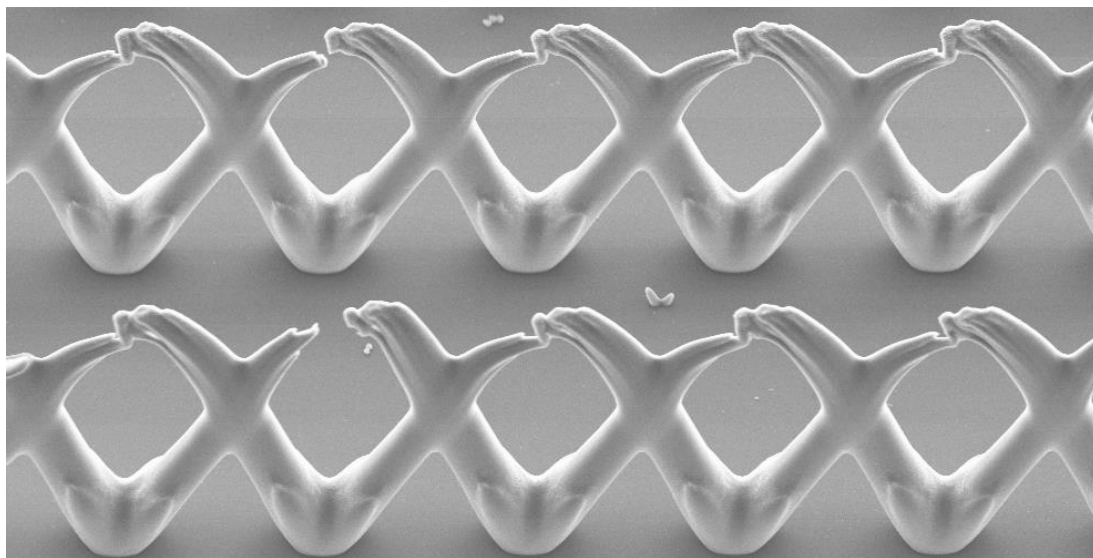


*Fig. 40 Inclined structure made with mask's holes size of 20  $\mu\text{m}$ . The dose used for the sample was not enough to expose the whole 75  $\mu\text{m}$  SU-8 layer.*

This is the main issue faced when working with SU-8 and inclined lithography, the size of the structures is dependent on the SU-8 layer thickness. An extensive analysis must be done to understand the limit dimensions for the structures in different layer thicknesses. The other main concern is the formation of defects in the structures when the exposure dose is higher than the one that the resist can sustain. The analysis of defects is presented later in the discussion.

The exposure of thick layers may present another problem related to the dose that the resist will receive. The thickness of the beams is decreasing from the bottom part to the top. This is again caused by the absorption of the light happening first in the bottom part of the structure with less photons arriving to the top part. In Fig. 41 the situation is presented with the measurements of the beam from the bottom to the top. The non-uniform exposure might be caused by the high intensity of the UV light coming from the lamp. The exposure dose is met with a short time but the bottom part of layer will receive the most of it. The time is simply not sufficient for the light to polymerize uniformly also the top layer (the exposure is from the bottom so the top layer is the one further away from the light source).



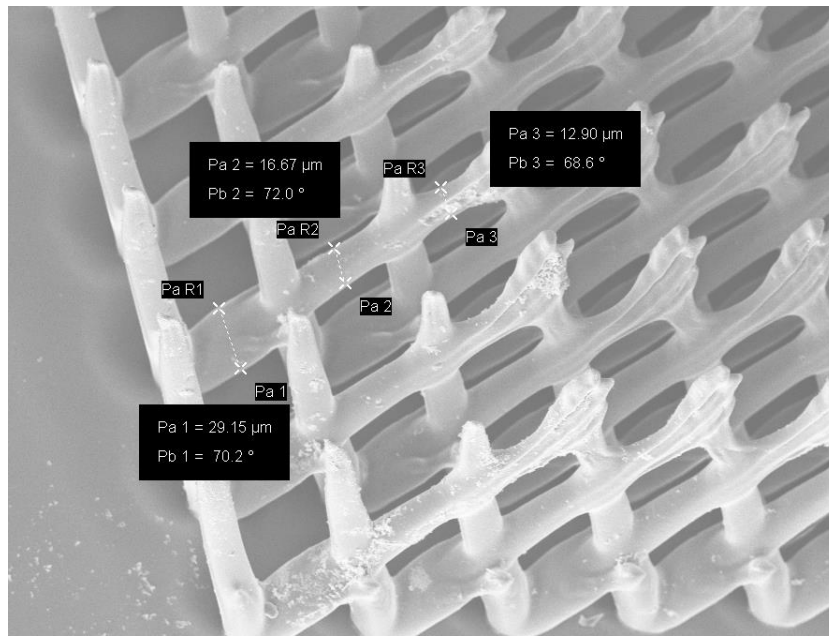


*Fig. 41 Inclined exposure mesh and measurements of the beam from the bottom to the top layer. Near the top the beam is less than half the thickness compare to the bottom.*

The structures that are reported here and characterized are all fabricated with the test pattern that was not created to test systematically the effects of the pattern dimensions to the fabricated structures. The analysis is done on the best samples obtained after several iterations. All kind of different pattern dimensions are present in the test sample so that some preliminary characterization and conclusions could be obtained. This study is not a comprehensive detail analysis of the pattern-structures relation. Further studies can be now carried on with the ready process and setup. The visual inspection of the meshes was very useful during the optimization in order to understand what parameters to change in the subsequent iteration.

### Analysis of the mesh structures

The basic structures in the pattern were simple rows of holes resulting in the inclined mesh in the Fig. 39. Some more different shapes of the opening in the mask are reported in the appendix. Different shapes of the mask's holes could potentially lead to novel structures that may have a precise application for them. Still further studies on those should be performed.

The spacing between rows is an important factor in the fabrication due to the emerging defects in structures too near to each other. Every time that the exposed areas are too near to each other the exposure dose might be too high and defects will appear (Fig. 52). After the discovery of this issue the subsequent structures were fabricated at a suitable distance to avoid these defects.

The primary features of the mesh is its openings size, the beams dimensions and inclination angle. In Fig. 42 the differences of aperture size in the structure when the mask's holes diameter is changed are shown.

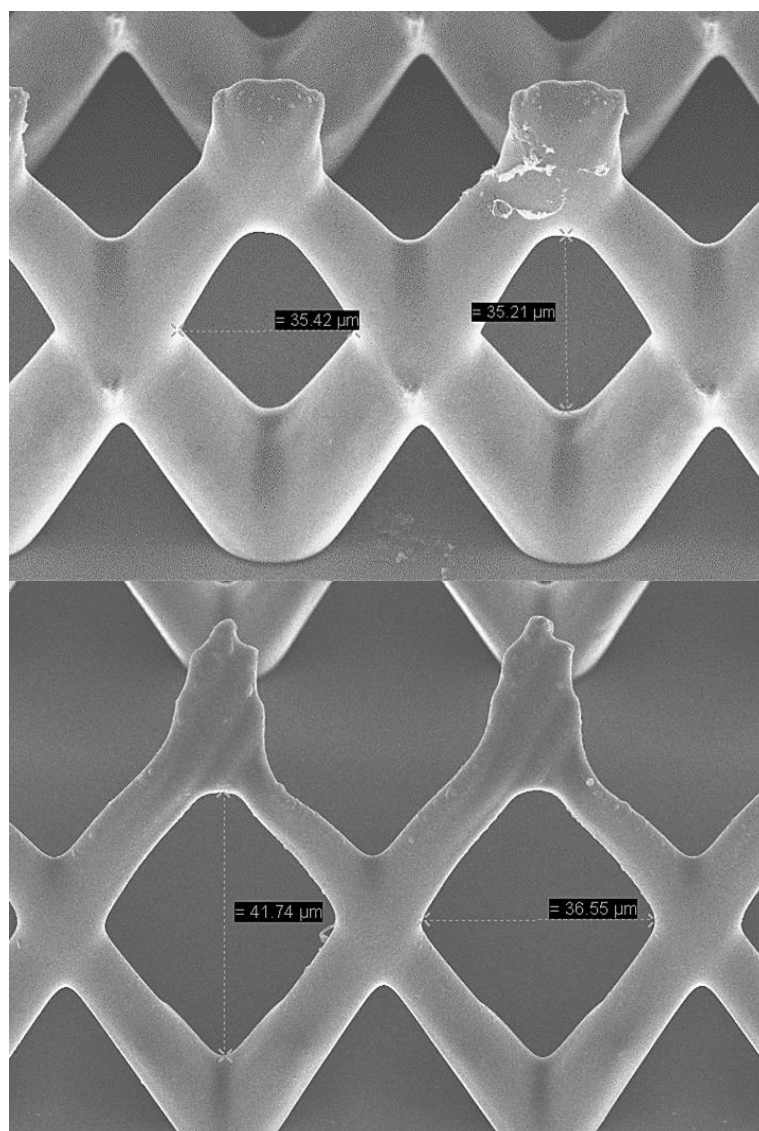


*Fig. 42 Structures in a 75  $\mu\text{m}$  thick SU-8 layer. On the top picture the structures are created by 15  $\mu\text{m}$  diameter holes while on the bottom one the holes were 10  $\mu\text{m}$  in diameter.*

In the picture on the top the holes on the mask are bigger and this is directly reflected on the size of the beams composing the mesh. Smaller holes in the mask will result in thinner beams (picture on the bottom Fig. 42) and bigger openings. The thickness of the layer is the same in both pictures (75  $\mu\text{m}$ ) and on the top of the structure we can notice that the exposure was not complete with the thinning of the extremities of the beams.

The separation of the holes in the pattern on the mask was the same in both structures (35  $\mu\text{m}$ ). This seems to reflect in the openings of the mesh since the horizontal dimension in both top and bottom structures is similar to the distance in the pattern (35,42  $\mu\text{m}$  on the left and 36,55  $\mu\text{m}$  on the right). The small difference is coming from the fact that in the bottom picture the structure's beams are thinner. The vertical

dimension of the holes is different between the two structures being 35,21  $\mu\text{m}$  on the top and 41,74  $\mu\text{m}$  on the bottom. This is one of the best examples to show how the dimensions of the apertures in the mesh is dependent directly on the size of the holes in the mask.

The number of openings in the mesh depends on both the thickness of the beams and, mostly, the distance between the holes in the mask. Fig. 43 shows two different structures fabricated in a 100  $\mu\text{m}$  SU-8 layer. On the left structure the bigger holes (20  $\mu\text{m}$ ) in the mask and larger separation (35  $\mu\text{m}$ ) between them creates only one opening in the mesh. On the right structure, on the other hand, both holes in the mask and separation are smaller (10  $\mu\text{m}$  holes with 25  $\mu\text{m}$ ) and the result is two opening in the mesh. The ratio between holes size and separation is 1,75 on the left and 2,5 on the right. These ratios, in combination with the exposure angle, determine the number of opening in the mesh for the specific thickness in consideration (100  $\mu\text{m}$ ). The nearest the beams will be the more they will intersect. The size of the opening is also directly related with the ratios, in addition to the thickness of the beams. If both thickness of the layer and the ratio holes size-separation is fixed then the holes size will, controlling the

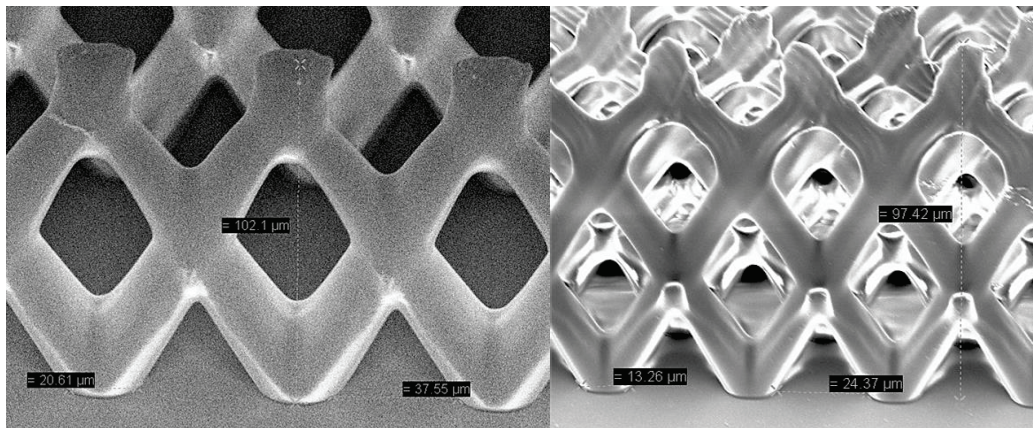


Fig. 43 Dimensions of the structures in 100  $\mu\text{m}$  thick SU-8 at 50° exposure angle. The height of the left structure is 102,1 $\mu\text{m}$  while in the right one is 97,42 $\mu\text{m}$ . The other values are indicating the approximate dimension of the holes in the mask and the spacing between them.

beams thickness, directly affect the openings dimensions. This is just an indication of how the holes size in the mask is related to the distance between them in the creation of the opening in the mesh. More specific analysis would be required to confirm the optimal ratio to obtain the required number of openings in the mesh.

The dimensions of the base of the beams and the separation are also measured with the SEM. The values are slightly higher than the one of the holes in the mask (on the left side of Fig. 43 the value of the base of the beams is 20,61  $\mu\text{m}$  while on the left side the beams are 13,26  $\mu\text{m}$ ). These differences are due to the presence of the under laying thin SU-8 layer that is completely cured prior to the inclined exposure. The bottom of the beams would result of the same dimension of the holes in the mask if the thin layer was not present.

The height of the structure is also measured with SEM (still Fig. 43). The values are both well into the precision range of the spinning step ( $\pm 5\%$ ) that in the case of a 100  $\mu\text{m}$  layer is  $\pm 5$   $\mu\text{m}$ . This is shown in Fig. 43 where the structures are 102  $\mu\text{m}$  and 97,4  $\mu\text{m}$

high. The measurements are the confirmation that the spinning step was correctly performed and that the exposure dose for that structures was good (or slightly low in the structure on the right).

The effect of light refraction is visible in the angles of the inclined structures. From the article by Ling and Lian [15], the exposed angle in the SU-8 should be less than  $30^\circ$  when the incident angle of the light is  $50^\circ$ . My calculation in Fig. 12 confirm this data, the refracted angle in the SU-8 should be around  $26^\circ$ - $27^\circ$ .

The angles of the structures measured with the SEM (Fig. 44) and the values were near to the expected ones. The angles measured are actually greater ( $30,8^\circ$ - $30,7^\circ$ ) and this is caused by distortion of the SEM images when the structures are seen inclined by  $50^\circ$

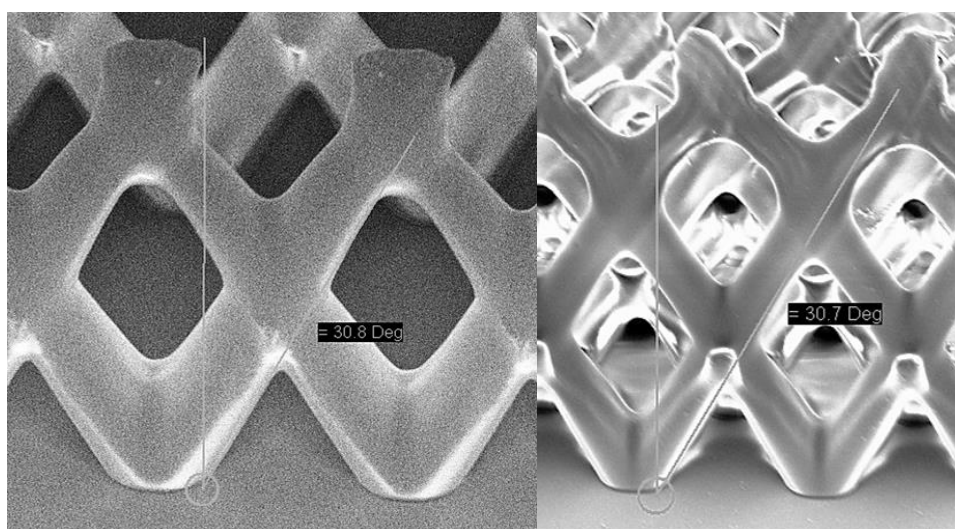


Fig. 44 Angle measurements for the structures fabricated at an exposure inclination of  $50^\circ$  in a  $100\ \mu\text{m}$  thick SU-8.

and the structures not being extremely precise. The angle in the real structures can vary for different reasons, mostly the narrowing of the mesh's beams towards the top of the structures. This is also making the actual measurement of the angle not straightforward. The few degree discrepancy between theoretical measurements and fabrication could even be completely due to the wrongly measured angle. That said the values of the angle are not too far off and they give a good idea on the fact that the refractive indexes difference is limiting the exposure angles.

### Contact angles measurements

Just to obtain some additional information contact angle measurements were performed on some of the structures to check whether the 3D mesh would be hydrophobic or hydrophilic. The structures were not designed so possess any of those but mealy as structural mesh. The test were performed using the contact angle measurements setup dropping a drop of water on the top of the structures and measuring the contact angle using the machine's software. The different structures (that were basically differing from one another by the holes size and distance in the mask) have a wide range of contact angle with water from  $70^\circ$  to  $145^\circ$ . This measurements was

more a proof of concept to see whether the mesh could be eventually used for creating super hydrophobic surfaces.

### Defects and possible improvements

After presenting the good sides of the fabricated structures the focus shifts on the defects of the structures and the problems encountered during the fabrication with some possible solution also reported.

To expose the whole SU-8 layer thickness a certain exposure dose is necessary with the bottom layer receiving a higher dose compare to the top. This situation is inevitable and defects in the structures are created, mostly in the bottom part of the structures, where the beams intersect. In these points the exposure dose is actually double thanks to the two exposures.

The defects on the meeting points are arising from the fact that the exposure dose in certain spots is excessive and the light is not anymore absorbed by the unexposed resist and it is polymerizing the resist also outside the wanted volume creating the protrusions on the first intersection of the beams (detailed on the right in Fig. 45). This protrusion are not formed in the intersection points higher in the structure since at that point the intensity of the light has already decreased due to the absorption of the SU-8.

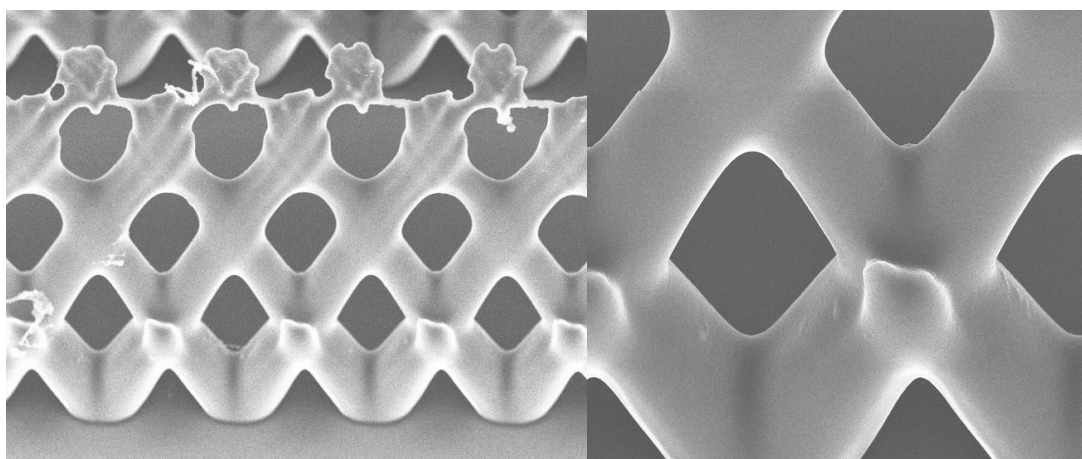


*Fig. 45 Defects on structures from a 100  $\mu\text{m}$  layer at 50° inclination. On the left we see both the overexposed areas on the meeting points of the beams near the bottom and the underexposed top part of the structures. On the right the zoomed view of the overexposure defects.*

Some of the defects are caused by underexposure of the top part of some structures (on the top of the left picture in Fig. 45). These defects are formed when the exposure dose is not sufficient to expose the whole layer if the light is coming from too small holes in the mask or if the exposure time is too short. The incomplete exposure is connected to the beams shrinkage from the bottom to the top (Fig. 41). The cause is a non-optimal exposure of the SU-8.

All the inclined exposure is done with a high intensity lamp (100 mW/cm<sup>2</sup>) because of the space necessary for the inclining stage that is not available in the MA-6 mask aligner. The UV setup used for the experiments is designed to be used for polymer curing. Its lamp power reflects that together with the poor control of the exposure time. The intensity is too high for good lithography where the accurate control of the exposure



dose in the sample is fundamental. Even though the exposure dose when using a powerful lamp for a short time or a less powerful lamp for a longer time is the same the results are usually not. Usually mask aligners have a power of 20-25 mW/cm<sup>2</sup> so around a quarter of the power of the UV light used for inclined lithography.

The lower power is beneficial because, during the exposure, there will be a lower photon density going through the resist layer and the polymerization will proceed slower into the layer compared to a high photon density exposure. Being the SU-8 a chemical amplified resist a single photon is initiating multiple polymerizations and the lower photon density will create a more uniform and controlled polymerization. The high photon density is causing unwanted polymerization in the layer near to the mask but then when the light is moving through the resist layer the dose is reduced and the beams are defects free while at the same time their diameter is decreased.

When analysing the size of the beams in the right side of Fig. 46 the beams made with the first exposure result always with a smaller diameter while the second exposure is creating bigger beams even though the exposure dose is the same. This is caused by the fact that the already exposed SU-8 is not absorbing photons as much as the unexposed one so that when the beams are formed during the second exposure they will receive higher dose after each intersection points.

To solve these problems and to eliminate the defects the best solution could be to use a less powerful lamp so that the dose can be better controlled exposing the sample for a longer time making the exposure more uniform through the SU-8 layer.

The thinning of the beams deep in the layer may be an intrinsic problem caused by the way the resist works and a solution could be impossible. Changing the resist is the only possibility to obtain the meshes in very thick layers (hundreds of  $\mu\text{m}$ ).

The fact that the mask used throughout the work was not optimized for the specific thickness but rather a collection of different patterns is creating a lot of defects that are then used to understand the working principle of the technology so that the optimization of a specific pattern for a specific sample can be performed. The final solution for most of the defects is a mixture of the general ways and then optimization of the process for the optimized pattern.

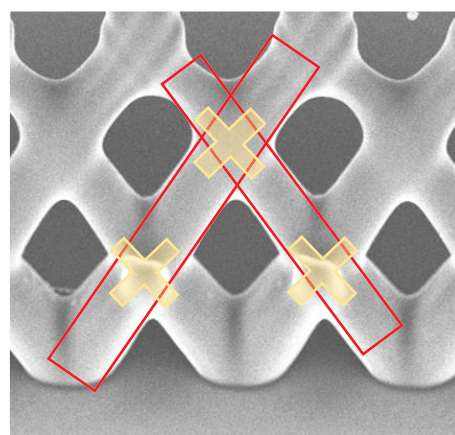


*Fig. 46 Detailed view of the difference in size of beams produced by the first (smaller rectangle) and the second (bigger rectangle) exposure. The intersection points are shown as yellow crosses.*

### Multiple exposure experiments

As the last development in the work some testing of four time exposure was done. The mask has a pattern of holes in a large area and the sample had an SU-8 layer on top of the Al mask that was 30  $\mu\text{m}$  thick. The layer was exposed four times for 2 s with a rotation of 90° after each one. The stage was inclined at 50°. A SEM picture of the result is shown here (Fig. 47) and this is just a proof of concept for now that could be developed into new applications later on.

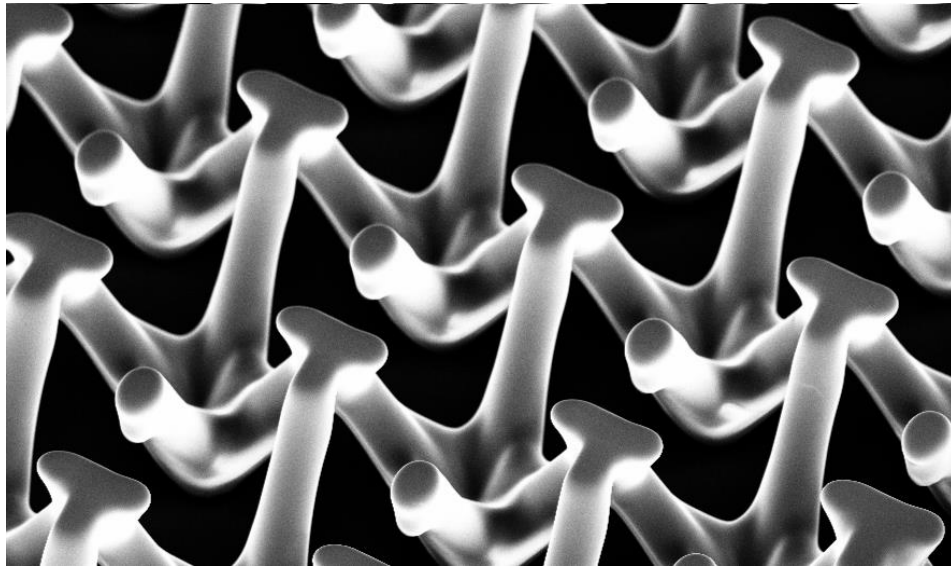


*Fig. 47 Structures fabricated using four exposure with the sample rotated 90° after each of them. From this picture is possible to visualize half of the box that could be created with a layer double the thickness.*

To perform multiple inclined exposure the equipment should be improved with the addition of another rotating stage on top of the existing one so that the sample could be turned easily while maintaining the angle set at the needed position. With a more expensive motorized rotating stage it would be possible to perform rotating inclined lithography still utilizing the same setup.

## 6. Conclusions and final remarks

In this section I will present ideas for applications and new processing that could be achieved if the work will be continued in the future. The applications for this kind of structures is ranging from microfluidics to chemical catalysis to mechanical enhanced structures.

Many microfluidic application were presented in the thesis but new application are now available when using the 3D meshes. When fabricated using four exposures rotated 90° from each, a 'cubic box' is obtained. The idea is to utilise these boxes cells incubators with the size of the box tuneable during the fabrication to match the cells size. An array of cells incubators is quickly produced with the cells occupying their own box or sharing it with a set number of other cells. The incubators can also be fabricated inside a microfluidic circuit to obtain a complete device. The cells could be loaded in the circuit and then transported to the incubator, where different experiments could be carried out. Eventually the incubators could be washed and reused again. The big advantage of using inclined lithography is that the fabrication of single box inside a small channel or arrays of boxes of different dimensions is as simple as two lithography steps.

Another interesting way to enhance the 3D inclined structure is to use coatings on them. Utilizing again the boxes array, the addition of coatings will make possible another set of experiments. The interaction of the cells with different materials can be studied on both single cells and groups of them. The meshes could also be used inside a microfluidic channel, as mixers for instance, where a catalyst coated on their surface would catalyse some chemical reactions.

The dimensions of the mesh can be tailored specifically for the application. In the case of catalysis the volume to surface ratio needs to be maximized to increase the catalysis power of the structure. Thin beams and a large number of openings will be necessary for this. The mesh structures possess an intrinsic high mechanical resistance to compression thanks to their shape [12]. Large areas with 3D meshes could provide mechanical support in a device. The use the meshes obtained from four exposures as flexible support in between two metal layers would enable the fabrication of a micro balance. The capacitance between the two metal layers would change when their distance is modified upon compression, with the meshes maintaining this distance in the wanted range. The shape of the mesh will ensure that the device will revert back to its initial stated after the compression is lifted.



Thinking outside of the box and trying to imagine some fancy processes we could arrive to the fabrication of structures that are now highly improbable. The fabrication flow in Fig. 48 is the example. The unexposed SU-8 layer is casted inside holes on thick positive resist to create columns of unexposed SU-8.

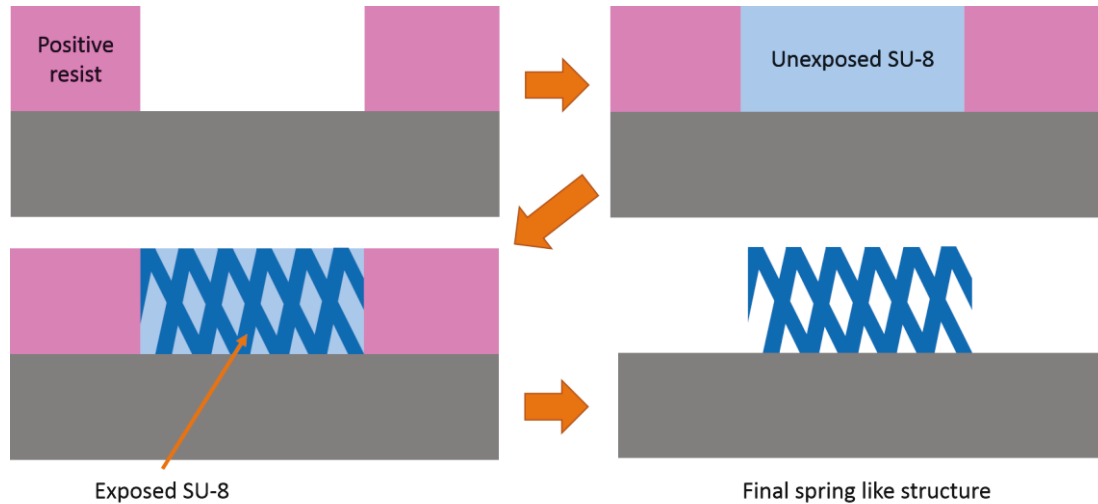


Fig. 48 Simple fabrication idea utilising positive tone resist to confine the unexposed SU-8. Then utilizing inclined lithography we can fabricate spring like structures in the SU-8.

In this way the mesh structure resulting from the inclined exposure of SU-8 will be confined in the horizontal dimensions as well as in the vertical dimension (due to the limited thickness of the layer). The inclined exposure is done for four times with the wafer rotated 90 every time. The four exposures will create the spring like structure inside the SU-8 columns. The beams are made as thin as possible to maximize the free space. When the SU-8 is developed and the positive resist is removed the structure resulting will be the spring made of SU-8. In order for this idea to work the fabrication of the beams must be highly optimized to ensure that the structure would be defect free. Many of these applications are only ideas and proof of concept that could be eventually fabricated if more research, in the processing of inclined lithography, I carried out.

Inclined lithography is a technology that is still at the beginning of its development even though the basic principles have been known for decades. The absence of some sort of standard in the processing gives the researchers a big freedom when developing their own inclined lithography processes. The setup and the processes developed in this work are part of the contribution to the development of the technology.

The inclinable stage built for this work was designed to fit a wide variety of devices that would require inclined lithography structures. The simplicity of the design makes it suitable for quick modifications. The design of a novel setup is always positive (when better options are not available) to create knowhow benefitting both me and the Microfabrication group, as well as the scientific field as a whole.

During the work different kind of mesh structures were fabricated in SU-8 layer ranging from 100 to 50  $\mu\text{m}$  thick obtaining different structures with good success in some cases.

The 3D mesh was also fabricated inside a microfluidic channel to demonstrate the possible integration of the inclined exposure structures with existing designs.

The quality of the fabricated structures are not dependent on the setup used for the inclined exposure but on the processing parameters such as exposure dose and SU-8 baking. The setup is responsible only for the reflection of the light from the stage and that problem was solved during the work. The processing parameters are, as now, limiting the fabrication of thick SU-8 layers because of the defects that are forming when we use the higher exposure dose required by the thick layer. The improvement on the exposure setup should boost the quality of the fabricated structures.

The structures fabricated in this work are not novel. Examples of similar structures are found in many articles cited throughout the thesis. The novelty in this work is the setup and the process developed that made possible the creation of new ideas. This work created the basis and the continuation of the research will eventually end with the fabrication of novel structures

One of the goal of this work was the creation of a cheap and simple process that could potentially be done completely outside of a cleanroom facility with inexpensive equipment. The setup is cheap, simple and it can be used with almost any UV light sources (provided enough space to fit it). The SU-8 processing is easily done in a normal laboratory space while the only step that needs specific and expensive equipment is the alignment of an external mask to the one present on the sample. If this issue could be solved then the process developed here would give the possibility to scientist to produce good quality 3D structures without the need for expensive equipment.

When inclined lithography fabricated structures are compared to others from different technology fields the first that come to mind are the ones from 3D printing. Similar 3D mesh structures are easily fabricated out of different hard polymers using 3D printing with the fundamental difference of feature size and the ratio area/speed of fabrication. One example of 3D printed meshes is present in the work of Balasubramanian et al. [64] where the mesh structures are used in thermally activated microfluidic structures. When a polymer with low enough glass transition temperature is used its rigidity can be modified with the use of the temperature. When the temperature is higher than the  $T_g$  the polymer will soften going then back to the original state when the temperature is lowered. An actuator could be then fabricated using this process or, in the case of the mesh structures by inclined lithography, different parts of a microfluidic device could be modified reversibly using only temperature difference. The biggest difference of this work to mine is the feature size in the order of mm while with inclined lithography the structures are easily fabricated in the order of  $\mu\text{m}$  with a better quality.

The structures fabricated with the two methods, although similar to each other, are used in different applications with all the microfluidic applications out of the reach of 3D printing but well in range for inclined lithography. The research needs to be continued since the 3D printing technology is advancing rapidly lowering the maximum features size barrier. The advantages of the inclined lithography are still strong with the fact that with lithography the speed of processing nor the quality of the structures are lowered if the device area is increased. This, the smaller features size achievable and the other characteristics discussed in this work must be the focus of the research in the

future so that the technique will keep improving with time giving a better tools to researcher to carry on their work in ever expanding different fields of science.

The most fascinating side of the inclined lithography technique, beside the already powerful fabrication capability, is the novelty of the process that gives possibilities to the researcher to discover and invent new and unexplored fields in the microfabrication technology.

## References

- [1] F. Faggin, M. Hoff and S. Mazor, "Memory system for a multi chip digital computer". USA Patent 3,821,715 , January 1973.
- [2] F. Faggin, "The history of the 4004," *Micro, IEEE*, vol. 16, no. 6, pp. 10-20, 1996.
- [3] W. Schrott, M. Svoboda, Z. Slouka, M. Pribyl and D. Snita, "PDMS microfluidic chips prepared by a novel casting and prepolymerization method," *Microelectronic engineering*, vol. 87, no. 5, pp. 1600-1602, 2010.
- [4] A. Bhagat, H. Bow, H. How, S. Tan, J. Han and C. Lim, "Microfluidics of cell separation," *Medical & Biological engineering & computing*, vol. 48, no. 10, pp. 999-1014, 2010.
- [5] P. Ang, A. Li, M. Jaiswal, Y. Wang, H. Hou, J. Thong, C. Lim and K. Loh, "Flow sensing of single cell by graphene transistor in a microfluidic channel," *Nano letters*, vol. 11, no. 12, pp. 5240-5246, 2011.
- [6] W. Biggs, A. Edison, J. Eastin, K. Brown, J. Maranville and M. Clegg, "Photosynthesis Light Sensor and Meter," *Ecology*, vol. 52, no. 1, pp. 125-131, 1971.
- [7] K. Kunz, P. Enoksson and G. Stemme, "Highly sensitive triaxial silicon accelerometer with integrated PZT thin film detectors," *Sensors and actuators A*, vol. 92, pp. 156-160, 2001.
- [8] A. Han, O. Wang, M. Graff, S. Mohanty, T. Edwards, K. Han and A. Frazier, "Multi-layer plastic/glass microfluidic systems containing electrical and mechanical functionality," *Lab on a chip*, vol. 3, no. 3, 2003.
- [9] B. Zheng, J. Tie, L. Roach and R. Ismagilov, "A Droplet-Based, Composite PDMS/Glass Capillary Microfluidic System for Evaluating Protein Crystallization Conditions by Microbatch and Vapor-Diffusion Methods with On-Chip X-Ray Diffraction," *Angewandte Chemie-international edition*, vol. 43, no. 19, pp. 2508-2511, 2004.
- [10] R. de Campos, I. Yoshida and J. de Silva, "Surface modification of PDMS microchips with poly(ethylene glycol) derivatives for  $\mu$ TAS applications," *Electrophoresis*, vol. 35, no. 16, pp. 2346-2352, 2014.
- [11] Sato, H. Matsumura, S. Keino and S. Shoji, "An all SU-8 microfluidic chip with built-in 3D fine microstructures," *Journal of Micromechanics and Microengineering*, vol. 16, pp. 2318-2322, 2006.
- [12] T. A. Schaedler, A. J. Jacobsen, A. Torrents, A. E. Sorensen, J. Lian, J. R. Greer, W. B. Valdevit and W. B. Carter, "Ultralight metallic microlattices," *Science*, no. 334, pp. 962-965, 2011.
- [13] M. Han, W. Lee, S.-K. Lee and S. S. Lee, "3D microfabrication with inclined/rotated UV lithography," *Sensors and actuators A*, no. 111, pp. 14-20, 2004.

- [14] G. Jiang, K. Shen and M. Wang, "Fabrication of 3D Micro- and Nano-Structures by Prism-Assisted UV and Holographic Lithography (Chapter 10)," in *Updates in advanced lithography*, InTech (open access book), 2013, pp. 227-252.
- [15] Z. Ling, "SU-8 3D microoptic components fabricated by inclined UV lithography in water," *Microsystem technology*, no. 13, pp. 245-251, 2007.
- [16] L. Meza, S. Das and J. Greer, "Strong, lightweight, and recoverable three-dimensional ceramic nanolattice," *Science*, vol. 354, no. 6202, pp. 1322-1326, 2014.
- [17] W. M. Moreau, *Semiconductor lithography principles, practices and materials*, Plenum press, 1988.
- [18] J. S. Kilby, "The integrated circuit's early history," *Proceedings of the IEEE*, vol. 88, no. 1, pp. 109-111, 2000.
- [19] H. Shlomo and M. Auslender, "Single-Crystal Silicon: Electrical and Optical Properties," in *Springer Handbook of Electronic and Photonic Materials*, Springer US, 2007, pp. 441-480.
- [20] S. Franssila, *Introduction to Microfabrication*, 2nd ed., Wiley, 2010.
- [21] H. K. Wen, B. Min-Hang and H. Yeun-Ding, "A high-sensitivity integrated-circuit capacitive pressure transducer," *IEEE transactions on electron devices*, vol. 29, no. 1, pp. 48-56, 1982.
- [22] T. Rogers and J. Kowal, "Selection of glass, anodic bonding conditions and material compatibility for silicon-glass capacitive sensors," *Sensors and Actuators A: Physical*, vol. 46, no. 1-3, pp. 113-120, 1995.
- [23] W. H. Grover, A. M. Skelley, C. N. Liu, E. T. Lagally and R. A. Mathies, "Monolithic membrane valves and diaphragm pumps for practical large-scale integration into glass microfluidic devices," *Sensors and actuators B*, vol. 89, pp. 315-323, 2003.
- [24] J. Nilsson, M. Evander, T. Hammarström and T. Laurell, "Review of cell and particle trapping in microfluidic systems," *Analytica chimica acta*, vol. 649, no. 2, pp. 141-157, 2009.
- [25] P. Abgrall and G. A-M, "Lab-on-chip technologies: making a microfluidic network and coupling it into a complete microsystem—a review," *Journal of Micromechanics and Microengineering*, vol. 17, no. 5, 2007.
- [26] J. Mellros, V. Gorbounov, R. Ramsey and J. Ramsey, "Fully Integrated Glass Microfluidic Device for Performing High-Efficiency Capillary Electrophoresis and Electrospray Ionization Mass Spectrometry," *Analytical chemistry*, vol. 80, pp. 6881-6887, 2008.
- [27] N.-N. Deng, Z.-J. Meng, R. Xie, X.-J. Ju, C.-L. Mou, W. Wang and L.-Y. Chu, "Simple and cheap microfluidic devices for the preparation of monodisperse emulsions," *Lab on a chip*, vol. 11, pp. 3963-3969, 2011.

- [28] X. Liu, W. Wu, Z. Wang, Z. Luo, Y. Liang and F. Zhou, "A replication strategy for complex micro/nanostructures with superhydrophobicity and superoleophobicity and high contrast adhesion," *Soft matter*, vol. 5, no. 16, pp. 3097-3105, 2009.
- [29] Y. Yoon, D. Kim and J.-D. Lee, "Hierarchical micro/nano structures for super-hydrophobic surfaces and super-lyophobic surface against liquid metal," *Micro and Nano Systems Letters*, vol. 2, no. 3, 2014.
- [30] V. Jokinen, P. Sakha, P. Suvanto, C. Rivera, S. Franssila, S. Lauri and H. Huttunen, "A microfluidic chip for axonal isolation and electrophysiological measurements," *Journal of Neuroscience Methods*, vol. 212, pp. 276-282, 2013.
- [31] G. Scotti, D. Trusheim, P. Kanninen, D. Naumenko, M. Schulz-Ruthenberg, V. Snitka, T. Kallio and S. Franssila, "Picosecond laser ablation for silicon micro fuel cell fabrication," *journal of micromechanics and microengineering*, vol. 23, pp. 1-14, 2013.
- [32] V. Cadarso, K. Pfeiffer, U. Ostrzinski, A. Voigt, G. Gruetzner and J. Brugger, "FAST PROTOTYPING OF  $\mu$ TAS BY DIRECT LASER WRITING," in *16th international conference on miniaturized systems for chemistry and life science*, Okinawa, Japan, 2012.
- [33] M. Brunet, T. O'Donnel, J. O'Brien, P. McCloskey and S. Mathuna, "Thick photoresist development for the fabrication of high aspect ratio magnetic coils," *Jornal of micromechanics and microengineerings*, vol. 12, pp. 444-449, 2002.
- [34] S.-Y. Moon and J.-M. Kim, "Chemistry of photolithographic imaging materials based on the chemical amplification concept," *Journal of photochemistry and photobiology C: Photochemistry reviews*, vol. 8, pp. 157-173, 2007.
- [35] Microchem, *SU-8 50 material safety sheet*, 2001 (12 december).
- [36] A. Campo del and C. Greiner, "SU-8: a photoresist for high-aspect-ratio and 3D submicron lithography," *journal of micromechanics and microengineering*, no. 17, pp. R81-R95, 2007.
- [37] W. Teh, U. Dürig, U. Drechsler, C. Smith and H.-J. Güntherodt, "Effect of low numerical-aperture femtosecond two-photon adsorption on (SU-8) resist for ultrahigh-aspect-ratio microstereolithography," *journal of applied physics*, no. 97, 2005.
- [38] R. Martinez-Duarte and M. Madou, "SU-8 Pholithography and its impact on microfluidics," in *Microfluidics and Nanofluidics Handbook: Fabrication, Implementation and Applications*, NewYork, CRC Press, 2011, pp. 231-268.
- [39] T. Anhoj, A. Jorgensen, D. A. Zauner and J. Hübner, "The effect of soft bake temperature on the polymerization of SU-8 photoresist," *Jornal of micromechanics and microengineering*, vol. 16, pp. 1819-1824, 2006.
- [40] Microchem, *Nano SU-8 50-100 data sheet*, Rv.2/02.
- [41] Microchem, *SU-8 3000 material safety data sheet*, 2009 (13 april).

- [42] S. Preuss and M. Stuke, "Sub-Picosecond UV laser ablation of metals," *Applied physics A*, vol. 61, no. 1, pp. 33-37, 1995.
- [43] A. Lyuovich, K. Maile, A. Gusko, K. Ashurov and S. Morozov, "Characterisation of the generation of ions in electron beam evaporator for the control of metal deposition processes," *Surface and coating technology*, Vols. 151-152, pp. 105-109, 2002.
- [44] I. Blech, "Evaporated film profiles over steps in substrates," *Thin solid films*, vol. 6, no. 2, pp. 113-118, 1970.
- [45] Seshan and Krishna, *Handbook of Thin Film Deposition - Techniques, Processes, and Technologies*, Elsevier, 2002.
- [46] A. Porcellato, V. Palmieri, L. Bertazzo, A. Capuzzo, D. Giora, F. Stivanello, S. Stark and S. Kar, "Production, installation and test of Nb-sputtered QWRs for ALPI," *Pramana*, vol. 59, no. 5, pp. 871-880, 2002.
- [47] G. Abadias and P. Guerin, "In situ stress evolution during magnetron sputtering of transition metal nitride thin films," *Applied physics letters*, vol. 93, p. 11908, 2008.
- [48] D. S. Gardner, X.-C. Mu and D. Fraser, "Method for the anisotropic etching of metal films in the fabrication of interconnects". U.S.A. Patent US5350484 A, 27 september 1994.
- [49] J. Bhardwaj, H. Ashraf and A. McQuarrie, "Dry silicon etching for MEMS," in *Symposium on Microstructures and Microfabricated systems at the Annual meeting of the electrochemical society*, Quebec, Canada, 1997.
- [50] F. Marty, L. Rousseau, B. Saadany, B. Mercier, O. Français, Y. Mita and T. Bourouina, "Advanced etching of silicon based on deep reactive ion etching for silicon high aspect ratio microstructures and three-dimensional micro- and nanostructures," *Microelectronics journal*, vol. 36, pp. 673-677, 2005.
- [51] L. Laerme, A. Schilp, K. Funk and M. Offenberger, "Bosch deep silicon etching: improving uniformity and etch rate for advanced MEMS applications," in *Micro electro mechanical systems*, Orlando, FL, USA, 1999.
- [52] H. Winters and J. Coburn, "The etching of silicon with XeF<sub>2</sub> vapour," *Applied physics letters*, vol. 34, p. 70, 1979.
- [53] M. J. Madow, *Foundamentals of Microfabrication 2 ed.*, CRC press, 2002.
- [54] G. Jiang, S. Baig and M. R. Wang, "Prism-assisted inclined UV lithography for 3D microstructure fabrication," *Journal of micromechanics and microengineering*, no. 22, pp. 1-8, 2012.
- [55] T. Suzuki, H. Yamamoto, M. Ohoka, A. Okonogi, H. Kabata, I. Kanno, M. Washizu and H. Kotera, "Hight throughput cell electroporation array fabricated by single-mask inclined lithography exposure and oxygen plasma etching," in *transudecs & eurosensors '07*, Lyone, France, 2007.

- [56] Y.-K. Yoon, J.-H. Park and M. Allen, "Multidirectional UV lithography for complex 3-D MEMS structures," *Journal of microelectromechanical systems*, vol. 15, no. 5, pp. 1121-1130, 2006.
- [57] Microresist technology GmbH, *Removers mr-Rem 660, mr-Rem 400 and mr-Rem 500 Process guidelines*, Berlin: Microresist technology gmbh, July 2013.
- [58] T. Shimizu, Y. Murakoshi, Z.-J. Wang, R. Maeda and T. Sano, "Microfabrication technique for thick structure of metals and PZT," vol. 3680, pp. 472-477, 1999.
- [59] k. Al-Arife, G. Knopf and A. Bassi, "Reconfigurable microfluidic chip based on a light-sensitive hydrogel," in *Optomechatronics actuators, manipulation, and systems control; Proc. of SPIE Vol. 6378*, 2006.
- [60] P. Obreja, D. Cristea, E. Budianu, R. Gavrilă, M. Kusko and V. Kuncser, "Poly (vinyl-alcohol) films for microphotonics," in *International Conference on Microelectronics - ICM*, 2004.
- [61] Microresist technology, *Negative tone photoresist series ma-N 1400*, Berlin, Germany, 22 february 2012§.
- [62] A. Voigt, M. Heinrich, K. Hauck, R. Mientus, G. Gruetzner, M. Töpfer and O. Ehrmann, "A single layer negative tone lift-off photo resist for patterning a magnetron sputtered Ti/Pt/Au contact system and for solder bumps," *Microelectronic engineering*, Vols. 78-79, pp. 503-508, 2005.
- [63] S. Tuomikoski and S. Franssila, "Free-standing SU-8 microfluidic chips by adhesive bonding and release etching," *Sensors and actuators A*, vol. 120, pp. 408-415, 2005.
- [64] A. Balasubramanian, M. Standish and C. Bettinger, "Microfluidic Thermally Activated Materials for Rapid Control of Macroscopic Compliance," *Advanced Functional Materials*, vol. 24, no. 30, p. 4860–4866, 2004.
- [65] G. Michler, *Electron microscopy of polymers*, Berlin: Springer-Verlag, 2008.
- [66] J. Lee, W. Choi, K. Lee and J. Yoon, "A simple and effective fabrication method for various 3D microstructures: backside exposure 3D diffuser lithography," *Journal of micromechanics and microengineering*, vol. 18, pp. 1-7, 2008.



## Table of figures

|  |    |
|--|----|
| <i>Fig. 1 Fabrication of a device using a single step lithography and a positive tone photoresist. a) Exposure of the resist through a mask, b) Development of the resist will dissolve away the exposed areas, c) The substrate is etched only in the areas non protected by the resist.</i>  | 5  |
| <i>Fig. 2 Difference between the positive tone resist on the left and the negative resist on the right. After development the exposed areas will be removed in the positive resist resulting in positive sloped walls while in the negative resist the exposed areas remain with negative sloped walls. From [20]</i>  | 6  |
| <i>Fig. 3 Chemical formula of the Novolak resin, main component of SU-8. From [53]</i>   | 8  |
| <i>Fig. 4 Components of the ma-N 1400 series resist. The Novolak is the main component of the resist while the Aromatic Bisazide is the optically active one.</i>  | 11 |
| <i>Fig. 5 Generation of nitrenes during the exposure of the resist. This reaction is the starting point of the polymerization of the novolak resin.</i>  | 11 |
| <i>Fig. 6 After the Aromatic Bisazide is activated it will promote the polymerization of the Novolak resin resulting in higher molecular weight compounds.</i>   | 12 |
| <i>Fig. 7 Magnetic and electric fields in a magnetron. a) The magnetic field is going from one magnet to the other and it is perpendicular to the electric field at half of the magnets distance creating the ExB drift path where the electrons are confined. In b) the drift path can be notice in its spiral motion over the target.</i>  | 15 |
| <i>Fig. 8 Lift-off processing work flow. The resist used is negative tone to obtain the V shaped walls that will help the stripping of the resist using acetone or a proper resist stripping solution.</i>   | 18 |
| <i>Fig. 9 Schematic of the inclined lithography and the final structure resulting from it..</i>  | 20 |
| <i>Fig. 10 Differences of the front side lithography on the left and the back side lithography on the right. On both picture the resist is positive tone and it is easy to visualize the exposed areas that are removed. When the exposure is performed from the bottom the base of the structures will be attached to the substrate. The opposite situation will happen with front side lithography.. The diffuser in the picture is inspired by [66]</i> | 21 |
| <i>Fig. 11 Relations between the incidence angles of the UV light when refracted travelling through different materials (air to glass and finally to SU-8). From [56]</i>  | 22 |
| <i>Fig. 12 Relation between exposure angle and refracted angle in the SU-8. The angle in the SU-8 is always smaller than the exposure angle and it is limited to values below 35°.</i>   | 23 |
| <i>Fig. 13 Structures fabricated with inclined lithography from the top side and bottom side on the bottom right. From [13]</i>  | 24 |
| <i>Fig. 14 Inclined lithography setup used in [13]. The setup is using just a UV light source and a tilting stage to hold the sample with a rotating motor integrated in it.</i>   | 24 |
| <i>Fig. 15 Schematic of the topside reflection inclined lithography and the resulting structures on the right. From [13].</i>  | 24 |
| <i>Fig. 16 On the left the setup used for the inclined exposure and on the right the process flow followed by the authors. (a) The mask is placed on the topside of the resist layer, (b) First exposure at a certain inclination angle, (c) second exposure at the same angle and finally the final structure in (d). From [56]</i>   | 25 |
| <i>Fig. 17 On the left side the microfluidic channel with the mesh structures inside of it and on the right the zoomed image of the mesh structure where we can appreciate the dimensions. From [11]</i>   | 26 |
| <i>Fig. 18 Example of a filter for microfluidics made out of a mesh structure fabricated with frontside inclined exposure. From [56]</i>   | 26 |

|  |    |
|--|----|
| <i>Fig. 19 Holder for optical fibres fabricated with inclined lithography of SU-8. a) the structure and b) with the fibre in place. From [15].</i>   | 27 |
| <i>Fig. 20 The mesh structure "filter" in action while breaking a big droplet into smaller ones inside a microfluidic channel. From [11]</i>   | 27 |
| <i>Fig. 21 Inclined lithography of thiol-ene monomers to obtain the final metal hollow metal mesh. a) the schematic of the exposure, b) exposed polymer and c) the polymer structure coated with the Nickel. The details of the structure are also illustrated. From [12]</i>                                  | 28 |
| <i>Fig. 22 Schematic of the inclined lithography assisted by the prism. The maxim exposure angle can be raised from 35° to 60° thanks to the reflections inside the prism. From [54]</i>   | 29 |
| <i>Fig. 23 Inclined structures fabricated using a combination of a slanted stage at different inclinations and a 45° prism. From [54]</i>  | 30 |
| <i>Fig. 24 Structure fabricated in SU-8 using a pyramid prism and traditional lithography. The inclination of prism's walls is refracting the light that creates the inclined structures when exposing the SU-8. From [14]</i>   | 30 |
| <i>Fig. 25 Process flow for generic back side exposure of SU-8 using a mask directly on the wafer. Information about the steps are found in the text.</i>  | 34 |
| <i>Fig. 26 Process flow for the fabrication of inclined exposure structures.</i>   | 36 |
| <i>Fig. 27 Schematic of the inclining stage. The support frame is 16 cm high and around 14 cm long. The rotating stage's dimensions are 8 by 5 cm.</i>   | 37 |
| <i>Fig. 28 Sample on the inclined lithography setup before exposure. The sample is attached simply with tape and this is not creating any problems since the SU-8 layer is touching the stage and the tape is attached to the glass support.</i>   | 38 |
| <i>Fig. 29 Pictures of the inclined lithography equipment showing the supporting frame and the rotating stage with the antireflection material attached. On the right a close up on the angles scale on the rotating stage.</i>  | 39 |
| <i>Fig. 30 DYMAX ECE 2000 setup as used in the experiments. From the manufacturer website.</i>   | 40 |
| <i>Fig. 31 Pictures showing the difference in walls slope when the developing time is longer at the same exposure dose. On the picture a) the developing time is 3:30 minutes and in d) 5 minutes. B) and c) are in between with 4 and 4:30 minutes respectively.</i>  | 42 |
| <i>Fig. 32 V-shaped resist's 2 <math>\mu\text{m}</math> lines and an evaporated metal layer that is deposited only in the areas not covered by the resist.</i>   | 43 |
| <i>Fig. 33 Schematic showing the sample ready after the multilayer SU-8 is spinned. The thickness of the exposed bottom layer is around 10 <math>\mu\text{m}</math> (and it could be also smaller) while the top unexposed layer thickness varies between samples from 50 to 100 <math>\mu\text{m}</math>.</i> | 45 |
| <i>Fig. 34 On the left the schematic of the first lithography to pattern the channels. On the right the second lithography (inclined) is performed to pattern the 3D structures inside the channel.</i>  | 45 |
| <i>Fig. 35 The inclined SU-8 structure after development while still on top of the carrier glass wafer.</i>  | 46 |
| <i>Fig. 36 Schematic of the bonding method using the PVA as release layer between the capping SU-8 and the carrier transparency.</i>   | 47 |
| <i>Fig. 37 Finished device with the capping layer bonded on top of it. Still the glass carrier is present.</i>   | 48 |
| <i>Fig. 38 Final all SU-8 device. The inclined structures are enclosed by the bottom layer and the capping bonded layer. At this point all the microfluidic channel are sealed and the device is ready to use.</i>   | 48 |
| <i>Fig. 39 The mesh structure inside a microfluidic channel fabricated using 10 <math>\mu\text{m}</math> holes in the mask, 50° exposure orientation and a 100 <math>\mu\text{m}</math> thick SU-8 layer. On the right the zoomed detail of the structure.</i>   | 49 |

|   |    |
|---|----|
| <i>Fig. 40 Inclined structure made with mask's holes size of 20 <math>\mu\text{m}</math>. The dose used for the sample was not enough to expose the whole 75 <math>\mu\text{m}</math> SU-8 layer.</i>   | 50 |
| <i>Fig. 41 Inclined exposure mesh and measurements of the beam from the bottom to the top layer. Near the top the beam is less than half the thickness compare to the bottom.</i>   | 51 |
| <i>Fig. 42 Structures in a 75 <math>\mu\text{m}</math> thick SU-8 layer. On the top picture the structures are created by 15 <math>\mu\text{m}</math> diameter holes while on the bottom one the holes were 10 <math>\mu\text{m}</math> in diameter.</i>  | 52 |
| <i>Fig. 43 Dimensions of the structures in 100 <math>\mu\text{m}</math> thick SU-8 at 50° exposure angle. The height of the left structure is 102,1<math>\mu\text{m}</math> while in the right one is 97,42<math>\mu\text{m}</math>. The other values are indicating the approximate dimension of the holes in the mask and the spacing between them.</i>   | 53 |
| <i>Fig. 44 Angle measurements for the structures fabricated at an exposure inclination of 50° in a 100 <math>\mu\text{m}</math> thick SU-8.</i>   | 54 |
| <i>Fig. 45 Defects on structures from a 100 <math>\mu\text{m}</math> layer at 50° inclination. On the left we see both the overexposed areas on the meeting points of the beams near the bottom and the underexposed top part of the structures. On the right the zoomed view of the overexposure defects.</i>  | 55 |
| <i>Fig. 46 Detailed view of the difference in size of beams produced by the first (smaller rectangle) and the second (bigger rectangle) exposure. The intersection points are shown as yellow crosses.</i>  | 56 |
| <i>Fig. 47 Structures fabricated using four exposure with the sample rotated 90° after each of them. The result shows the potential of this process to fabricate open boxes that could contain cells selectively when the volume inside of the box is the same of the volume needed by the cell. If different cells are bigger than the box they should not fit in it or they should adapt to the volume somehow.</i> | 57 |
| <i>Fig. 48 Simple fabrication idea utilising positive tone resist to confine the unexposed SU-8. Then utilizing inclined lithography we can fabricate spring like structures in the SU-8.</i>   | 59 |
| <i>Fig. 49 Example of single mesh structures with apertures of different sizes inside a microfluidic channel.</i>   | 71 |
| <i>Fig. 50 Structure fabricated in the 50 <math>\mu\text{m}</math> layer SU-8 showing the formation of defects on structures too near to each other's.</i>  | 71 |
| <i>Fig. 51 Inclined structures obtained by holes in the mask made with 2 triangles joined by one tip. Structures like this have no actual use but trying out different shapes in the mask could actually result in some useful strange shaped structures.</i>   | 72 |
| <i>Fig. 52 Top view of rows too near to each other. The overexposure defects on the sides of the structures are connected to the ones on the next row. The defects needs to be eliminated if we need to fabricate structures near to each other.</i>  | 72 |

## APPENDIX A (Inclined exposure additional data and pictures)

In this section some additional SEM pictures are presented for completeness sake. They are not fundamental for the work but helped during the iterations to understand what was going on in the samples.

A table with the parameters used for the fabrication of all the samples is presented. From the Table 5 is possible to visualize the process of optimization with the mask changing and the exposure time getting shorter.

| Sample             | Thickness (μm) | 1 <sup>st</sup> exposure (s) | Inclined Exposure(s) | Inclination | Mask version |
|--------------------|----------------|------------------------------|----------------------|-------------|--------------|
| <b>1.1 and 1.2</b> | 350            |                              |                      |             | 1.0          |
| <b>2.1</b>         | 100            | 28                           | 2x8                  | 50°         | 2.0          |
| <b>2.2</b>         | 50             | 18                           | 2x4                  | 50          | 2.0          |
| <b>2.3</b>         | 100            | 25                           | 2x8                  | 50          | 2.0          |
| <b>2.4</b>         | 100            | 25                           | 2x6                  | 50          | 2.0          |
| <b>2.5</b>         | 50             | 18                           | 2x3                  | 50          | 2.0          |
| <b>2.6</b>         | 70             | 20                           | 2x4                  | 50          | 2.0          |
| <b>2.7</b>         | 50             | 18                           | 2x3                  | 50          | 2.1          |
| <b>2.8</b>         | 70             | 20                           | 2x4                  | 50          | 2.1          |
| <b>3.1</b>         | 70             |                              | 4x5                  | 50          | Holes        |
| <b>3.2_rot</b>     | 70             |                              | 45                   | ~30         | Holes        |
| <b>3.3</b>         | 30             |                              | 4x3                  | 50          | Holes        |
| <b>3.4_rot</b>     | 30             |                              | 30+3 perpend.        | ~30         | Holes        |
| <b>3.5</b>         | 30             |                              | 4x2                  | 50          | Holes        |
| <b>3.6_rot</b>     | 30             |                              |                      |             | Holes        |

*Table 5 All the sample fabricated during the work are reported here. We can notice that the mask was changed and improved during the iteration as well as the exposure.*

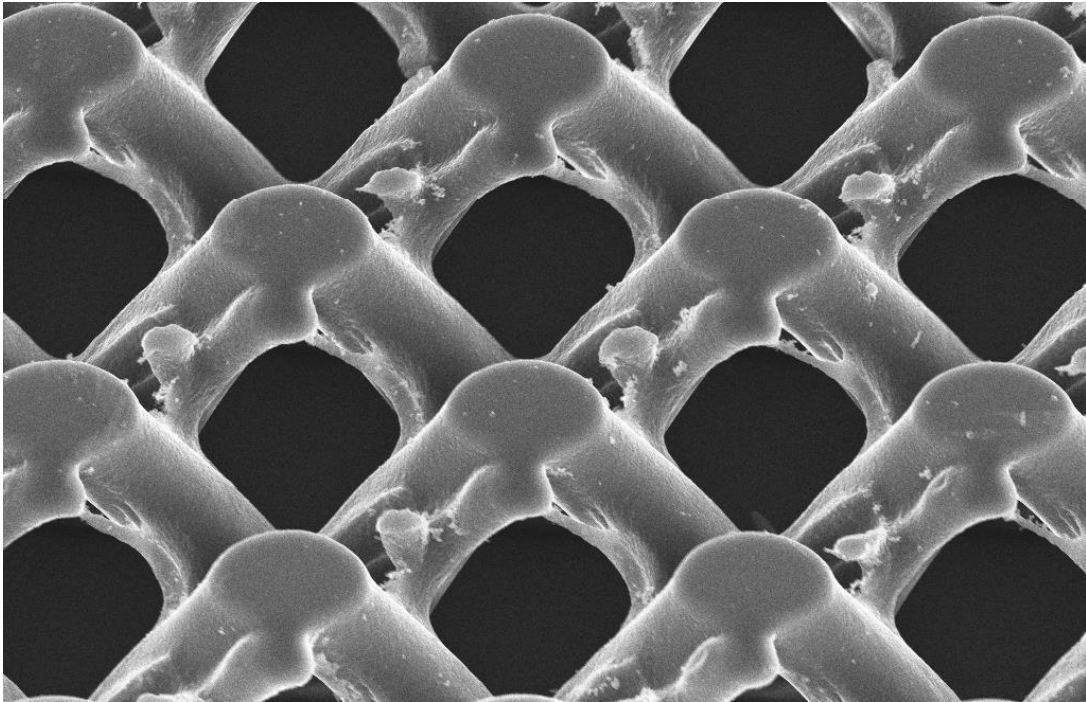


*Fig. 50 Structure fabricated in the 50  $\mu\text{m}$  layer SU-8 showing the formation of defects on structures too near to each other's.*

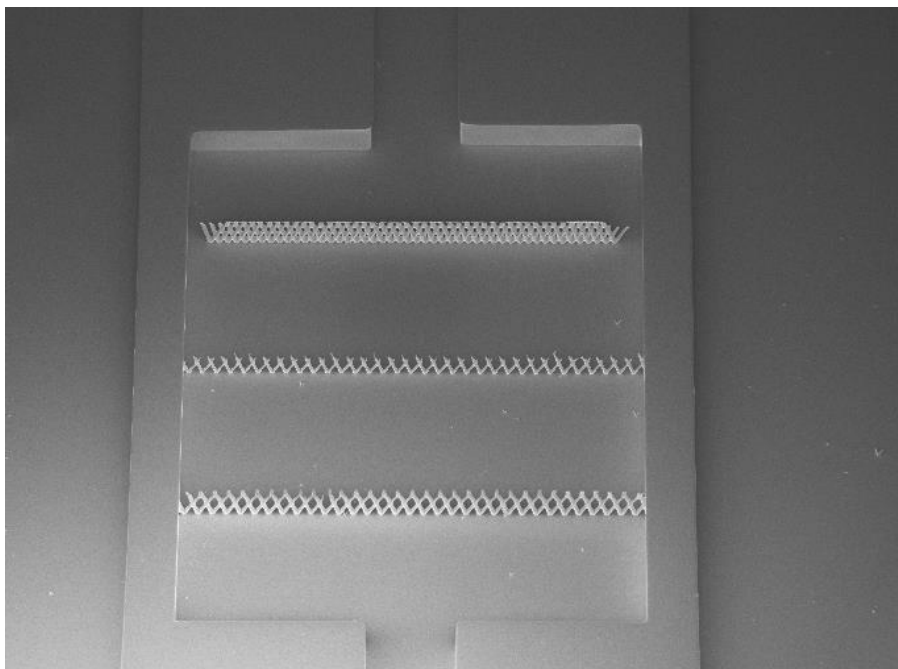


*Fig. 49 Example of single mesh structures with apertures of different sizes inside a microfluidic channel.*

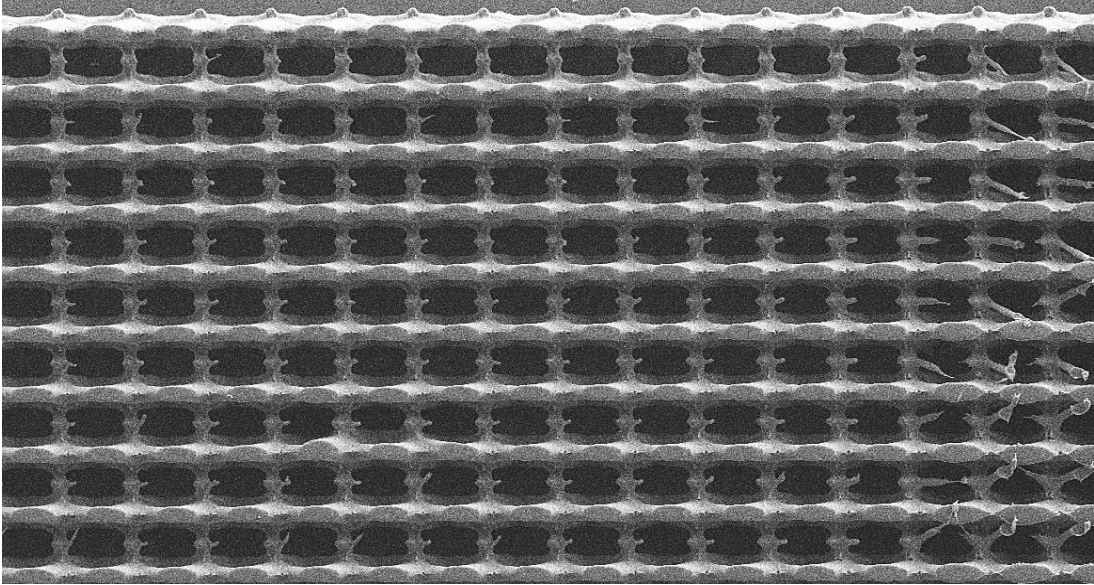


*Fig. 52 Top view of rows too near to each other. The overexposure defects on the sides of the structures are connected to the ones on the next row. The defects need to be eliminated if we need to fabricate structures near to each other.*

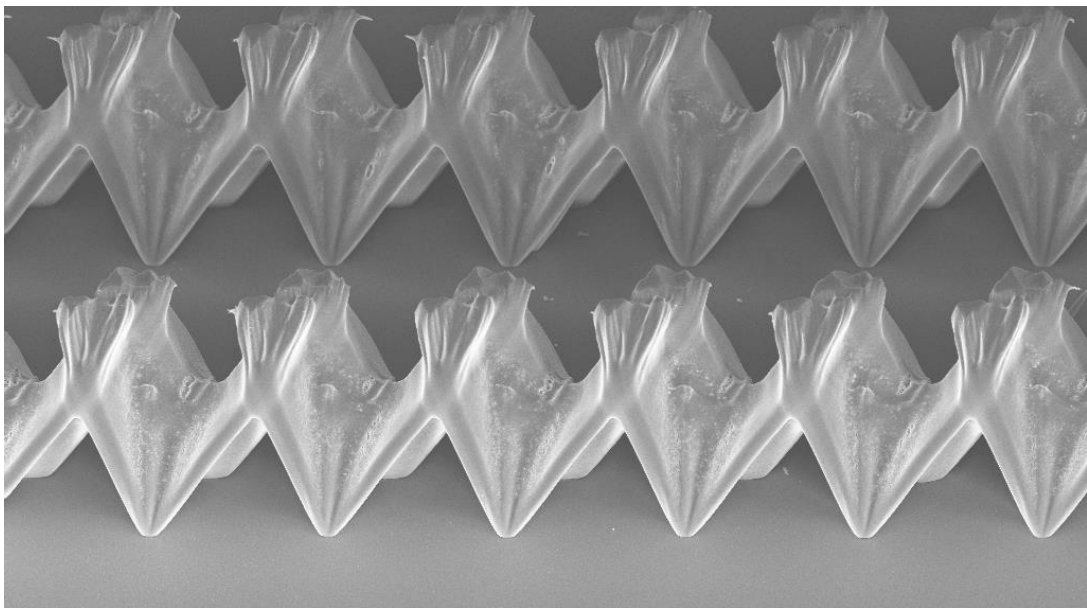


*Fig. 51 Inclined structures obtained by holes in the mask made with 2 triangles joined by one tip. Structures like this have no actual use but trying out different shapes in the mask could actually result in some useful strange shaped structures.*

## APPENDIX B (Scanning electron microscope)

The scanning electron microscope is the tool that makes possible the imaging of small structures (up to 1 nm resolution) in bulk samples. The SEM is based on the interaction of an electron beam and the sample surface. The focussed electron beam scans the surface of the sample line by line with the interaction of beam-surface forming signals that are then detected. In the analogic era the signal from the sample was displayed as a brightness modulation in a CRT screen whose electron beam was driven simultaneously to the beam in the SEM. In the digital era the CRTs are replaced by computer techniques of analysis.

The magnification in the SEM is provided by the fact that the area of the displayed image remains unchanged while the dimensions of the scanned area are reduced. The resolution of the SEM is determined by both the diameter of the electron beam focused on the surface and interaction of the primary electrons (PE, the electrons from the beam) and the sample. The electron beam is focused on the sample using a series of electromagnetic lenses coupled with diaphragms. The diameter of the electron beam on the sample's surface is dependent on the aperture angle of the objective (the last lens, or lenses, of the column), the current intensity and gun brightness with the formula:

$$d_0 = \left( \frac{4I_0}{\pi^2 R} \right)^{1/2} \frac{1}{\alpha_0} = \frac{C_0}{\alpha_0}$$

Where  $I_0$  is the current intensity,  $R$  is the gun brightness and  $\alpha_0$  is the aperture angle that is  $\alpha_0 = \frac{r}{L}$ , the ratio of the diameter of the last diaphragm ( $r$ ) and the working distance  $L$  (distance between the specimen and the lenses column). Of course the  $d_r$ , the real diameter of the beam, is always bigger than  $d_0$  due to aberrations [65].

Another important characteristic of the SEM is the large depth of focus. On a normal optical microscope the depth of focus is in the  $\mu\text{m}$  range for a 200x magnification whereas in the SEM the depth of focus is in the mm range at the same magnification. This characteristic is particularly useful when observing the sample at very high magnification. In the case of low depth of focus the imaging at high magnification would not be possible since most of the picture would be out of focus and only a small area would be properly focused.

The imaging in a SEM can be done using many different detectors but the most used for imaging are the ones detecting secondary electrons (SE) and back scattered electrons (BSE).

The SE are collected with an Everhardt-Thornley detector, a combination of a scintillator and a photomultiplier. The secondary electrons are formed from the interaction of the primary electrons in the beam with the electron clouds of the sample's atoms and they possess low energy in the order of 50 eV. These electrons are collected using a grid electrode positively biased at 200V. The scintillator will accelerate the electrons that will enter the photomultiplier with higher kinetic energy, sufficient to create photons in the multiplier tube. The result is a large number of photons that will create the detected signal. The resolution of the SE detector is the better of the two and it is used for imaging when the shaped are important since the images are three dimensional and the morphology of the sample can be analysed.

The BSE detector is a solid state detector (semiconductor diodes) used to collect the backscattered electrons. The BSE are the PE that interact with the nucleus of the atoms and are deflected back. These electrons are used to analyse the different materials in the sample since the BSE characteristics are connected to the Z value of the nucleus. In this way it is possible to check the composition of the sample. Using different diodes for the detection it is also possible to have topography-sensitive signals in addition to the material-specific signal. This detector is used for example to observe the different material in a multilayer structure.